Identification of Protein-Protein Interactions in the Type Two Secretion System of *Aeromonas hydrophila*

A Thesis Submitted to the College of

Graduate Studies and Research

in Partial Fulfillment of the Requirements

for the Degree of Master of Science

in the Department of Microbiology and Immunology

University of Saskatchewan

Saskatoon

By

Sue Zhong

PERMISSION TO USE

In presenting this thesis in partial fulfillment of the requirements for a Postgraduate degree from the University of Saskatchewan, I agree that the Libraries of this University may make it freely available for inspection. I further agree that permission for copying of this thesis in any manner, in whole or in part, for scholarly purposes may be granted by the professor or professors who supervised my thesis work or, in their absence, by the Head of the Department or the Dean of the College in which my thesis work was done. It is understood that any copying or publication or use of this thesis or parts thereof for financial gain shall not be allowed without my written permission. It is also understood that due recognition shall be given to me and to the University of Saskatchewan in any scholarly use which may be made of any material in my thesis.

Requests for permission to copy or to make other uses of materials in this thesis in whole or part should be addressed to:

Head of the Department of Microbiology and Immunology
University of Saskatchewan
Saskatoon, Saskatchewan S7N 0W0
Canada

ABSTRACT

The type II secretion system is used by many pathogenic and non-pathogenic bacteria for the extracellular secretion of enzymes and toxins. *Aeromonas hydrophila* is a Gram-negative pathogen that secretes proteins via the type II secretion system.

In the studies described here, a series of yeast two-hybrid assays was performed to identify protein-protein interactions in the type II secretion system of *A. hydrophila.* The periplasmic domains of ExeA and ExeB were assayed for interactions with the periplasmic domains of Exe A, B, C, D, K, L, M, and N. Interactions were observed for both ExeA and ExeB with the secretin ExeD in one orientation. In addition, a previously identified interaction between ExeC and ExeD was observed. In order to further examine and map these interactions, a series of eight two-codon insertion mutations in the amino terminal domain of ExeD was screened against the periplasmic domains of ExeA and ExeB. As a result, the interactions were verified and mapped to subdomains of the ExeD periplasmic domain. To positively identify the region of ExeD involved in the interactions with ExeA, B, C and D, deletion mutants of ExeD were constructed based on the two-codon insertion mutation mapping of subdomains of the ExeD periplasmic domain, and yeast two-hybrid assays were carried out. The results showed that a fragment of the periplasmic domain of ExeD, from amino acid residue 26 to 200 of ExeD, was involved in the interactions with ExeA, B and C. As an independent assay for interactions between ExeAB and the secretin, His-tagged derivatives of the periplasmic domains of ExeA and ExeB were constructed and co-purification on Ni-NTA agarose columns was used to test for interactions with untagged ExeD. These experiments confirmed the interaction between ExeA and ExeD, although there was background in the co-purification test.

These results provide support for the hypothesis that the ExeAB complex functions to organize the assembly of the secretin through interactions between both peptidoglycan and the secretin that result in its multimerization into the peptidoglycan and outer membrane layers of the envelope.

ACKNOWLEDGMENTS

I would like to thank my supervisor, Dr. Howard.. I am grateful that you gave me a chance to come to the lab although I knew nothing about Microbiology and could not answer your question at the interview. Thank you for teaching me the basic knowledge and guiding me in my experiments and thesis. Sometimes I could not follow you because I was very nervous and my English was poor. Thank you for your time and patience. Also I would like to thank my committee members Dr. Goldie and Dr. Xiao, and the external examiner Dr. Napper. Thank you for reading my thesis and giving me advice. A special thank also goes to the people in Dr. Xiao's lab who helped me with the yeast two-hybrid assay. And of course I must thank all my lab-mates, Tim, Li, Alicia and Qibing, you are not only my friends but also my teachers. Li and Tim, I thank you in particular for guiding me in my early experiment. In addition, I would like to extend my gratitude to Dr. Yu Luo and Dr. Yan-wu Luo, thank you for providing me your house to live in and giving me good suggestions when I had just landed in Canada. To my cousin Zhu Jing, thank you for thinking of me and calling me often in the first year when I was in Saskatoon. Your voice made me less homesick. My last but most heartfelt thanks goes to my parents, thank you for your love and encouragement for all these years, I could not have finished this project without your understanding and support. Although we live far away from each other, you are always in my mind.

DEDICATION

Dedicated to my parents,
Yongchun Jing and Yi-e Zhong

TABLE OF CONTENTS

Page

LIST OF TABLES

LIST OF FIGURES

Figure **Page**

LIST OF ABBREVIATIONS`

3-AT	3-aminotriazole
Ade	adenine
Amp	amplcillin
conc.	concentration
DMSO	dimethyl sulfoxide
dNTPs	Deoxyribonucleotide triphosphate
EDTA	ethylenediaminetetraacetic acid
FPLC	Fast Protein Liquid Chromatography
GAL_{AD}	DNA activation domain in GAL4 yeast two-hybrid system
GAL_{BD}	DNA binding domain in GAL4 yeast two-hybrid system
GSP	general secretory pathway
HR domain	high homology region
IM	inner membrane
Inc.	Incorporation
IPTG	Isopropyl β-D-1-thiogalactopyranoside
Kan	Kanamycin
Li	Lithium Acetate
LPS	lipopolysaccharide
Ni-NTA	nickel-nitrilotriacetic acid
NTPases	nucleoside triphosphatases
OD	optical density
OM	out membrane
PCR	polymerase chain reaction
PDZ	protein interaction domain, named after post synaptic density protein (PSD95), Drosophila disc large tumor suppressor (DlgA), and zonula occludens-1 protein (zo-1)
peri	periplasmic domain
PG	peptidoglycan
PMSF	phenylmethylsulphonyl fluoride
SDS	sodium dodecyl sulphate
SDS-PAGE	dodecyl sulphate-polyacrylamide gel electorphoresis
Sm	Streptomycin
T2SS	type II secretion system
TCA	trichloroacetic acid
Temp	temperature
TM/HR domain	a fragment between the TM and HR domain
TMS	transmembrane segment
WT	wild-type
YaeT	the general OM insertion factor Omp85

1.0 INTRODUCTION

The genus *Aeromonas* is a group of Gram-negative pathogens found in aqueous environments, which secrete a variety of extracellular protein toxins associated with pathogenicity and environmental adaptability. Some members of the genus are highly lethal to aquatic mammals, fish, reptiles and cows, while others also cause disease in humans (Altwegg and Gless, 1989; Fivaz *et al*., 2001, Schoenhofen *et al*., 2005). The *Aeromonas* infection is mainly associated with gastroenteritis, wound infections and systemic illness, but in immuno-compromised individuals infection may lead to lethal disease such as septicemia and meningitis (Fivaz *et al*., 2001, Yu *et al*., 2007). One member of this genus, *Aeromonas hydrophila*, can cause motile aeromonad septicemia in both fish and humans (Yu *et al*., 2007). The major virulence mechanism of this species involves secretion of degradative enzymes and toxins into the external milieux (Schoenhofen *et al*., 2005). Some of the virulence factors produced by *A. hydrophila* are surface structures, including pili, S-layers, polar flagella, and lateral flagella. Other extracellular virulence factors are secreted enzymes such as proteases, glycerophospholipid-cholesterol acyltransferase, hemolysins, aerolysin, lipases and metalloprotease (Yu *et al*., 2007). Among these toxins, aerolysin is the best characterized (Fivaz *et al*., 2001). These virulence factors are secreted into the media *via* different secretion pathways (Yu *et al*., 2007). *A. hydrophila* secretes many of the protein toxins such as aerolysin via the type II secretion system (T2SS) (Ast *et al*., 2002).

1.1 The type II protein secretion system

The T2SS is part of the general secretory pathway (GSP) which includes 2 steps, passage across the inner and outer membranes (for recent reviews, see Sandkvist, 2001a,b**;** Filloux, 2004 and Johnson *et al*, 2006) (Fig. 1-1). Table 1-1 shows T2SS nomenclature. In the first step, exoproteins to be secreted are synthesized as precursors containing N-terminal cleavable signal peptides that target them to either the Sec or Tat machinery in the inner membrane (IM) (Voulhoux *et al*., 2001; de Keyzer *et al*., 2003; Palmer *et al*., 2005). Following secretion into the periplasm, signal peptides are removed by the activity of leader peptidase, and the mature exoproteins are released into the periplasmic space, where they fold. Up to now, several branches have been identified for the second step. Among these branches, the T2SS, also known as the main terminal branch of the GSP, is used by many species of Gram-

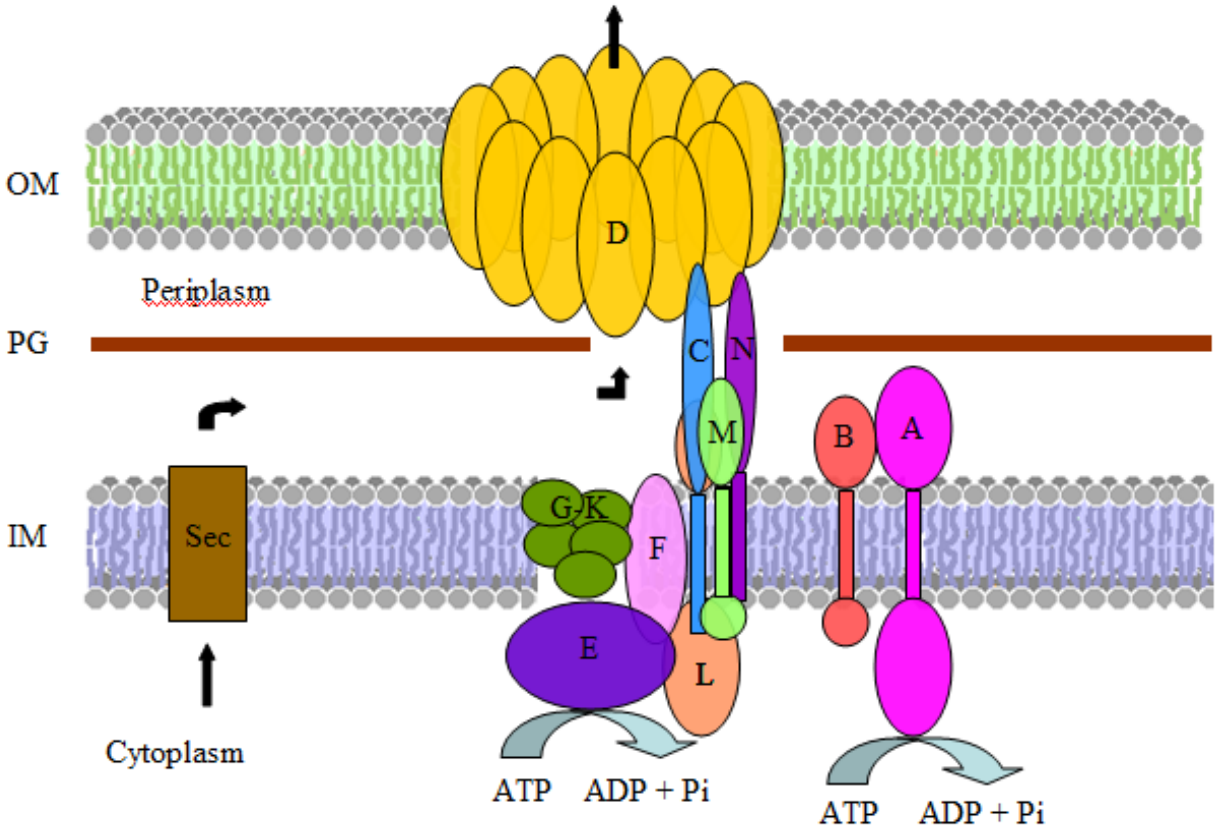

FIG. 1-1. Model of the type II secretion apparatus of *A. hydrophila*. ExeA and ExeB form a complex in the IM and are required for the assembly and/or multimerization of the ExeD secretin in the outer membrane (OM). The secretin consists of approximately 12-14 monomers which form a large oligomeric ring that functions as the translocation channel. Proteins E, F, L and M form a complex which may be involved in the assembly of the pseudopilus. Both ExeA and ExeE are ATPases. ExeC and ExeN connect the IM complex and ExeD, and may be involved in regulating the opening of the ExeD channel. The pilus-like structure composed of protein G to K extends from the IM complex and may reversibly block the secretin channel or push the folded exoproteins out of the cell. The Sec machinery secretes the exoproteins from the cytoplasm to the periplasm.

TABLE 1-1. T2SS nomenclature

Bacteria	Protein name*	Gsp Equivalent
Aeromonas hydrophila	Exe	Gsp
Erwinia chrysanthemi	Out	Gsp
Klebsiella oxytoca	Pul	Gsp
Pseudomonas aeruginosa (*Pseudomonas Alcaligenes*)	XcpR, S, Y,Z XcpT, X XcpP, Q	GspE, F, L, M GspG, K GspC, D
Vibrio cholerae	Eps	Gsp
Xanthomonas campestris	XpsP	GspC

* The individual protein nomenclature for each bacterium is the same as that for the general secretion pathway (Gsp) protein unless listed in the table.

negative bacteria, including *A. hydrophila*. In this step, the fully folded exoproteins in the periplasm are recognized and translocated across the OM by components of the T2SS. Since this apparatus apparently functions after the signal sequence-dependent transfer across the IM, it has been considered to form an extension of the Sec pathway and therefore to be part of the GSP. The T2SS differs from most other membrane transport systems, in that its substrates consist of folded proteins (Sandkvist, 2001a). Another distinguishing feature of the T2SS is that it has the ability to assemble a pilus-like structure, which is quite similar to the type IV pilin assembly system. It is proposed to move like a piston to push the folded exoproteins out of the cell through the channel of the GspD secretin.

The T2SS of *A. hydrophila* spans both inner and outer membranes and is comprised of at least 14 proteins encoded by *exe* genes which are clustered into 2 operons, *exe*C-N and *exe*AB (Howard *et al*., 1993; Jahagirdar and Howard, 1994; Ast *et al*., 2002; Schoenhofen *et al*., 2005). The proteins encoded by these 2 operons form a secretion structure or machinery called the secreton. The genes *gsp*O and *gsp*S occur in the T2SS of other species but are not found in that of *A. hydrophila.* The T2SS is generally considered as consisting of three subassemblies: an IM platform, a periplasmic pseudopilus and an OM complex (Johnson, *et al*., 2006).

1.2 The inner membrane complex

Of the five integral cytoplasmic membrane proteins C, F, L, M and N, three of them including GspF, L and M, together with the cytoplasmic protein GspE, form an IM complex (Py *et al*., 2001, Robert *et al.*, 2005b). The IM ternary complex appears to connect the secretion pore and the GspE protein component that is located in the cytoplasm. In addition, it is presumably used as a platform for assembling other parts of the T2SS, especially the pseudopilus.

GspL and GspM are two key components of the T2SS present in the IM. Some studies have shown that EpsL and EpsM, homologs of GspL and GspM from *Vibrio cholerae*, are likely to form homodimers or homomultimers (Py *et al*., 1999; 2001; Johnson *et al*. 2007). Yeast two-hybrid analysis revealed that both the N-terminal cytoplasmic domains and the C-terminal periplasmic domains (peri) of EpsL and OutL, a homolog from *Erwinia chrysanthemi*, are involved in homodimer or homomultimer formation (Py *et al*., 1999, Douet *et al*., 2004, Abendorth *et al*., 2004a). Furthermore, the peri-EpsM has been proved to be a part of the

interface between the IM platform and other components of the machinery (Abendorth *et al*., 2004b). This region of EpsM has further been revealed to be a binding site of an unknown ligand or part of a protein partner. In addition, the specific regions of EpsM involved in oligomerization were identified and mapped by Johnson *et al*. (2007) showing that a periplasmic region, from residue 100 to 135, is responsible for homo-oligomer formation. Specifically, co-purification and co-immunoprecipitation of truncated EpsM mutants with Histidine-tagged EpsM showed that EpsMΔ14, EpsMΔ30 (C-terminal 14 and 30 amino acids were removed respectively) bound to $EpsM_{His6}$, while binding of EpsMΔ66, EpsMΔ82 (C-terminal 66 and 82 amino acids were removed respectively) to $EpsM_{His6}$ was undetectable, suggesting that the C-terminus of EpsM (the last 30 residues) was not necessary for EpsM dimerization while the last 66 residues were required to stably interact with another EpsM molecule. A yeast two-hybrid assay in both directions showed that the last 79 amino acids of the C-terminal region of OutM (OutM contains 162 amino acids), from residue 84 to 162, were responsible for OutM homodimer formation as well as for the OutLM interaction (Py *et al*., 2001). Based on these results, it can be hypothesized that a region near the TM in the peri-ExeM or the whole periplasmic domain including the C-terminus contributes to the dimerization or oligomerization. Although different regions were mapped for the self-interaction, these results suggest that GspM may form dimers or larger oligomers through interactions involving the C-terminal end of the periplasmic domain. It has also been demonstrated that GspL and GspM homologs in *Pseudomonas aeruginosa, Klebsiella oxytoca*, *E. chrysanthemi* and *V. cholerae* are capable of protecting each other from proteolytic degradation (Michel *et al*. 1998; Sandkvist *et a*., 1999; Py *et al.*, 2001; Robert *et al*., 2002, 2005b; Johnson *et al*., 2007). In *V. cholerae*, EpsL and EpsM seem to interact with each other directly as no other Eps protein is needed for their assembly when they are expressed in *Escherichia coli* (Sandkvist *et al*., 1999). Analysis of truncated EpsM mutants and co-immunoprecipitation revealed that EpsMΔ83 still appeared to interact with EpsL, though not as well as full-length EpsM, indicating that this fragment (residues 1-82) of EpsM is partially dispensable for EpsLM interaction. These and other data on truncated EpsM mutants suggested that a region from residue 84 to 99 is required for a stable interaction with EpsL (Johnson *et al*., 2007). This result is in agreement with Py *et al.* (2001).

Another component of the IM complex, termed XpsN, a homolog of GspC of *Xanthomonas campestris*, could be co-immunoprecipitated with both XpsL and XpsM, suggesting that it might be involved in formation of the XpsL-XpsM complex in the T2SS (Lee *et al*., 2001). This result was further confirmed by metal-chelating chromatography and immunoblot analysis which revealed that both XpsL and XpsN co-eluted with His-tagged XpsM, and XpsL and XpsN co-immune precipitated with each other (Tsai *et al*, 2002). Further purification by size-exclusion chromatography followed by nickel affinity chromatography demonstrated that XpsL, XpsM and XpsN form a reversible ternary complex, that is, there is a dynamic relationship among the three components of the XpsLMN complex. XpsN was not stably maintained in the complex and detached from it before dissociation of the other two components. Conversely, XpsN preferentially associated with the XpsLM complex rather than to XpsM alone. In addition, the dissociation rate of XpsL from the XpsLM complex was significantly greater than from XpsLMN complex, suggesting the presence of XpsN in the complex probably strengthens the association between XpsL and XpsM (Tsai *et al*, 2002), which corresponds to a previous study showing that XpsN was required for maintaining both XpsL and XpsM at normal steady state levels (Lee *et al*., 2001).

Protein GspF, a polytopic integral cytoplasmic protein in secreton, is the least studied component of the IM complex. The function of GspF and its interactions with other components of the ternary complex are not well known. Yeast two-hybrid assays in one direction have revealed interactions of the N-terminal 172 residues of OutF with OutE, and with the cytoplasmic segment of OutL in *E. chrysanthemi* (Py *et al.*, 2001). Further co-immunoprecipitation studies demonstrated that OutF formed a stable complex with OutE and OutL *in vivo*. However, OutF was not necessary for the production of the OutE-OutL complex while OutL was required for the formation of the OutE-OutF complex. Interactions between GspF and other components of the complex have also been demonstrated in *P.aeruginosa*. Reversible cross-linking and co-purification of XcpR (GspE), XcpS (GspF), XcpY (GspL) and XcpZ (GspM) suggested that these four components associated as a complex in the IM (Robert *et al*., 2005b). Similarly, XcpS has been demonstrated to be stabilized by co-expression with XcpR and XcpY, indicating an interaction between these three components of the machinery (Arts *et al*., 2007). Arts *et al*. (2007) also found that the cytoplasmic loop of XcpS was

involved in the stabilization by XcpR and XcpY, and the cytoplasmic domain of XcpS, from residue 240 to 376, seemed to be important for interaction with XcpRYZ. In addition, two GspE and GspF homologs, BfpD and BfpE, which are required for biogenesis of the bundle-forming pilus of enteropathogenic *E. coli.*, have also recently been demonstrated to interact with each other (Crowther *et al*., 2004). Further study by this group showed that the ATPase activity of BfpD was slightly stimulated by a fragment of the N-terminal cytoplasmic domain of BfpE (Crowther *et al*., 2005). It can be concluded that the cytoplasmic proteins E, F, L, M and N form an IM complex via reversible association.

1.3 GspE, the putative ATPase

GspE belongs to a large family of TypeII/TypeIV secretion nucleoside triphosphatases (NTPases), which are proposed to couple NTP hydrolysis to bacterial protein secretion (Planet *et al.*, 2001). GspE as well as other members of the NTPase family contain several conserved motifs including Walker A and B boxes, a histidine box and an aspartate box (Robin *et al*., 2003). It has been demonstrated that purified EpsE from *V. cholerae* is an Mg^{2+}-dependent ATPase, and the 3D structure of an N-terminal deletion derivative was determined (Robien *et al*., 2003; Camberg and Sandkvist, 2005). It was also shown that EpsE displays cooperative ATPase activity as the specific activity of EpsE was influenced by its concentration (conc.), and this result together with previous studies on OutE (Py *et al*., 1999), indicated that type II secretion ATPases can assemble into oligomers (Camberg and Sandkvist, 2005). Gel filtration showed that purified EpsE contained a small fraction of hexamers with increased specific activity and the crystal structure of the N-terminal deletion derivative (Δ90EpsE) revealed a helical filament with six fold symmetry (Robien *et al*., 2003). In addition, several structural homologues of EpsE such as HP0525, a type IV secretion NTPase of *Helicobacter pylori*, and PilT, the type IV pilus retraction ATPase, have been shown to be hexameric ATPases (Yeo *et al*., 2000; Forest *et al*., 2004). These findings suggest that functional GspE may form a hexameric ring associated with the IM that is involved in pseudopilus assembly (Robien *et al*., 2003). EpsE of *V. cholerae* and OutE of *E. chrysanthemi* were both demonstrated to associate with the cytoplasmic membrane through interactions with the N-terminal cytoplasmic domain of EpsL and OutL (Sandkvist *et al*, 1995, 1999; Py *et al*, 1999). Yeast two-hybrid assays in both directions in *E. chrysanthem* also suggested that the N-terminal cytoplasmic domain of

OutL was involved in OutE-OutL interaction (Py *et al*, 1999). These results have been confirmed by the X-ray crystal structure of a hetero-tetrameric complex formed between subdomains of EpsL and EpsE showing that two regions, both located in the cytoplasmic domain of EpsL, are involved in interactions with the N-terminal cytoplasmic region of EpsE (Sandkvist *et al*, 2000; Abendroth *et al.* 2005).

Although a recent study demonstrated that *X. campestris* XpsE oligomerization was triggered by ATP binding, which led to its association with the N-terminal domain of XpsL (Shiue *et al*., 2006), the HP0525 ATPase of *H. pylori* oligomerized independent of ATP (Savvides *et al*., 2003), and yeast two-hybrid assay demonstrated that mutations of the Walker A box in OutE did not influence its interaction with OutL (Py *et al.*, 1999). Shiue *et al*. (2006) also showed that XpsE–XpsL association precedes ATP hydrolysis and stimulates this activity. The weak ATPase was stimulated two-fold by a fusion protein containing the cytoplasmic domain of XpsL. Shiue *et al*. (2007) further identified a key residue, R286, of the ATPase XpsE which facilitates a critical role in coupling ATP hydrolysis to protein translocation. The result was obtained by site-directed mutation of XpsE. Although mutation of R286 to alanine increased the rate of XpsE ATP hydrolysis five times compared to that of the wild-type (WT) XpsE, the mutant lost ATP-binding affinity and ability to oligomerize. As a result, the mutant was not able to associate with the IM via $XpsL_N$, and ATP hydrolysis by XpsE was uncoupled from protein secretion. Therefore, the mutant became non-functional in protein secretion. Conversely, Camberg *et al*. (2007) found that ATP-binding was not a requirement for complex formation of EpsE with EpsL. EpsE of *V. cholerae* was shown to be a hexamer with weak ATPase activity (Camberg and Sandkvist, 2005). The ATP hydrolysis assay demonstrated that acid phospholipids, including phosphatidylglycerol and cardiolipin, stimulated ATPase activity of EpsE by 30 fold and 130 fold respectively; however, the stimulation was observed for the EpsE/EpsL (1-253) complex but not for EpsE alone. By altering the order of addition of ATP and cardiolipin in the ATP hydrolysis assay, they revealed that direct binding of the EpsE/EpsL (1-253) complex to acid phospholipids was required for the activation. These studies thus suggested that the stimulation of ATPase activity requires a properly formed conformation of EpsE, which results from association of EpsE and the cytoplasmic domain of EpsL and is responsive to the presence of acid phospholipids. In addition, EpsE and EpsL (1-253) could be cross-linked to form a larger molecular species which could be recognized by both anti-EpsE

and anti EpsL antibodies, and EpsL (1-253) substitution mutants showed a reduced rate of ATP hydrolysis compared to the non-mutated EpsE/EpsL (1-253), suggesting that EpsL (1-253) might be involved in fine tuning the interaction of EpsE with phospholipids in the IM and thus regulating its oligomerization and promoting ATPase activity (Camberg *et al*. 2007).

1.4 The pseudopilins

The pseudopilins of T2SS encoded by *gsp*G-K have been proposed to extend from the IM complex and form a pilus structure in the pore of the OM complex spanning the cell envelope, acting as a piston and/or plug to translocate substrates and exoproteins through the OM secretin pore (Hobbs and Mattick, 1993; Nunn, 1999; Sauvonnet *et al.* 2000; Ast *et al*., 2002; Peabody *et al*., 2003). The pseudopilus may extend from the GspEFLM complex in the IM complex, which may be involved in its assembly. The T2SS pseudopilins are similar to the pilins that are assembled into the type IVa pilus (Filloux *et al*., 1998; Mattick *et al*., 1995; Sandkvist 2001). The recently published crystal structure of a truncated form of PulG from *K. oxytoca* revealed that PulG and the type IV pilins displayed a similar structure made up of an N-terminal hydrophobic α-helix followed by four β-strands arranged in a globular domain (K¨ohler *et al*., 2004). Among the T2SS pseudopilins, GspG, termed 'major' pseudopilin, is the most abundant, whereas GspH, GspI, GspJ and GspK are low abundance 'minor' pseudopilins, which may contribute to initiation, stabilization, regulation, or capping of the periplasmic piston filaments to achieve secretion (Nunn and Cleavage, 1993; Sauvonnet *et al*., 2000; Forest, 2008). Cross-linking and immunoblot analysis showed that XpsG interacts directly with secretin XpsD and XpsN in *X. campestris pv.Campestris*, and the association of XpsG with XpsD was strongly dependent on the expression of XpsN (Lee *et al*., 2005), suggesting that GspG and the secretin GspD are in contact at certain stages during the secretion process, and this contact may be regulated by GspC, indicating that GspC may play a direct role during pseudopilus assembly or activity as well. GspK has been shown to control the pseudopilus assembly and may interact directly with GspG (Durand *et al.* 2005). The same study further confirmed that only XcpT (GspG) of *P. aeruginosa*, the major pseudopilin, could be assembled in a multifibrillar structure termed the pseudopilus, while none of the four minor pseudopilins had this characteristic, suggesting that the assembly into a pseudopilus is a unique property of GspG. Furthermore, XcpX (GspK) was shown to destabilize XcpT (GspG) when

overexpressed, and this phenomenon together with cross-linking experiments revealed that GspK interacts with GspG. In addition, the study revealed that the pseudopilin XcpX is important in controlling the pseudopilus elongation process, and this control was probably exerted via a direct interaction between XcpX and XcpT. These results suggest that GspK may be involved in the interactions with other pseudopilins during pseudopilus assembly and/or functioning. A recent study showed that GspK forms a ternary complex with GspI and GspJ in *E. coli.* (Korotkov and Hol., 2008). The X-ray crystal structure of the GspK–GspI–GspJ heterotrimer suggested that this complex might be located at the tip of the pseudopilus, and an inserted α-helical domain of GspK might form the tip of the piston with GspK and GspJ positioned in such a way that additional pseudopilin subunits extend below but not above the tip of GspK. This result is in agreement with the previous study showing that XcpX (GspK) controls the length of the pseudopilus in *P. aeruginosa* (Durand, *et al.* 2005). The GspK–GspI–GspJ tip probably interacts at least transiently with T2SS components in the OM, in particular with the secretin GspD (Korotkov and Hol, 2008).

1.5. **GspC and GspN, the connecting components**

GspC is a bitopic IM protein which is proposed to connect the IM platform and OM components of the T2SS (Bleves *et al.*, 1999; Possot *et al*., 2000; Gérard-Vincent, *et al*., 2002). GspC consists of a short N-terminal cytoplasmic sequence, a single TMS (transmembrane segment), and a large C-terminal hydrophilic periplasmic region (Bleves *et al.*, 1996; Thomas *et al*., 1997; Gérard-Vincent, *et al*., 2002; Robert *et al*., 2005a; Korotkov *et al*., 2006).

The majority of the GspC homologs contain a PDZ domain near their C termini (Pallen and Ponting, 1997). However, the PDZ domain is absent in some GspC family members and replaced by a coiled coil domain (Gérard-Vincent, *et al*., 2002; Peabody *et al*., 2003). Both PDZ domains and coiled coil domains are known to be involved in protein-protein interactions (Bleves *et al.*, 1999; Bouley *et al*., 2001; Gérard-Vincent, *et al*., 2002; van Ham & Hendriks, 2003). These two domains may also be responsible for multimerization. Analysis of XcpP (GspC)-OutC chimeras composed of the XcpP coiled coil exchanged for the PDZ domain of OutC revealed that these two structurally different regions could be exchanged and the resulting hybrid could be integrated into a functional secreton, suggesting that both the coiled coil

domain of XcpP and the PDZ domain of OutC could be involved in the formation of homo-multimeric complexes but not required for interaction with other proteins (DaeGérard-Vincent *et al*., 2002). However, a recent study showed that the absence of the PDZ domain does not affect OutC self-interaction (Login and Shevchik, 2006). Thus the PDZ region or the coiled coil structure of GspC homologs may be either involved in homotypic interactions in the formation of homomultimers or interaction with other proteins. Other regions of GspC may also contribute to homo-oligomerization. Login and Shevchik (2006) suggested that the TM domain drives the self-association of OutC that is essential for the formation of a functional secretion system, whereas the periplasmic region is dispensable for homodimerization, corresponding to the previous studies by Robert *et al*. (2005a) and Korotkov *et al* (2006).

In addition to homodimerization and protein-protein interaction, the PDZ domain or a coiled coil domain may also be involved in the recognition of secreted proteins and confer secretion specificity to a subgroup of secreted proteins. Bouley *et al*. (2001) found that OutC of *E. chrysanthemi* containing partial or complete deletions of the PDZ motif became selectively functional in that the secretion of three exoproteins was unaffected while the secretion of the majority of pectate lyase was completely abolished. Conversely, by domain swapping between XcpP of *P. aeruginosa* and OutC of *E. Chrysanthemi*, Gérard-Vincent *et al*. (2002) suggested that 35 residues in the TM/HR domain [a fragment from residue 50 to 85 between the TM and high homology domain (HR)] of XcpP might contribute species specificity since this region was non-exchangeable and was involved in the stability of the XcpYZ secreton subcomplex and the functionality of the XcpP machinery. However, this hypothesis was later questioned by the study of Robert *et al*. (2005a). In this study, the specificity function of the TM/HR domain was further analyzed by domain swapping of XcpP of *P. aeruginosa* with XcpP of *Pseudomonas Alcaligenes*. In contrast to the T2SS of *E. chrysanthemi*, the T2SS of *P. alcaligenes* promotes heterologous protein secretion in *P. aeruginosa*. The results showed that the TM/HR domain of *P. aeruginosa* XcpP could be substituted by the corresponding domain of *P. alcaligenes* XcpP without affecting the functionality of the Xcp system, indicating that the TM/HR domain might not contribute to species specificity.

GspC has been suggested to interact with the OM protein GspD since homo-trimer formation, stability and proper function of GspC required GspD (Shevchik *et al*., 1997; Bleves *et al.*, 1999; Possot *et al*., 1999; Lee *et al*., 2000). However, previous results have shown discrepancies concerning the region of GspC involved in the interaction with GspD. As described above, the PDZ domain or a coiled coil domain of GspC may be involved in protein-protein interactions. An earlier study suggested that the N-terminal TM and the coiled coil structure at the C terminus of XcpP (179-212) might be responsible for the protein-protein interaction during assembly of the secretory machinery (Bleves *et al*., 1999). Analysis of truncated XcpP mutants showed that XcpPΔ19, a mutant lacking the coiled coil structure, failed to complement an *xcp*P deletion mutant, while XcpPΔM which lacked the XcpP C-terminus including the coiled coil structure and the 22 C-terminal residues of the wild type (WT) protein not only complemented the mutation but also resulted in an increased level of secretion. These results suggested that the coiled coil structure at the C terminus of XcpP play a key role for XcpP function. Moreover, the contradictory results of the two mutants led to a hypothesis that the N-terminal domain of XcpP of *P. aeruginosa* may negatively control the opening of the XcpQ (GspD) secretin channel directly or via interaction with another Xcp protein, leading to efficient secretion. Although XcpPΔ19 also contained the N-terminal domain, the 22 C-terminal residues which were absent in XcpPΔM might be involved in negatively controlling the secretion process via maintaining the XcpQ pores in a closed conformation, resulting in the noncomplementation of the Xcp deletion mutant strain by the XcpPΔ19 variant. In contrast to this result, recent studies suggested that the C-terminal peri-GspC is involved in the interaction with GspD (Robert *et al*., 2005a; Korotkov *et al*., 2006), while the PDZ domain or coiled-coil structure of GspC does not interact with GspD (Korotkov *et al*., 2006). Robert *et al*. (2005a) constructed hybrid proteins by domain swapping with the corresponding regions of *P. alcaligenes* XcpP and *E. chrysanthemi* OutC, and then tested the stability of the hybrids in the presence or absence of XcpQ. The results suggested that it is the C-terminal domain of XcpP that might be involved in the interaction with XcpQ. In addition, other experiments with XcpP also excluded the possibility that the interaction was in a species-specific manner. Although the XcpP-XcpQ interaction promoted via the C-terminal domain of XcpP was not essential for the secretion process, the study suggested that this region might be involved in a fine tuning control of the channel opening of the secreton, corresponding to the previous study by Bleves *et al.*

(1999). The exact region in the C-terminus of GspC that interacts with GspD was further mapped by Korotkov *et al*. (2006) with co-purification showing that the periplasmic HR domain of EpsC of *V. cholerae* (residue 75 to 177) interacts with EpsD. Based on these results, it has been hypothesized that different exoproteins secreted by the T2SS of a given species possess a variable number of targeting signals which are recognized by different regions of GspC and GspD. In addition, this complex mechanism probably involves a structural recognition signal (Robert *et al*., 2005a).

Genetic and biochemical studies suggested that GspC interacts, at least transiently, with the IM proteins GspL and GspM and stabilizes the GspLM subcomplex (Possot *et al*., 1999, 2000; Gérard-Vincent *et al*., 2002; Robert *et al*., 2002, 2005b; Lee *et al*., 2004).
Gérard-Vincent *et al*. (2002) suggested the existence of an XcpP–XcpY–XcpZ (GspCLM) subcomplex in *P. aeruginosa*. The evidence showed that XcpZ45, an XcpZ (GspM) derivative that lost its function in conferring XcpY (GspL) stability when co-produced in *E. coli*, could stabilize XcpY in the presence of XcpP (GspC). The study showed that introducing the genes encoding *xcp*Z45 and *xcp*Y into *E. coli* resulted in a low level of XcpY, however, this defect was compensated by the introduction of the WT *xcp*P gene, but not by introduction of the *out*C gene. Therefore, to determine which domains of XcpP might be involved in this effect, *xcp*P–*out*C chimeras carrying the TM/HR region of OutC were expressed in *E. coli* containing *xcp*Z45 and *xcp*Y. The chimeras were not able to restore the stabilizing activity of XcpZ45 on XcpY, indicating that the TM/HR domain of XcpP might be involved in the stability of the XcpP–XcpY–XcpZ subcomplex. Similarly, TM domain was also supposed to contribute to this function. In contrast to the interaction between GspC and the IM complex, the interaction between GspC and GspD described above suggests that those regions of GspC are essential for linking the IM complex to the OM secretin. In addition, subcellular fractionation has revealed that PulC of *K. oxytoca* partly fractionates in the OM (Bleves *et al.*, 1999; Possot *et al*., 1999). For example, the subcellular fractionation done by Possot *et al*. (1999) showed that the N-terminal hydrophobic domain of PulC of *K. oxytoca* inserted into IM while the C-terminal region of PulC (residue 245 to 285) was involved in the regulation of the association with the OM. The study also used cross-linking of proteins in whole cells and found formation of a 110 kDa band which reacted with PulC-specific serum and whose detection required the presence of

PulD. However, the band was not a PulC-PulD hetero-dimer (31 kDa + 68 kDa), because it did not react with antibodies specific for PulD, indicating that the 110 kDa band could be a homo-PulC trimer whose formation required PulD. In addition, PulC was not stabilized by PulD since no difference was observed in the yields of PulC in strains with or without PulD. Based on the results of GspC-D interactions, GspC-GspLM interactions and the fractionation of GspC into both the IM and OM, it can be hypothesized that GspC connects the IM complex GspEFLM and the OM complex GspDS by interacting with GspLM of the IM complex and the OM protein GspD.

In addition to GspC, GspN is also a bitopic IM protein which has been suggested to connect the IM and OM. It has been identified only in some T2SS, such as *A. hydrophila, K. oxytoca, Erwinia carotovora, X. campestris* and *Pseudomonas putida,* while it is absent in many other T2SS (Filloux, 2004). In *X. campestris*, XpsN has been considered as a homolog of GspC for the following reasons. First, there is no GspC component in the secretion apparatus, and the function of XpsN is quite similar to that of GspC; second, the membrane topology of *xps*N is similar to that of *xps*P (*gsp*C); third, XpsN, as well as GspC, contains a coiled coil domain in its C-terminal section. Immunoblot analysis and nickel-nitrilotriacetic acid (Ni-NTA) affinity chromatography revealed that XpsN formed a stable complex with the C-terminal region of XpsD (residue 650-759), confirming the interaction between GspC and GspD (Lee *et al*., 2000). In addition to the interaction with XpsD, others studies also found that XpsN was involved in the formation of the XpsLM subcomplex (Lee *et al*. 2001; Tsai *et al*., 2002). Furthermore, residue 47 to 97 have been identified to play an important role in interacting with XpsL and XpsM, and the N-terminal 46 residues were shown to be important for maintaining the two IM proteins at normal levels as well as maintaining a stable association with the subcomplex (Lee *et al*., 2004). Since most T2SS contain both GspC and GspN, it is not clear what the relationship is between the two proteins or whether their functions overlap.

1.6 The outer membrane complex

GspD belongs to a large family of homologous proteins generically designated secretin. It is an OM protein required for the T2SS, type IV pilus biogenesis, type III protein secretion, filamentous bacteriophage extrusion and uptake of DNA (Genin and Boucher, 1994).

Therefore, secretins constitute a very important group of macromolecule transporters in the OM of Gram-negative bacteria. Some of the GspD homologues have been purified and characterized by electron microscopy. They form highly stable [heat and detergent sodium dodecyl sulphate (SDS)-resistant] large oligomeric rings in the OM, consisting of approximately 12-14 monomers with a central cavity that ranges from 50 to 100 Å in diameter that are occluded with a centrally located plug (Bitter *et al*., 1998; Nouwen *et al*., 1999, 2000; Chami *et al*., 2005). However, the regulation of the opening and closing of the central cavity and the components involved in this activity is not well studied. A recent study on the very C-terminal region of XcpP (GspC) of *P. aeruginosa* showed that either deletion or modification of this region results in increased levels of secreted proteins released to the extracellular environment, therefore it can be hypothesized that this region may contribute to regulation of the gating of the pore (Robert *et al*., 2005a). In addition, the exoprotein pullulanase of *K. oxytoca* has been suggested to be a regulator of the channel (Chami *et al*., 2005). In this study, the PulD polypeptide was found to be comprised of an N domain, which formed the walls of one of the chambers, and a trypsin-resistant C domain, which contributed to the outer chamber, the central disc, and the plug. The pullulanase may bind to the inner chamber which is proposed to constitute a docking site for the secreted proteins. As a result, the outer chamber allows displacement of the plug to open the channel and permit the exoprotein to be secreted.

Sequence comparisons have shown that the C-terminal domain is highly conserved in all members of the secretin family whereas the N-terminal domain is variable and only shows conservation within the different subfamilies (Genin and Boucher, 1994; Peabody *et al*., 2003). Limited proteolysis and protease protection experiments have shown that the conserved C-termini of XcpQ (GspD) and PilQ of *P. aeruginosa* and PulD of *k. oxytoca* are protease-resistant and remain a multimer after proteolysis. This domain contains several putative amphipathic transmembrane β-strands, suggesting that the C-terminal domain of GspD may be embedded in the OM and is likely to form the actual channel, while the N-terminal domain is probably exposed to the periplasmic space, where it facilitates interactions with other components of the secretion apparatus (Bitter *et al*., 1998, Brok *et al*., 1999; Nouwen *et al*., 2000). It has also been suggested that the C-terminal domain is responsible for OM insertion and multimerization, while the N-terminus may interact with exoproteins in the periplasmic space in addition to other T2SS components (Shevchik *et al*., 1997; Bouley *et al*., 2001).

Deletion mutations, gel filtration and ion exchange chromatography analysis revealed that two fragments, from residue 429 to 544 and from residue 544 to 759 in the C-terminal domain of XpsD were required for OM insertion and multimerization. This is because the WT XpsD protein could co-fractionate with XpsD (Δ29–428) or XpsD (Δ448–650) but not with XpsD (Δ74–303) or XpsD (Δ553–759) (Chen *et al*., 1996). Although the fragments from residue 429-544 and from residue 544-759 were partially contained in the XpsD (Δ448–650) protein, the mutant could neither form functional multimers by itself nor function in protein secretion. In addition, the XpsD (Δ74–303) mutant contained these two fragments, however, it only formed non-functional multimers. Another study showed that the N-terminus may interact with exoproteins in the periplasmic space in addition to other T2SS components (Shevchik *et al.*, 1997). *In vivo* co-immunoprecipitation and co-sedimentation in sucrose density gradients showed that PelB, a secreted protein, co-migrated with the OM fraction in the presence of OutD, and co- precipitation of the two proteins revealed that OutD bound to streptavidin–agarose in the presence of biotinylated PelB, suggesting that OutD interacts with PelB. The N-terminal region of OutD was required for the interaction with secreted proteins since a 50 amino acid N-terminal deletion of OutD prevented its interaction with PelB. The study also suggested that the N-terminal domain may gate the pore it is forming, and a modification of the structure of the channel was provoked by the interaction of the secreted proteins with OutD.

In addition to the two functions of the N and C termini described above, Guilvout *et al*. (1999) also suggested that both the N-terminal and C-terminal region of PulD were required for multimerization. Linker and deletion mutagenesis and gene fusions showed that the SDS-resistant multimer formation of the C domain strongly depended on N domain production in *trans*. In detail, insertion of 24 amino acids near or within the C-terminus abolished SDS-resistant multier formation, whereas insertions elsewhere had less effect on multimerization. However, the C-terminal domain did not form multimers unless part of the N-terminal region was produced in trans. Furthermore, the function of all of a group of insertion mutants of PulD was abolished, except one close to the C terminus of the protein. In addition, the highly unstable N domain did not form SDS-resistant multimers even in the presence of the C domain produced in *trans*. All these results suggested that the C-terminal domain is responsible for

multimer stability while the N domain contributes to multimer formation. Similar to the study of Guilvout *et al*. (1999), limited proteolysis and analysis of a three-dimensional model of the homomultimeric complex PulD identified a lower proportion of transmembrane β-structure of the trypsin resistant C domain than classical OM proteins, suggesting that only a small part of it is embedded within the OM (Chami *et al*., 2005). This result leads to a hypothesis that the centrally plugged channel formed by C domain penetrates both the peptidoglycan (PG) on the periplasmic side and the lipopolysaccharide (LPS) and capsule layers on the cell surface. Therefore, the basic core structure formed by the C-domain is not only required for stable mutimerization but also interaction with other envelope components such as LPS and PG.

Species specificity is another function in which GspD is involved. T2SS is highly specific and secretion of heterologous exoproteins is rarely observed despite strong conservation of this secretion pathway, even when they are expressed in closely related species, such as *E. chrysanthemi* and *E. carotovora* (Lindeberg *et al*., 1996), or *P. aeruginosa* and *P. alcaligenes* (de Groot *et al*., 2001). In *Erwinia*, GspE-N can be exchanged between the two different species, but GspC and GspD are not exchangeable, and these proteins have thus been suggested to be the gatekeepers of the T2SS (Lindeberg et al., 1996) and to confer specificity for substrate recognition (Bouley *et al*., 2001). Bouley *et al.* (2001) identified an N-terminal region of OutD important for secretion specificity by using complementation tests with chimeric constructs between $OutD_{Eca}$ and $OutD_{Ech}$. The results showed that the N-terminal region of OutD, including a linker segment between the N and C-terminal domains, is involved in secretion specificity in *E. chrysanthemi*. However, these results seem to be contradictory to a study by Guilvout *et al*. (1999) which indicated that substrate recognition did not require the N domain of PulD. This conclusion was based on complementation tests showing that chimeric constructs containing the N-terminal region of $OutD_{Ech}$ and the C-terminal part of the secretin PulD were able to complement a Δ*pulD* mutation. A recent study demonstrated that both C terminal and N-terminal domains of XcpQ of *P. alcaligenes* are involved in species specificity (Bitter *et al*., 2007). Although XcpP and XcpQ of *P. alcaligenes* could not substitute for their respective *P. aeruginosa* counterparts, these bacteria could secrete exoproteins of each other, indicating that species-specific recognition of exoproteins was not the reason for these complementation failures (de Groot *et al*., 2001). Furthermore, complementation occurred

when *P. alcaligenes xcpP* and *xcpQ* were expressed simultaneously in a *P. aeruginosa xcpPQ* deletion mutant on agar plates. Therefore, to map the region in the C-terminal domain (amino acid residue 326 to 606) of XcpQ of *P. alcaligenes* contributing to species specificity, Bitter *et al*. (2007) constructed chimeras between $xcpQ_{alc}$ and $xcpQ_{aer}$ secretins since expression of $xcpQ_{alc}$ in an *xcpQ* mutant of *P. aeruginosa* does not restore protein secretion via the T2SS. Specifically, chimeras contained variable N-terminal fragments of $XcpQ_{aer}$ and the complementing C-terminal domain of $XcpQ_{alc}$. The analysis showed that the elastase secretion defect of a chromosomal *xcp*Q mutant strain could be complemented efficiently with the F478 hybrid containing an N-terminal pre-$XcpQ_{aer}$ fragment consisting of 478 or more amino acid residues, whereas no complementation occurred in the fusions with an N-terminal pre-$XcpQ_{aer}$ fragment consisting of less than 331 amino acid residues. Moreover, secretion in the *P. aeruginosa xcpQ* mutant could be completely restored by a hybrid containing the same C-terminal segment of $XcpQ_{alc}$ that was present in hybrid F497 and another $XcpQ_{alc}$ segment extending from residue 68 up to residue 344. Thus it was concluded that the region in the C-terminus of $XcpQ_{aer}$ between amino acid residues 344 and 478 appears to contain an important determinant for species-specific function in *P. aeruginosa.* This study also suggested that the N-terminal 63 amino acid residues may contribute to this function. In addition to investigating the species-specific function of $XcpQ_{aer}$, the study also revealed that LPS had a role in the functioning of secretins. First, the C-terminal domain involved in the species specificity was probably in close contact with LPS as this region is located in the OM. Second, mutations affecting LPS structure had a negative effect on the endogenous secretin of *P. aeruginosa*, but a positive effect on the $XcpQ_{alc}$ secretin, indicating that there was a direct interaction between LPS and XcpQ. Third, both *P. alcaligenes* XcpQ and inactive hybrids functioned properly in *P. aeruginosa* under high cons. of divalent cations known to affect the structure of LPS. Therefore, changes in LPS structure influence the functioning of the protein transport channel in the secretin.

1.7 GspS, the pilotin for GspD

A number of studies have focused on how secretin inserts into the OM and assembles into an oligomeric ring. It has been found that some secretins contain an S domain at the C-terminal region that is the binding site for an OM-associated lipoprotein chaperone, GspS (termed

pilotin) (Daefler *et al*, 1997), which is specifically required to protect secretins from proteolysis and to direct its insertion to the OM (Hardie *et al*, 1996a, b; Daefler and Russel, 1998; Shevchik and Condemine, 1998). In the absence of PulS, PulD assembles in the IM and induces the phage shock response, resulting in the production of great amounts of PspA, a 26 kDa peripheral membrane protein (Hardie *et al*, 1996a, b; Guilvout *et al*., 2006). In addition, neither the PulS signal sequence, which protected PulD from cleavage, nor a periplasmic MalE-PulS hybrid protein facilitated the proper localization of PulD to the OM, suggesting that PulD and PulS interact with each other directly (Hardie *et al*., 1996b). A chimeric protein composed of bacteriophage f1 pIV and the C-terminal domain of PulD required properly localized PulS to support phage assembly, therefore the region of PulD required for protection by PulS was examined by analysis of the stability of a series of chimeric proteins composed of variable C-terminal segments of PulD fused to variable N-terminal segments of fl pIV (Daefler *et al*, 1997). The result showed that a hybrid lacking the C-terminal 65 amino acids of PulD could not be stabilized by PulS, indicating that this fragment was the PulS-binding site. Similar results were found in *E. chrysanthemi* by ligand-blotting experiments which showed that OutS did not bind to OutD lacking the C-terminal 62 and 328 amino acids, indicating that at least the 62 C-terminal amino acids of OutD are required for interaction with OutS (Shevchik and Condemine, 1998). Furthermore, the 62 C-terminal amino acids of OutD might only be involved in the stabilization of OutD while not contributing to its insertion to the OM in the presence of OutS because a hybrid composed of this fragment and the secreted pectate lyase PelD was only stabilized by OutS without OM insertion. The insertion of OutD in the OM might require other proteins. Guilvout *et al*.(2006) revealed that a PulD-CS (C and S domain) fragment was targeted to the OM via association with PulS. The same experiment further suggested that the regions of PulD which were responsible for its special requirements for extraction from the OM were completely determined by the C (and S) domains. This is because the PulS-bound PulD-CS in cell envelopes could only be extracted under conditions that also extracted PulD. The study also purified PulD-CShis from *E. coli* together with PulS by affinity chromotography, which was then treated with phenol. Dodecyl sulphate-polyacrylamide gel electorphoresis (SDS-PAGE) and Coomassie blue staining showed that the multimers disappeared after phenol treatment and generated a band which migrated faster than monomeric PulDhis and reacted with PulD antibodies, suggesting that PulD-CS formed PulD-like

multimers in the OM. However, PulS was not required for the formation of PulD multimers as PulD-CShis (a His tag inserted in the S-domain) formed multimers without PulS. To determine the role of PulS, the envelopes from a protease-deficient strain were centrifuged in floatation sucrose gradients, and immunoblotting of the resulting fractions after phenol-treatment revealed that PulD-CS and full-length PulD monomers predominantly inserted in the IM without PulS, suggesting that PulS prevents mislocalization of PulD-CS and PulD to the IM (Guilvout *et al*., 2006). However, the T2SS of some other bacteria do not have GspS pilotin; instead, secretin assembly requires other ancillary factors, such as ExeA and ExeB proteins in *A. hydrophila* (Ast *et al*, 2002) and the ExeB homolog OutB in *E. chrysanthemi* (Condemine and Shevchik, 2000). In addition, it was suggested that YaeT (the general OM insertion factor Omp85) in *Neisseria meningitides* may be involved in secretin assembly since it is required for porin assembly (Voulhoux *et al*, 2003; Bayan *et al*, 2006). However, Guilvout *et al*. (2006) suggested that multimerization and OM association of PulD could be YaeT-independent since PulD formed dodecamers in the IM without PulS, and thus do not contact the OM protein YaeT. This suggestion is confirmed by a recent study showing that PulD was resistant to extraction by either the detergent Sarkosyl and or by urea, and susceptible to trypsin digestion (Collin *et al*. 2007).

1.8 Isolation of *exe* genes of *A. hydrophila*

To study T2SS of *A. hydrophila*, a group of *exe* genes belonging to two operons have been isolated and analyzed in our lab. In previous studies of aerolysin secretion, Jiang and Howard (1991) isolated a number of Tn5-751 insertion mutants of *A. hydrophila* strain Ah65 using transposon mutagenesis, and analysis showed that these mutants were unable to secrete extracellular proteins. Furthermore, two of these mutants, including C5.84 and L1.97 were pleiotropic, essentially devoid of any of the major extracellular proteins normally secreted by the WT. However, immunoblot and cell fraction experiments revealed that these extracellular proteins were synthesized and accumulated in the periplasm, indicating that the genes inactivated by the transposon are important only for OM translocation of the proteins. In addition, the WT fragment corresponding to the L1.97 mutation could partially restore the mutation in C5.84, suggesting that these two genes or their products may interact with each other during OM translocation.

To identify mutant genes, a *Kpn*I 4.1 kb fragment which complemented the L1.97 mutant was isolated and sequenced (Jiang and Howard, 1992). Analysis showed that this fragment contained two complete genes, *exe*E and *exe*F. To identify the rest of the *exe* operon, Howard *et al*. (1993) and Howard unpublished results isolated and sequenced an additional ten genes which constituted *exe*C and *exe*D at the 5' end of the operon and *exe*G to *exe*N at the 3' end of the operon. Then Kanamycin (kan) resistance cassettes were inserted into three different regions of the operon by marker exchange mutagenesis, and analysis indicated that the extracellular proteins aerolysin and protease could not be secreted by any of these mutants and were instead accumulated in the periplasm. Moreover, immunoblot and cell fraction experiments showed that these mutants displayed altered membrane protein profiles. This phenotype is identical to that of the original Tn5-751 insertion mutant L1.97, indicating that the entire operon is required for extracellular secretion.

Another Tn5-751 insertion mutant, C5.84, isolated by Jiang and Howard (1991) displayed the same character as the mutant L1.97. To identify the genes involved, Jahagirdar and Howard (1994) isolated and sequenced a 3.5-kb fragment which complemented the C5.84 mutant. Subcloning followed by sequence analysis of this fragment revealed that this locus consists of an independent operon composed of two genes, *exe*A and *exe*B. Furthermore, complementation test showed that both genes were required to restore the mutant to normal extracellular secretion, and this result was further confirmed by marker exchange mutagenesis. In addition, in vitro expression and sequence analysis indicated that ExeA is a 60 kDa protein with a consensus ATP binding site, and ExeB is a 25 kDa basic protein. ExeB was later shown to bear sequence as well as topological similarity to TonB by Howard *et al*. (1996). Both ExeA and ExeB fractionate with the IM, and are anchored to the IM by a single hydrophobic domain, with large domains localized in the periplasm (Jahagirdar and Howard, 1994; Howard *et al*., 1996).

1.9 GspA and GspB, secretin assembly factors in the T2SS of *A. hydrophila*

Based on the previous results, it can be concluded that ExeA and ExeB, the components of the smaller *exe* operon of *A. hydrophila*, are two additional proteins required for type II secretion of aerolysin and other extracellular proteins. ExeA and ExeB homologues in T2SS have been found in many bacterial species, including *V. cholerae*, *Shewanella putrefaciens*, *Geobacter*

sulfurreducens, and *E. coli* K-12 (Francetic and Pugsley, 1996; Heidelberg *et al*., 2000; Francetic *et al*., 2000; Sandkvist, 2001a). OutB of *E. chrysanthemi* is also an essential component for efficient secretion in T2SS, although no OutA has been identified (Condemine and Shevchik, 2000).

A series of experiments were done by Howard *et al*. (1996) to more specially examine the role of ExeA and ExeB. First, site specific mutations of highly conserved amino acids of the ATP-binding site in ExeA showed that the secretion efficiency of the toxin aerolysin was compromised, suggesting that the consensus ATP-binding site is important to the function of ExeA. In addition, an ExeA/ExeB complex was first suggested by examination of the stability of ExeB overexpressed in the presence and absence of ExeA. Specifically, ExeB was protected from proteolytic digestion in the presence of ExeA, while degraded when synthesized without ExeA. Based on these results, it can be hypothesized that the role of ExeA may be to provide energy by ATP hydrolysis. This hypothesis was further confirmed by a study of the energetic requirements for extracellular secretion. Letellier *et al*. (1997) and Wong and Buckley (1989) showed that both ATP and protonmotive force are required for secretion across the OM.

Schoenhofen *et al*. (1998) demonstrated that ExeA formed a stable complex with ExeB in the IM via cross-linking and immunoprecipitation. Pulse-chase immunoprecipitation with ExeA anti-serum showed that synthesis of ExeA in the absence of ExeB resulted in rapid degradation of ExeA. In addition, both ExeA and ExeB could be cross-linked into an 85 kDa complex by the cross-linking reagent Bis [sulfosuccinimidyl] suberate, and the cross-linked samples could then be co-immunoprecipitated with ExeA and ExeB anti-serum, confirming the presence of both ExeA and ExeB in the same 85 kDa complex. ExeA was found to cross-link into a 120 kDa homodimer as well. In addition, Schoenhofen *et al*. (2005) examined the structure of the ExeAB complex via gel filtration analysis and suggested that ExeA dimerized and formed a very large complex with ExeB which might be comprised of three dimers of each protein and that the soluble N-terminal domain of ExeA did not contribute to ExeA mutimerization.

Sequence analysis revealed that ExeA contains three motifs commonly found in kinases. One is a typical Walker A consensus motif or kinase-1a motif, A/GX_4GKS/T (50-GEVGTGKT-57),

involved in ATP- binding and phosphate-binding and transfer (Walker *et al*., 1982; Traut, 1994); and the other two belong to the Walker B motif 126-VVLVD-130, and the Mg^{2+} binding kinase-2a motifs (105-KLLFD-109) and kinase-3a motifs (228-GGIPR-232). To examine the role of the potential ATP-binding site in ExeA, Schoenhofen *et al*. (1998) determined the stability of mutations in conserved ATP binding and catalytic residues including K56R of kinase-1a motif and G229 of kinase-3a motif with pulse-chase immunoprecipitation. The results showed that mutations in the consensus ATP-binding site of ExeA abolish or decrease the rate of protein secretion, suggesting that secretion required ATP hydrolysis. Schoenhofen *et al*. (2005) further demonstrated that the purified cytoplasmic domain of ExeA (cytExeA), including 278 N-terminal residues, displayed Mg^{2+} ATPase activity. Specifically, the N-terminal domain of ExeA (cytExeA) with a C-terminal hexahistidine tag containing the putative ATP binding/hydrolysis motifs was overproduced in *E. coli* and purified by metal chelate affinity and anion-exchange chromatography. The malachite green dye-binding assay showed that purified cytExeA displayed ATPase activity.

In addition to forming an IM complex with ExeA, ExeB also shows structural and some sequence similarity to TonB; this similarity is also found between GspC and TonB (Howard *et al*., 1996). Moreover, GspB as well as GspC/N have been proposed to interact directly with GspD in a TonB-like fashion to open the secretin channel (Howard *et al*., 1996; Ast *et al*., 2002; Filloux, 2004). TonB is an integral IM protein that translocates various ligands inwardly across the OM by opening gated channel proteins in the OM to which the ligands bind. This process is dependent on the electrochemical gradient across the IM. OutB also has been suggested to play an important role in promoting OM insertion and stabilization of the secretin oligomer (Condemine and Shevchik, 2000). Specifically, analysis of OutB showed that a mutation in OutB can be suppressed by overproduction of OutD, suggesting that OutB interacts with OutD (Condemine and Shevchik, 2000). Furthermore, OutB can be stabilized in the presence of OutD and OutD expressed in *E. coli* can be protected from proteolytic degradation by the coexpression of a fragment of OutB without the N-terminal TMS. These results were further confirmed by cross-linking experiments using formaldehyde.

The studies described above indicate the ExeAB complex is very important in T2SS protein secretion. Therefore, a series of experiments has been performed to further characterize the role

of the ExeAB complex in the T2SS of *A. hydrophila* (Ast *et al*., 2002). Complementation tests showed that the secretion deficiency of an *exe*AB mutant could be overcame by overexpression of ExeD. However, *exeC-N* operon expression analysis in *exeAB* mutants showed that the ExeAB complex did not regulate the expression or stability of the components of the *exe*C-N operon, and thus did not cause secretion deficiency through a regulatory effect. Immunoblot analysis demonstrated that the ExeD secretin was not able to multimerize and remained in the IM as a monomer in the absence of ExeAB. Furthermore, expression of ExeAB from a plasmid in an *exe*AB mutant strain resulted in an increased amount of ExeD multimer and also restored aerolysin secretion. Pulse-chase radiolabelling experiments also indicated that induction of ExeAB complexes could promote the assembly of previously synthesized labelled ExeD monomer into the multimer. All these results suggest that the ExeAB complex is required for the assembly and/or multimerization of the ExeD secretin in the OM, possibly using energy derived from ATP hydrolysis. The function of the ExeAB complex in secretin assembly was further examined by Howard *et al*. (2006). First, a series of two-codon insertion mutants of ExeA was constructed and aerolysin secretion assays showed that amino acid 495, located within a putative PG binding motif in the peri-ExeA, was required for ExeD secretin assembly while not involved in ExeAB complex formation. That is, the mutant lost the ability to assemble the ExeD secretin or secrete aerolysin, while retaining the ability to form a complex with ExeB. This secretion negative phenotype also occurred for substitution mutants of three highly conserved amino acids in the PG binding motif, suggesting that the C-terminal PG binding domain of ExeA was critical to its function in secretin assembly. Furthermore, *in vivo* cross-linking with 3, 3′-Dithiobis (sulfosuccinimidylpropionate) showed that WT ExeA could be cross-linked to PG, whereas the three substitution mutants of ExeA could not, suggesting that there was an interaction between ExeA and PG. All these experiments suggest that PG binding to ExeA is required for the function of the ExeAB complex in ExeD secretin assembly. In addition, the *in vivo* cross-linking analysis also showed that ExeB and ExeC interact with PG in the presence of ExeA, suggesting that there are interactions between ExeA and ExeC as well as ExeA and ExeB. All of these results suggest that there may be a complex that involves ExeA, B, C, D and PG during assembly of the ExeD secretin.

1.10 Research objective of this study

As described above, many studies have focused on the function of the components of three subassemblies, including the IM complex, the OM complex and the periplasmic pseudopilus in the T2SS. However, the IM GspA and GspB proteins are two ancillary factors for secretin GspD assembly and/or transport that occur in some bacteria such as *A. hydrophila*, and the role of these two proteins in the T2SS is still not clear. Previous studies have suggested that GspA and GspB play important roles in promoting OM insertion and stabilization of secretin multimers (Ast *et al*., 2002; Howard *et al*., 2006). Howard *et al*. (2006) also revealed that PG can be cross-linked to ExeA and that ExeB and ExeC can be cross-linked to PG in the presence of ExeA, suggesting that there are interactions between ExeA and ExeC as well as ExeA and ExeB. However, the characterization of GspA and GspB is still not complete and how these two proteins link to other components of the T2SS is not yet clear. Therefore, the research objective of this project was to identify and characterize protein-protein interactions between GspA, GspB and other components of the T2SS using *A. hydrophila* as the model bacterium.

The yeast two-hybrid system was used as the experimental approach to identify the protein-protein interactions. Although this method has quite a few advantages compared with traditional methods, it contains several limitations (Yang *et al*., 1995; Phizicky and Fields, 1995; Luban and Goff, 1995). One of the disadvantages of this method is that highly hydrophobic membrane domains may cause insolubility or instability in yeast (Phizicky and Fields, 1995; Luban and Goff, 1995; McAlister-Henn *et al*., 1999). Therefore, the periplasmic domains of Exe proteins were assayed for interactions. The protein domains selected for the yeast two-hybrid assay with ExeA and ExeB were thus based on the topology revealed by previous studies.

It has been demonstrated that both ExeA and ExeB are bitopic IM proteins. The topological orientation of ExeA (60 kDa) and ExeB (25 kDa) was determined by Howard *et al*. (1996) with the alkaline phosphatase reporter system. The results showed that an N-terminal domain of 31 kDa of ExeA carried the consensus ATP-binding site exposed to the cytoplasm, while a C-terminal 28 kDa domain extended to the periplasmic space, indicating that ExeA is nearly evenly distributed between cytoplasm and periplasm. For ExeB, only a small N-terminal

domain located in the cytoplasm while a large 18 kDa C-terminal domain extended to the periplasm, suggesting that the majority of ExeB remains in the periplasm. Although not well studied in *A. hydrophila*, the topology of the components of the *gsp*C-N operon in other bacteria has been studied. It has been demonstrated that the OM protein GspD contains two structurally distinct C-terminal and N-terminal domains, with the N-terminal domain exposed to the periplasm where it interacts with other components of the secretion apparatus while the C-terminal region containing several putative amphipathic transmembrane β-strands may be embedded in the OM and is likely to form the actual channel (Bitter *et al*., 1998, Brok *et al*., 1999; Nouwen *et al*., 2000). Except for GspD, the other T2SS components are all IM proteins. GspC is a bitopic IM protein which consists of a short N-terminal cytoplasmic sequence, a single TMS, and a large hydrophilic periplasmic region (Bleves *et al.*, 1996; Thomas *et al*., 1997; Gérard-Vincent, *et al*., 2002; Robert *et al*., 2005a; Korotkov *et al*., 2006). GspN is a homolog of GspC in many species, and thus probably shares the same topology. Of the IM complex components GspE, F, L and M, GspE appears to be associated with the IM on the cytoplasmic side (Sandkvist 1995, 2001a) and thus can not be used for the interaction test in the periplasm. GspL contains a single TM helix with a large cytoplasmic domain and a smaller periplasmic region (Bleves et al., 1996; Ball *et al*., 1999; Sandkvist 2000); GspM is a small IM protein with a short segment residing in the cytoplasm whereas a larger portion extends into the periplasm (Bleves *et al*., 1996; Sandkvist 2000). GspF is a polytopic integral cytoplasmic protein crossing the IM three times with a small loop in the periplasm and two large segments extending into the cytoplasm (Thomas *et al*., 1997). Although the pseudopilin proteins G, H, I, J and K are found associated with both membranes after fractionation and part of them are in the periplasmic space (Sandkvist, 2001a), they may act as a piston and therefore have less possibility to interact with ExeAB than other proteins. Therefore, the periplasmic domains of proteins C, D, L, M and N were chosen as the prey for protein-protein interaction studies with the baits ExeA and ExeB.

1.11 Yeast two-hybrid experimental strategies

The Gal4 yeast two-hybrid system was employed to identify protein-protein interactions involving Exe proteins. The yeast two-hybrid system was first described by Stan Fields in 1989 (Fields and Song, 1989). It is a genetic method used to identify and analyze protein-protein

interactions via transcriptional activity in vivo. One of the commonly used two-hybrid systems is derived from the yeast Gal4 protein. The intact yeast Gal4 protein is a transcriptional activator which consists of two domains: an N-terminal domain which interacts with promoters by binding to upstream activation sequences; and a C-terminal domain which interacts with polymerase and therefore is necessary to activate transcription. The system is based on the observation that the two domains of the activator need not be covalently linked and can be brought together by the interaction of any two fusion protein partners to reconstitute a transcriptional activator. The application of this system requires two hybrid proteins to be constructed: one hybrid consists of the Gal4 DNA binding domain fused to a known protein X, which is termed the bait; another hybrid consists of the Gal4 activating domain fused to a test protein Y or proteins derived from genomic or cDNA libraries which are termed the prey. If binding occurs between the prey and the bait, transcriptional activity will be restored and will produce normal Gal4 activity. This can be detected by expression of reporter genes. The most commonly used reporter genes in the Gal4 system are *lac*Z and HIS3, which are inserted in the yeast genomic DNA immediately after the GAL promoter, so that if binding occurs, LacZ and His3 are produced.

The vectors to be used for the yeast two-hybrid system are pGBT9 (the Gal4 DNA-binding domain vector or the bait vector) and pGAD424 (the Gal4 activating domain vector or the prey vector) (Bartei *et al*., 1993a). One major problem in performing the yeast two-hybrid system is the elimination of false positives, clones that cause the activation of reporter genes, but not as a result of protein-protein interaction between the bait and the prey. False positives occur frequently in most host strains, such as Y190 and Y153 (Bartei *et al*., 1993a, b). In addition all these strains use a single promoter element to drive the transcription of the individual reporter gene, thus increasing the growth of the background colonies because many false positives are specific to the promoter element. Promoter-specific false positives are even more difficult to eliminate due to the utilization of the single promoter element (James *et al*., 1996). In this project, an improved yeast strain, PJ69-4A was employed in the two-hybrid screens. This host strain was first constructed and described by James, Halladay and Craig in 1996 (James *et al*., 1996). PJ69-4A contains three different reporter genes, including HIS3, ADE2 and *lac*Z, each under control of an appropriate inducible promoter, they are Gal1, Gal2 and Gal7, which can be induced to high levels (James *et al*., 1996). These promoters respond to the same inducer

(Gal4) and share a minimum of sequence identity. As a result, the ability to discriminate between false positives and real interactions is improved. Among these three reporter genes, HIS3 and *lacZ* have been shown to be extremely sensitive to weak or transient interactions, while ADE2 is the most stringent and provides a low background of false positives.

2. MATERIALS AND METHODS

2.1 Strains and plasmids

The bacterial and yeast strains used in this study are listed in Table 2-1. The cloning vectors of bacteria and yeast, and recombinant plasmids are listed in Table 2-2A and B.

2.2 Polymerase chain reaction

The PCR (polymerase chain reaction) was routinely used to amplify DNA fragments for the purposes of cloning, mutagenesis and co-purification. A PTC-100 programmable thermal controller from MJ Research Incorporation (Inc.) (Watertown, MA, USA) and from Mandel Scientific (England) were used to carry out routine amplifications. Annealing temperature (temp) gradient PCRs were performed by a PCR machine of Biometra obtained from Montreal Biotech Inc. (Montreal, Canada).

To construct the bait and prey plasmids for the yeast two-hybrid assay, the Ah65 chromosome was used as the template for amplifying the periplasmic domain of *exe*A, B, C, D, L, M and N (Table 2-3). Chromosomal DNA was isolated using the following method. The strain Ah65 was grown on LB-Agar plate containing 2.5 μg/ml chloramphenicol (Cm) at 30 ºC for 3 days. A single colony was picked and resuspended in 500 μl sterile H_2O, and then the suspension was heated at 95 ºC for 10 min and vortexed to lyse the cells. PCR reaction mixtures were created based on the guidelines in the instruction manual for *Pfx* DNA polymerase (Invitrogen). Specifically, 1 μl of the 500 μl Ah65 chromosomal DNA template was used in a 50 μl reaction with a buffer containing 1 × *Pfx* amplification buffer, 1-2 mM $MgSO_4$, deoxyribonucleotide triphosphate (dNTPs) at a final concentration of 300 μM for each dNTP, 0.4 μM of oligonucleotide primer (Table 2-4), and 1.25 unit *Pfx* DNA polymerase. The program was started with 1 cycle of denaturation (95 ºC, 2 min), then five cycles of denaturation (95 ºC, 1 min), annealing (the lower temperature listed in Table 2-3) and extension (72 ºC, 1 min), followed by twenty five cycles of the same conditions except for the annealing temperature used (the higher temperature listed in Table 2-3).

TABLE 2-1. Bacterial and yeast strains

Strain	Genotype/Phenotype	Source/Reference
A. hydrophila		
Ah65	WT	This laboratory
E. coli		
XL1-Blue	*recA1 endA1 gyrA96 thi-1 hsdR17 supE44 relA1 lac* [F′ *proAB lacI*qZΔ*M15* Tn*10* (Tetr)].	Stratagene
BL21(DE3)	F^- *ompT hsdS*$_B$ (r_B^- m_B^-) *gal dcm* (DE3)	Novagen
Yeast		
pJ69-4A	*MATa trp1-901 leu2-3,112 ura3-52 his3-200 gal4D gal80D LYS2::GAL1-HIS3 GAL2-ADE2 met2::GAL7-lacZ*	Dr. Wei Xiao

TABLE 2-2A. Bacterial cloning vectors and recombinant plasmids

Plasmid	Description	Source/Reference
pET30a	A cloning vector for expression of recombinant proteins in *E. coli*; carries an N-terminal His•Tag	Novagen
pET47b	A cloning vector for expression of recombinant proteins in *E. coli*; carries an N-terminal His•Tag coding sequence	Novagen
pCDFDuet	An coexpression vector for two target genes; high-level protein expression;	Novagen
pRJ31-1	Encodes *exe*AB sequence	Dr. Howard
pVA1.3.1	Encodes *exe*CD sequence carrying a two-codon insertion mutant at amino acid residue 58	Vivan Ast
pVA23.6.2	Encodes *exe*CD sequence carrying a two-codon insertion mutant at amino acid residue 127	Vivan Ast
pVA2.3.2	Encodes *exe*CD sequence carrying a two-codon insertion mutant at amino acid residue 137	Vivan Ast
pVA24.7.1	Encodes *exe*CD sequence carrying a two-codon insertion mutant at amino acid residue 182	Vivan Ast
pVA29.2.2	Encodes *exe*CD sequence carrying a two-codon insertion mutant at amino acid residue 201	Vivan Ast
pVA6.2.1	Encodes *exe*CD sequence carrying a two-codon insertion mutant at amino acid residue 247	Vivan Ast
pVA8.1.1	Encodes *exe*CD sequence carrying a two-codon insertion mutant at amino acid residue 256	Vivan Ast
pVA36.1.1	Encodes *exe*CD sequence carrying a two-codon insertion mutant at amino acid residue 269	Vivan Ast

TABLE 2-2B. Yeast cloning vectors

Plasmid	Description	Source/Reference
pGBT9	A shuttle vector that replicates autonomously in both *E. coli* and *S. cerevisiae*; carries the *bla* gene [for ampicillin (Amp) resistance in *E. coli*] and the *TRP1* nutritional marker that allow yeast auxotrophs carrying pGBT9 to grow on limiting synthetic medium lacking Tryptophan (Trp); generates a hybrid protein that contains the sequence of the Gal4 DNA-binding domain (Gal_{BD}).	Dr. Xiao
pGAD424	A shuttle vector that replicates autonomously in both *E. coli* and *S. cerevisiae*; carries the *bla* gene (for Amp resistance in *E. coli*) and the *LEU2* nutritional marker that allow yeast auxotrophs carrying pGAD424 to grow on limiting synthetic medium lacking Leucine (Leu); generates a hybrid protein that contains the sequence of the Gal4 DNA- activation domain (Gal_{AD}).	Dr. Xiao

2-3. Amplification of fragments for the bait and prey plasmids construction

Target DNA	$MgSO_4$ Conc.	Annealing Temp.	Resulting clone
*exe*A	2 mM	64-68 °C	pGBT9-*exe*A pGAD424-*exe*A
*exe*B	1 mM	64-68 °C	pGBT9-*exe*B pGAD424-*exe*B
*exe*C	1 mM	54-58 °C	pGBT9-*exe*C pGAD424-*exe*C
*exe*D	2 mM	64-68 °C	pGBT9-*exe*D pGAD424-*exe*D
*exe*L	1 mM	45-55 °C	pGAD424-*exe*L
*exe*M	2 mM	64-68 °C	pGAD424-*exe*M
*exe*N	1 mM	58-62 °C	pGAD424-*exe*N

Note:

Annealing tempreatures were obtained by oligo design and analysis tools from IDT integrated DNA Tecnologies. Each of the higher tempreature was designed based on the GC content of the whole oligo, while each of the lower tempreature was designed based on the GC content of the oligo without flanking region.

TABLE 2-4. PCR primers for amplification of *A. hydrophila* DNA

Template	Target DNA	Primers (5'-3')	Resulting clone
Ah65 chromosome	*exe*A	u, e: ATCCAGAATTCCAGTTCTTCGGCTTCTTCCC d, b: ATACTGGATCCTCAGGAAGCCTCCTCCGAC	pGBT9-*exe*A pGAD424- *exe*A
Ah65 chromosome	*exe*B	u, e: TTAAAGAATTCAACCGCCCCATCGAGAAGAC d,b: TTAATGGATCCTCAGCCGCGCCAGTCCTG	pGBT9-*exe*B pGAD424- *exe*B
Ah65 chromosome	*exe*C	u, e: TTAAAGAATTCCGTCTGCTGGATCTCGGC d, b: TTAAAGGATCCTTATTCTGACAAGCCGACATAAAC	pGBT9-*exe*C pGAD424- *exe*C
Ah65 chromosome	*exe*D	u, e: TTAATGAATTCACCGAGTATTCTGCCAGCTTC d, b: TTAATGGATCCTCACAGTACCTGGGCGCGG	pGBT9-*exe*D pGAD424- *exe*D
Ah65 chromosome	*exe*L	u, e: TTAATGAATTCCAGCTGGCGGAGCAGG d, b: TTAATGGATCCTCAACCTTGCCCTCTGTGC	pGBT9-*exe*L pGAD424- *exe*L
Ah65 chromosome	*exe*M	u, e: TTAATGAATTCGCCAACCGCATCGCCG d, b: TTAATGGATCCTCATTGGGGACGGCTCAACTG	pGBT9-*exe*M pGAD424- *exe*M
Ah65 chromosome	*exe*N	u, e: TTAAAGAATTCAACCTGGTGCAGCTGGAAG d, bg: TTAATAGATCTTTAAATCCGGCCCTGATAGCG	pGBT9-*exe*N pGAD424- *exe*N
pGBT9-ExeD	*exe*D:Δ121-355	u, e: TTAATGAATTCACCGAGTATTCTGCCAGCTTC d, b: TTAATGGATCCTTAGCCCGGGTTGGTCTCAT	pGBT9-*exe*DΔ121-355
pGBT9-ExeD	*exe*D:Δ26-120	u, e: TAGCTGAATTCATAGGCGACGAGATGGTGACC d, b: TTAATGGATCCTCACAGTACCTGGGCGCGG	pGBT9-*exe*DΔ26-120
pGBT9-ExeD	*exe*D:Δ201-355	u, e: TTAATGAATTCACCGAGTATTCTGCCAGCTTC d, b: ATAATGGATCCTTAGGCATATTTCAGCTTGATGAT	pGBT9-*exe*DΔ201-355 pGAD424-*exe*D Δ201-355
pGBT9-ExeD	*exe*D:Δ26-200	u, e: AATATGAATTCTCCGCCGGCGAGATGGT d, b: TTAATGGATCCTCACAGTACCTGGGCGCGG	pGBT9-*exe*DΔ26-200 pGAD424-*exe*D Δ26-200
pGBT9-ExeD	*exe*D:Δ140-355	u, e: TTAATGAATTCACCGAGTATTCTGCCAGCTTC d, b: AATATGGATCCTTATTCGCGCACCGAGACGTT	pGBT9-*exe*D:Δ140-355 pGAD424-*exe*D Δ140-355

Template	Target DNA	Primers (5'-3')	Resulting clone
pGBT9-ExeD	*exe*D:Δ26-139, Δ257-355	u, e: ATATAGAATTCCTGGCGCCTCTGCTGCG d, b: ATATAGGATCCTTACACCATCTGTATGATGCGGGC	pGBT9-*exe*D:Δ26-139, Δ257-355 pGAD424-*exe*D:Δ26-139, Δ257-355
pGBT9-ExeD	*exe*D:Δ26-256	u, e: ATATAGAATTCCGCCAGCTCGATCGGGATCTG d, b: TTAATGGATCCTCACAGTACCTGGGCGCGG	pGBT9-*exe*D:Δ26-256 pGAD424-*exe*D:Δ26-256
pRJ31-1	*exe*A	u, e: CATATGCACCATCATCATCATCATCAGTTCTTCGGCTTCTTCCCC d, x: CTCGAGTCAGGAAGCCTCCTCCGACAATGTG	pET30- *exe*A
pRJ31-1	*exe*B	u, e: ATATGCACCATCATCATCATCATAACAACCGCCCCATCGAGAAG d, x: CTCGAGAAGGGGAGCTCTCAGGCTCC	pET30- *exe*B
pGBT9-exeC	*exe*C	u, s: TTAAACCGCGGCTCGTCTGCTGGATCTC d, x: AATTTCTCGAGTTATTCTGACAAGCCGACATAAAC	pET47-ExeC
pGBT9-exeD	*exe*D	u, s: TTAAACCGCGGCTACCGAGTATTCTGCCAGCTTC d, x: TTAATCTCGAGTTACAGTACCTGGGCGCGGCGGAT	pET47-ExeD
pGBT9-exeA	*exe*A	u, n: ATCCACATATGCAGTTCTTCGGCTTCTTCCC d, x: ATACTCTCGAGGGAAGCCTCCTCCGACAATG	pCDFDuet-*exe*A
pGAD424-exeB	*exe*B	u, n: TTAAACATATGAACCGCCCCATCGAGAAGAC d, x: TTAATCTCGAGGCCGCGCCAGTCCTGCAG	pCDFDuet-*exe*B
pGBT9-exeC	*exe*C	u, n: TTAAACATATGCGTCTGCTGGATCTCGGC d, x: ATATTCTCGAGTTCTGACAAGCCGACATAAAC	pCDFDuet-*exe*C
pGBT9-exeD	*exe*D	u, n: TTAATCATATGACCGAGTATTCTGCCAGCTTC d, x: TTAATCTCGAGCAGTACCTGGGCGCGG	pCDFDuet-*exe*D

u- upstream primer; d- downstream primer; e-primer contains a *Eco*RI site; b-primer contains a *Bam*HI site;
bg-primer contains a *Bgl*II site; s-primer contains a *Sac*II site; x-primer contains a *Xho*I site; n-primer contains a *Nde*I site

To construct the bait and prey plasmids containing the *exe*D two-codon insertion mutations, the recombinant plasmids carrying the mutations were used as the templates for amplifying the eight *exe*D mutants 1.3, 23.6, 2.3, 24.7, 29.2, 6.2, 8.1 and 36.1 (Table 2-5). The oligonucleotide primer used here is the same as the one use for amplifying *exe*D (WT) (Table 2-4). PCR reaction mixtures were made according to the guidelines for *Pfu* DNA polymerase (Fermentas). In more detail, 1 μl of 0.2-1 μg/μl plasmid template was used in a 50 μl reaction with a buffer containing 10 × *Pfu* buffer with $MgSO_4$, dNTPs at a final concentration of 300 μM for each dNTP, 0.4 μM of oligonucleotide primer, and 1.25 units *Pfu* DNA polymerase. The PCR program was the same as described above, and the annealing temperature was the same as that used for amplifying *exe*D (64-68 ºC). The program was started with 1 cycle of denaturation (95 ºC, 2 min), then five cycles of denaturation (95 ºC, 1 min), annealing (64 ºC) and extension (72 ºC, 1 min), followed by twenty five cycles of the same conditions except for the annealing temperature used (68 ºC).

The target DNAs for cloning of the ExeD deletion mutants (Table 2-6A) were amplified based on the guidelines for Phusion Hot Start DNA polymerase (Finnzymes). In detail, 0.1 μl of 0.2-1 μg/μl purified plasmid pGBT9-*exe*D obtained from a miniprep was used as the template in a 10 μl reaction with a buffer including Phusion HF reaction buffer containing 1.5 mM $MgCl_2$, dNTPs at a final concentration of 200 μM for each dNTP, 0.6 μM of oligonucleotide primer (Table 2-4), 0.1 μl of Phusion Hot Start DNA polymerase. For the PCR program, an annealing temperature gradient was used as shown in Table 2-6B. The program started with 1 cycle of denaturation (98 ºC, 2 min), followed by four cycles of denaturation (98 ºC, 15 s), annealing (Low) (30 s) and extension (72 ºC, 30 s), and 25 cycles of denaturation (98 ºC, 15 s), annealing (High) (30 s) and extension (72 ºC, 30 s), and finally an extension of 72 ºC for 5 min.

To construct the bait and the prey for co-purification test, the purified plasmids constructed in this study were used as the template (Table 2-7), and PCR reaction mixtures were created according to the guidelines for *Pfu* DNA polymerase (Fermentas). In more detail, 1 μl of 0.2-1 μg/μl plasmid template was used in a 50 μl reaction with a buffer containing 10 × *Pfu* buffer with $MgSO_4$, dNTPs at a final concentration of 300 μM for each dNTP, 0.5 μM of oligonucleotide primer, 1.25 units *Pfu* DNA polymerase. For the PCR program, all the steps were as described above except that the annealing temperature was 55-60 ºC. For pET30-*exe*A

TABLE 2-5. Amplification of fragments for two-codon insertion mutants of peri-*exe*D

Target DNA	Template	Annealing Temp.	Resulting clone
*exe*D (1.3.1)	pVA1.3.1	64-68 ºC	pGBT9-*exe*D (1.3.1) pGAD424-*exe*D (1.3.1)
*exe*D (23.6.2)	pVA23.6.2	64-68 ºC	pGBT9-*exe*D (23.6.2) pGAD424-*exe*D (23.6.2)
*exe*D (2.3.2)	pVA2.3.2	64-68 ºC	pGBT9-*exe*D (2.3.2) pGAD424-*exe*D (2.3.2)
*exe*D (24.7.1)	pVA24.7.1	64-68 ºC	pGBT9-*exe*D (24.7.1) pGAD424-*exe*D (24.7.1)
*exe*D (29.2.2)	pVA29.2.2	64-68 ºC	pGBT9-*exe*D (29.2.2) pGAD424-*exe*D (29.2.2)
*exe*D (6.2.1)	pVA6.2.1	64-68 ºC	pGBT9-*exe*D (6.2.1) pGAD424-*exe*D (6.2.1)
*exe*D (8.1.1)	pVA8.1.1	64-68 ºC	pGBT9-*exe*D (8.1.1) pGAD424-*exe*D (8.1.1)
*exe*D (36.1.1)	pVA36.1.1	64-68 ºC	pGBT9-*exe*D (36.1.1) pGAD424-*exe*D (36.1.1)

TABLE 2-6A. Amplification of fragments for constructing the *exe*D deletion mutants

Fragments	ExeD deletion mutants
*exe*D:Δ121-355	pGBT9-*exe*D:Δ121-355
*exe*D:Δ26-120	pGBT9-*exe*D:Δ26-120
*exe*D:Δ201-355	pGBT9-*exe*D:Δ201-355 pGAD424-*exe*D Δ201-355
*exe*D:Δ26-200	pGBT9-*exe*D:Δ26-200 pGAD424-*exe*D:Δ26-200
*exe*D:Δ140-355	pGBT9-*exe*D:Δ140-355 pGAD424-*exe*D:Δ140-355
*exe*D:Δ26-139, Δ257-355	pGBT9-*exe*D:Δ26-139, Δ257-355 pGAD424-*exe*D:Δ26-139, Δ257-355
*exe*D:Δ26-256	pGBT9-*exe*D:Δ26-256 pGAD424-*exe*D:Δ26-256

TABLE 2-6B. Annealing temperature gradient of PCR for amplification of the *exe*D deletion mutant fragments

	1	2	3	4	5	6
Low	55.5 ºC	56.9 ºC	60.3 ºC	63.9 ºC	67.4 ºC	70.1 ºC
High	60.5 ºC	61.9 ºC	65.3 ºC	68.9 ºC	72.4 ºC	75.1 ºC

TABLE 2-7. Amplification of fragments for co-purification expression vectors

Target DNA	Template	Annealing Temp.	Resulting clone
*exe*A	pRJ31-1	55 ºC	pET30-*exe*A
*exe*B	pRJ31-1	55 ºC	pET30-*exe*B
*exe*C	pGBT9-*exe*C	55-60 ºC	pET47-*exe*C
*exe*D	pGAD424-*exe*D	55-60 ºC	pET47-*exe*D
*exe*A	pGBT9-*exe*A	55-60 ºC	pCDFDuet-*exe*A
*exe*B	pGAD424-*exe*B	55-60 ºC	pCDFDuet-*exe*B
*exe*C	pGBT9-*exe*C	55-60 ºC	pCDFDuet-*exe*C
*exe*D	pGBT9-*exe*D	55-60 ºC	pCDFDuet-*exe*D

and pET30-*exe*B, diluted plasmid pRJ31-1 was used as the template for amplifying the periplasmic domains of *exe*A and *exe*B. The PCR mixture was the same as for the other reactions except that 0.4 μM of oligonucleotide primer and 2.5 units of *Pfu* DNA polymerase were used. The program started with 1 cycle of denaturing (95 ºC, 2 min), then twenty seven cycles of denaturation (95 ºC, 1 min), annealing (55 ºC, 1 min) and extension (72 ºC, 1 min), followed by 72 ºC, 3 min.

The PCR fragments were visualized by 1.2% agarose gel electrophoresis as described in 2.4. Following confirmation that the PCR products had the expected size, the rest of the PCR reaction was purified following 1.2% agarose gel electrophoresis, as described in 2.4.

2.3 Restriction digestion and ligation

All enzymes used in digestion including *Eco*RI, *Bam*HI, *Bgl*II, *Msc*I, *Nde*I, *Xho*I and *Sac*II were obtained from New England Biolabs (Pickering, Ontario, Canada), except that *Aar*I was obtained from Fermentas (Burlington, Ontario, Canada). 5-10 units of enzyme were used in a 40 μl reaction. After 2 h incubation at 37 ºC, the resulting digest was purified by QIAquick PCR Purification Kit as described in 2.4. The purified DNA including the digested PCR fragment and the digested vector were then ready for ligation.

T4 DNA ligase and 5 × T4 DNA ligase buffer (Invitrogen, Canada) or T4 DNA ligase and 10 × T4 DNA ligase buffer (New England Biolabs) was used for ligation. The ratio of the vector and the DNA insert ranged from 1:4 (1-3 μg/μl) to1:8 (0.2-1 μg/μl) depending on the concentration of DNA. 0.5-1.0 μl digested vector and 4 μl digested insert DNA were used in a 10 μl or 20 μl reaction. 1 μl T4 DNA ligase and T4 DNA ligase buffer was added to the mixture. The ligation mixture was either put in room temperature water bath and the bath then placed at 4 ºC overnight, or kept at room temperature for 4 h and then placed at 4 ºC overnight.

2.4 DNA electrophoresis, extraction and purification

DNA fragments including PCR products and digests of plasmids were separated by electrophoresis in 0.8-1.2% agarose in 1 × TBE buffer [0.089 M Tris base, 0.089 M boric acid, 0.002 M ethylenediaminetetraacetic acid (EDTA), pH8.0]. A constant current of 100 mA was applied until the desired migration was reached. Gels were stained in 0.5 μg/ml ethidium

bromide for 5-10 min and then washed with distilled water for 10-20 min. The DNA was viewed at 260 nm by a UV trans-illuminator (Mitsubishi, Japan).

For extraction of PCR fragments, DNA was first isolated by 1.2% agarose gel electrophoresis. Then the target fragments were cut from the agarose gel with a surgical blade and put in a 1.5 ml tube. The DNA was extracted from the agarose gel using a QIAquick Gel Extraction Kit (QIAGEN Science, Maryland, USA), using the protocol supplied with the kit. DNA digests and miniprep plasmids for sequencing were purified using a QIAquick PCR Purification Kit (QIAGEN Science, Maryland, USA), using the protocol supplied with the kit.

2.5 Electroporation and transformation

2.5.1 Electroporation of bacteria

0.2-1.0 µl plasmid (0.2-2 µg/µl) was added to 40 µl competent bacteria cells. The mixture was transferred to a cold 0.2 mm gap cuvette. Electroporation was performed at 1.5 volts and the time constant was 4.5-4.7. Recovery media [LB broth (1% tryptone, 0.5% yeast extract, 1% NaCl, 10 mM $MgCl_2$, 0.2% glucose] was added immediately to the electroporated cells. Then the culture was mixed by pipetting up and down several times and transferred to a sterile glass tube. The cells were incubated for either 1 h (plasmids encoding Amp resistance) or 2 h (plasmids encoding either Kan or streptomycin (Sm) resistance) to increase expression time at 37 ^{o}C. The culture was then plated on the LB agar plate containing the appropriate concentration of antibiotic (100 µg/ml Amp, 50 µg/ml Kan and 50 µg/ml Sm) and incubated at 37 ^{o}C overnight.

2.5.2 Co-transformation of yeast

PJ69-4A cells were cultured at 30 °C in a complete YPD medium (5% Bacto YPD Broth). The cells were transformed using a modified dimethyl sulfoxide (DMSO)-enhanced protocol (Hill *et al*., 1991). For each transformation, approximately 1.7 ml of early log-phase yeast cells were pelleted and washed with 400 µl LiTE [0.1 M LiOAc in 1 × TE buffer: 0.1 M lithium acetate (Li), 10 mM Tris- HCl, 0.1 mM EDTA, pH 8.0]. The suspension was pelleted again and resuspended in 100 µl of LiTE. An appropriate amount of DNA was then added as well as 4 µl of denatured sheared salmon sperm DNA (10 mg/ml in TE). In addition, 280 µl 50%

polyethylene glycol (40% in LiTE) was added and the samples were mixed gently by inversion. After incubation at 30 ºC for 4 min, 39 µl 10% DMSO was added and the samples were mixed by inverting several times. The cells were then heat-shocked at 42 ºC for 5 min. The cells were pelleted and the supernatant was removed. The resulting pellet was washed and resuspended in 500 µl sterile water. The cells were pelleted for the last time, and the pellets were resuspended in 100 µl sterile water and spread on -Trp-Leu plates (0.67% Difco yeast nitrogen base without amino acids, 2% glucose, 2% Difco Bacto agar, amino acid mix, including 20 mg/L Adenine (Ade) SO_4, 20 mg/L Histidine HCl, 30 mg/L Lysine HCl, 20 mg/L Methionine and 20 mg/L Uracil). Plates were incubated at 30 ºC for 68 h or 72 h to allow colony growth.

2.6 Miniprep plasmid extraction from *E. coli.*

A single colony of positive transformants was inoculated in 2 ml 2 × YT (tryptone 1.6%, yeast extract 1%, NaCl 0.5%) with appropriate antibiotic. The culture was shaken vigorously at 37 ^{o}C for 16-18 h. The 1.5 ml overnight culture was poured into a tube and centrifuged at room temperature for 1 min. The supernatant was aspirated completely and the pellet was resuspended in 200 µl of cold solution I (50 mM glucose, 20.5 mM Tris, 20 mM EDTA, 1% RNAse, pH 8.0) and vortexed. The mixture was kept at room temperature for 5 min. To lyse the cells, 200 µl solution II (0.8% NaOH, 1% SDS) was added, the mixture was gently inverted several times, and the tube was placed on ice for 5 min. Then the base was neutralized by adding 200 µl of solution III (3 M KOH, 11.5% glacial acetic acid). The tube was inverted vigorously 5 times and then placed on ice for 15 min. Then the sample was centrifuged at 4 ^{o}C for 20 min. 400-500 µl of supernatant was transferred to a new tube containing 250 µl of isopropanol. The tube was inverted vigorously 5 times and then centrifuged at room temperature for 20 min. The supernatant was aspirated completely and the pellet was resuspended in 250 µl of cold 70% ethanol, followed by centrifugation at 4 ^{o}C for 5 min**.** The supernatant was aspirated completely and the pellet was dried at 37 ºC for 10 min. The extracted plasmid was resuspended in 25 µl or 50 µl 0.1 × TE buffer (10 mM Tris-HCl, 0.1 mM EDTA, pH8.0). The plasmids were stored at -20 ºC. The plasmids were then purified as described in 2.4. All centrifuge steps were carried out at 17, 900 × g using Hettich centrifuge (Germany).

2.7 Plasmid construction

2.7.1 Yeast two-hybrid constructs of periplasmic *exe* fragments

Periplasmic domains of *exe*A, B, C, D, L, M and N (Table 2-8) were amplified by PCR with restriction sites incorporated into the primers as described in 2.2. In more detail, *Eco*RI and *Bam*HI sites were incorporated into the upstream primer and downstream primer respectively for amplifying *exe*A, B, C, D, L and M. In addition, *Eco*RI and *Bgl*II sites were incorporated into the upstream primer and downstream primer respectively for amplifying *exe*N since the *exe*N fragment contained a *Bam*HI restriction site. To construct the bait plasmids, the bait vector pGBT9 was double digested with *Eco*RI and *Bam*HI, and then the PCR fragments of *exe*A, B, C and D containing the *Eco*RI and *Bam*HI sites were cloned into the vector. Similarly, the prey plasmids were made by ligating the *exe*A, B, C, D, L, M fragments into the prey vector pGAD424 (*Eco*RI and *Bam*HI) as well as inserting the *exe*N fragment carrying *Eco*RI and *Bgl* II restriction sites.

2.7.2 Yeast two-hybrid constructs of *exe*D two-codon mutants

The 2-codon insertion mutants of *exe*D were constructed by Vivan Ast using single stranded hexameric oligonucleotides (Barany, 1985). In the peri-*exe*D encoding region, there are *Msp*I (CCGG) and *Hha*I (GCGC) cohesive end restriction sites (Fig. 2-1, Table 2-9). Single stranded hexameric linkers CGGATC and GATCCG were inserted into 4 *Msp*I and 4 *Hha*I restriction sites in the peri-*exe*D, thus creating a unique *BamH*I site.

The 8 fragments of the *exe*D mutants were amplified by PCR as described in 2.2. The 2 primers used were the same as those used for the *exe*D (WT) fragment. To construct the bait plasmids, the PCR products were digested with *EcoR*I and *Msc*I and cloned into pGBT-*exe*D (*Eco*RI and *Msc*I). Similarly, the prey plasmids were constructed by digesting the PCR fragments with *Eco*RI and *Aar*I and ligating the digests into pGAD424-*exe*D (*Eco*RI and *Aar*I).

2.7.3 Yeast two-hybrid constructs of *exe*D deletion mutants

To construct the deletion mutants of *exe*D, seven fragments (Table 2-10) of peri-*exe*D were amplified as described in 2.2. In more detail, *Eco*RI/*Bam*HI was incorporated into the upstream primers and downstream primers respectively for amplifying all the ExeD fragments. To construct the bait plasmids, the *Eco*RI and *Bam*HI digested fragments (3-7) were cloned into

TABLE 2-8. Periplasmic domains of Exe fragments

exe fragments	Amino acid residues (Whole sequence)	Amino acid residues (Periplasmic domain)
A	547	288-547
B	226	38-226
C	290	47-290
D	678	26-355
L	389	273-389
M	163	41-163
N	252	37-252

1 minkgkgwrl atvaaalmma gsawa**t**eysa sfknadieef intvgknlsk tiiieps*****vrg

61 kinvrsydll neeqyyqffl svldvygfav vpmdngvlkv vrskdaktsa ipvvdetnpg

121 igdemv*****trvv pvrnvs*****vrel apllrqlndn agggnvvhyd psnvllitgr aavvnrlvev

181 v*****rrvdkagdq evdiiklkya *****sagemvrlvt nlnkdgnsqg gntslllapk vvadertnsv

241 vvsgep*****kara riiqm*****vrqld rdlqsqgn*****tr vfylkygkak dmvevlkgvs ssieadkkgg

301 gtattaggga sigggklais adettnalvi taqpdvmael eqvvakldir raqv**l**veaii

FIG. 2-1. Amino acid sequence of peri-ExeD. The bold **t** and **l** represent the ends of the fragment amplified in this study. * Insertion sites of the single stranded hexameric linkers CGGATC and GATCCG

TABLE 2-9. Linker insertion mutagenesis of peri-*exe*D

Plasmid	Insertion site (aa)	Restriction site
pVA1.3.1	58	*Hha*I
pVA23.6.2	127	*Msp*I
pVA2.3.2	137	*Hha*I
pVA24.7.1	182	*Msp*I
pVA29.2.2	201	*Msp*I
pVA6.2.1	247	*Hha*I
pVA8.1.1	256	*Hha*I
pVA36.1.1	269	*Msp*I

TABLE 2-10. Fragments of peri-ExeD for deletion mutants

Fragment	Amino acid residues
1	26-120
2	121-355
3	26- 200
4	201-355
5	26-139
6	140-256
7	257-355

the bait vector pGBT9 (*Eco*RI and *Bam*HI) and all the 7 fragments were inserted into the prey vector pGAD424 (*Eco*RI and *Bam*HI). The constructed *exe*D deletion mutants are listed in Table 2-11.

2.7.4 Construction of vectors encoding tagged and untagged proteins for co-purification

Co-expression and co-purification assays require a tagged and an untagged protein. For co-expression, it is also necessary that the two vectors contain different antibiotic resistance genes and plasmid replicons. In this study, pET30 (Novagen, NJ, USA) and pET47b (Novagen) were used as the His-tag vector, and pCDFDuet (Novagen) was used as an S-tag vector in case both directions were required. To construct the N-terminal His-tagged protein, *Nde*I/*Xho*I were incorporated into the upstream primers and downstream primers respectively for amplifying *exe*A and B, and *Sac*II and *Xho*I were incorporated into the upstream primers and downstream primers respectively for amplifying *exe*C and D fragments. Six *his* codons were also incorporated into the upstream primers for *exe*A and B for construction of N-terminal His tag. pET30a and pET47b were double digested with *Nde*I and *Xho*I and *Sac*II and *Xho*I respectively. Then the *exe*A and B fragments were cloned into pET30a, the *exe*C and D fragments were inserted downstream of the N-terminal His tag sequence of pET47b. To construct the C-terminal S-tagged proteins, *Nde*I and *Xho*I were incorporated into the upstream primers and downstream primers respectively for amplifying *exe*A, B C and D fragments. Then the *Nde*I and *Xho*I double digested fragments were cloned into pCDFDuet (*Nde*I and *Xho*I). In this study, the pCDFDuet constructs were used as untagged proteins. All the primers used in this experiment are listed in Table 2-4.

2.7.5 Determination of the expression of the His-tag fused and unfused protein

To check the expression of the constructed His tag and S tag Exe proteins, the plasmids were electrophorated to BL21 and the transformants induced with Isopropyl β-D-1-thiogalactopyranoside (IPTG). Electroporation was accomplished according to 2.5.1. A single colony was picked from each transformation plate containing the appropriate antibiotic and resuspended in 2 ml 2 × YT containing 50 µg/ml Kan or 50 µg/ml Sm. The culture was shaken at 37 °C for 16 h. 200 µl over night culture was transferred to 20 ml 2 × YT supplemented with appropriate antibiotics. Cultures were induced with 1 mM IPTG (final concentration) when the

TABLE 2-11. Deletion mutants of pGBT9-*exe*D and pGAD424-*exe*D

	Bait	Prey
1		pGAD424-*exe*D:Δ121-355
2		pGAD424-*exe*D:Δ26-120
3	pGBT9-*exe*D:Δ201-355	pGAD424-*exe*D:Δ201-355
4	pGBT9-*exe*D:Δ26-200	pGAD424-*exe*D:Δ26-200
5	pGBT9-*exe*D:Δ140-355	pGAD424-*exe*D:Δ140-355
6	pGBT9-*exe*D:Δ26-139, Δ257-355	pGAD424-*exe*D:Δ26-139, Δ257-355
7	pGBT9-*exe*D:Δ26-256	pGAD424-*exe*D:Δ26-256

OD_{600} (optical density) reached 0.6-0.8. After induction for 3 h, the cultures were centrifuged at 8, 820 × g, 4 °C for 10 min, the supernatant was then removed and the pellet was resuspended in 10 ml NTA buffer. 10 µg/ml RNase and 20 µg/ml DNase and 40 µl protease inhibitor (one tablet/2 ml of redistilled H_2O) were added prior to three passes through a French Pressure Cell Press (SLM Instruments, INC) at 1, 000 p.s.i. The lysed cells were centrifuged at 31, 000 × g for 20 min or 19, 800 × g for 30 min, 4 °C to pellet inclusion bodies and unbroken cells. The supernatant and pellet obtained from the last centrifugation after French Press as well as the sample taken before cell collection was used for SDS-PAGE and immunoblot to determine the expression of the His-tag fused and unfused Exe proteins. Rotor JA-17, Avanti J-E centrifuge (USA) was used in all centrifugation steps.

2.8 Yeast two-hybrid assay

The bait and the prey plasmids were co-transformed into pJ69-4A, and initially plated on SD-Leu-Trp to select for colonies containing both plasmids. To test the activation of the P_{GAL1}-*HIS3* reporter gene, the cell growth assay was performed where at least six independent colonies were grown in SD-Leu-Trp media and then replica plated onto either SD-Trp-Leu-Histidine (His) alone or SD-Trp-Leu-His containing 3-aminotriazole (3-AT), with a gradient of concentration of 0.2 mM, 0.4 mM, 0.6 mM, 0.8 mM, 1.0 mM and 1.2 mM. For the first yeast two-hybrid assay, the activation of the P_{GAL2}-*ADE*2 reporter gene was also determined by replica plating onto SD-Leu-Trp-Ade. At the same time, an auto activation test was performed for each fragment to verify if the cloning vector alone would activate the reporter genes. To do so, the bait plasmids and the empty prey vector were co-transformed into strain pJ69-4A as were the empty bait vector (pGBT9) and the prey plasmid (pGAD424-*exe*C-N). In addition, pGBT9-MUS81 and pGAD424-MMS4 were co-transformed into PJ69-4A and was used as the positive control while the empty bait vector pGBT9 and the empty prey vector pGAD424 were co-transformed into PJ69-4A and used as the negative control. Plates were incubated for 60 h or 72 h at 30 ºC.

2.9 Co-purification test

His tag co-purification was performed using FPLC (Fast Protein Liquid Chromatography, Amersham Biosciences, AKTA purifier). pET30-*exe*A (bait) and pCDFDuet-*exe*D (prey) were

transformed into BL21(DE3) separately. The two transformants were grown in 20 ml 2 × YT contain 50 μg/ml Kan or Sm respectively. Cultures were induced with 0.4 mM IPTG when the OD_{600} reached 0.6-0.7. After induction for 3 h, the cultures were centrifuged at 8, 820 × g, 4 °C for 10 min, the supernatant was then removed and the pellet was resuspended in 10 ml binding buffer [50 mM Tris-HCl, 1 mM phenylmethylsulphonyl fluoride (PMSF), 20 mM imidazol, pH 7.5]. 10 μg/ml RNase and 20 μg/ml DNase and 40 μl protease inhibitor were added prior to three passes through a French Pressure at 1, 000 p.s.i. The lysed cells were centrifuged at 31, 000 × g for 20 min or 19, 800 × g for 30 min, 4 °C to pellet inclusion bodies and unbroken cells. 10 ml of the cell lysate of pET30-*exe*A and 5 ml pCDFDuet-*exe*D was applied to a Ni-NTA agarose column equilibrated with binding buffer (50 mM Tris-HCl, 1 mM PMSF, 20 mM imidazol, pH7.5) to detect the His-tag binding of the bait and background binding of the prey respectively. For ExeA and ExeD interaction, 10 ml of the cell lysate of pET30-*exe*A and 5 ml pCDFDuet-*exe*D was mixed and incubated at 4 °C for 5 h. The His-tagged bait protein was bound to the column and the column was washed with binding buffer before being eluted with a gradient of 0 to 100% elution buffer (50 mM Tris-HCl, 1 mM PMSF, 500 mM imidazol, pH 7.5). Elution fractions were kept at -20 °C for SDS-PAGE and immunoblot analysis. Rotor JA-17, Avanti J-E centrifuge (USA) was used in all cetrifugation steps.

2.10 Immunoblot

In the co-purification experiments of pET30-*exe*A and pCDFDuet-*exe*D, the Amersham ECL Advance Western Blotting Detection Kit (GE Healthcare, NJ, USA) was used. The primary antibody used was anti-ExeD (1:50,000 dilution), the secondary antibody added was affinity purified anti-rabbit (1:100,000 dilution). To examine the expression of the pGBT9-*exe*D mutants and pGAD424-*exe*D mutants, the Immun-Star HRP Chemiluminescent Kit obtained from Biorad (CA, USA) was used. The primary antibody used was anti-ExeD (1:20,000 dilution), the secondary antibody was affinity purified anti-rabbit (1:100,000 dilution). To determine the induction of CDFDuet-*exe*C, the same protocol was used except that the first antibody was anti-ExeC.

3. RESULTS

3.1 Yeast two-hybrid assay of the interactions between ExeA, B and Exe A, B, C, D, L, M and N.

Initially, the interactions between the periplasmic domains of ExeA and ExeB and those of ExeA, B, C, D, L, M and N were assayed. The bait plasmids pGBT9-*exe*A and pGBT9-*exe*B, and the prey plasmids pGAD424-*exe*C, D, L, M and N were constructed as described in 2.7.1. Co-transformation of the baits and the preys into the yeast host strain pJ69-4A and the yeast two-hybrid assay were performed as described in 2.5.2 and 2.8. The results are listed in Table 3-1. For the assay between the bait pGBT9-*exe*A and the prey pGAD424-*exe*A-N, only pGBT9-*exe*A and pGAD424-*exe*D showed protein-protein interaction; for pGBT9-*exe*B and the preys, no protein-protein interaction was observed. Neither pGBT9, the empty bait vector and the prey pGAD424-*exe*A-N, nor the baits pGBT9-*exe*A and pGBT9-*exe*B and the empty prey vector pGAD424 showed autoactivation except for pGBT9 and pGAD424-*exe*N (data not shown). Furthermore, the co-transformants of pGBT9-*exe*A and pGAD424-*exe*D could not grow on SC-Trp-Leu-Ade, and the interaction between pGBT9-*exe*A and pGAD424-*exe*D also could not be detected by the liquid β-galactosidase assay (data not shown), suggesting the interaction between the ExeA and ExeD fragments are weak. No other protein-protein interactions were identified by the yeast two-hybrid assay between ExeA/ExeB and ExeC-N except for the ExeA and ExeD interaction. The negative result for the ExeB and ExeD interaction is contradictory to previous studies which have suggested that the C-terminal domain including the peri-OutB interacts with OutD (Condemine and Shevchik, 2000). In addition, the ExeAB complex has been demonstrated to play either a direct or indirect role in the transport of ExeD into the OM (Ast *et al*., 2002). The negative result of ExeA/ExeA and ExeA/ExeB was also unexpected as ExeA has been shown to dimerize and to form a very large complex with ExeB (Schoenhofen *et al.*, 2005; Howard *et al*., 2006). The failure of interactions between ExeA/ExeA, ExeB/ExeB and ExeA/ExeB in the yeast two-hybrid assay may be because the conformation of these proteins required for interactions cannot be formed in yeast. Another possible explanation of the negative results could be that the protein-protein interactions occur in a different region of the proteins. Since the proteins ExeA and ExeB are cytoplasmic membrane proteins, the protein interactions may occur at the TM domain.

TABLE 3-1. Protein-protein interaction in T2SS of *A. hydrophila* identified by yeast two-hybrid assay 1

Bait	Prey	Interaction
pGBT9-*exe*A	pGAD424-*exe*A	No
	pGAD424-*exe*B	No
	pGAD424-*exe*C	No
	pGAD424-*exe*D	**Yes**
	pGAD424-*exe*L	No
	pGAD424-*exe*M	No
	pGAD424-*exe*N	No
pGBT9-*exe*B	pGAD424-*exe*A	No
	pGAD424-*exe*B	No
	pGAD424-*exe*C	No
	pGAD424-*exe*D	No
	pGAD424-*exe*L	No
	pGAD424-*exe*M	No
	pGAD424-*exe*AN	No

Similarly, the reason no interactions were identified between ExeA, B and the IM protein ExeC as well as the other components of the IM complex, ExeL, M and N may be because such interactions require the N-terminal TM domains instead of C-terminal periplasmic domain or in addition to the periplasmic domains. Previous studies, for example, showed that the N-terminal TM domain of GspC interacts with TM domains of other components of the IM complex (Bleves *et al*., 1999; Bouley *et al*., 2001; Lee *et al*., 2001; Filloux, 2004).

3.2 Yeast two-hybrid assay of the interactions between ExeC and ExeC, D, L, M and N, and between ExeD and ExeA, B, C and D

Based on the assay between ExeA and ExeB and Exe A, B, C, D, L, M and N, a second yeast two-hybrid assay was performed to identify interactions between pGBT9-*exe*C and pGAD424-*exe*C, D, L, M and N, as well as pGBT9-*exe*D and pGAD424-*exe*A, B, C and D. The interactions between pGBT9-*exe*D and pGAD424-*exe*L, M and N were not tested as these three proteins are components of the IM complex and less likely to interact with the secretin ExeD. pGBT9-*exe*C and pGBT9-*exe*D were constructed as described in 2.7.1, and the other plasmids as well as the protocol were same as those used in the first assay except that the co-transformants were not replica plated to SC-Trp-Leu-Ade. The results are listed in Table 3-2A. The results showed that there is an interaction between protein ExeD and protein ExeB and ExeC as well as an ExeD self-interaction (Table 3-2A, Fig. 3-1A). No autoactivation of the four protein fragments occurred (Fig. 3-1A). Furthermore, the interaction occurs between pGBT9-*exe*D and pGAD424-*exe*B and C, while not in the other direction including pGBT9-*exe*B and C and pGAD424-*exe*D (Table 3-2A, Fig. 3-1B). Similarly, no interaction was observed between pGBT9-*exe*D and pGAD424-*exe*A. This result, together with that of the first yeast two-hybrid assay, shows only one-direction interactions between ExeD and ExeA, ExeB and ExeC. This may be because the conformation of the protein required for interactions could not be formed in some of the fusion pairs. Previous studies have shown that the full-length GspD forms an oligomeric ring-like structure (Nouwen *et al*., 2000) that may be required for interaction with GspB. Such an assembly would be unlikely to form in the two-hybrid studies but could be present during biochemical approaches such as pull-down experiments or co-expression and co-purification (Gerard-Vincent *et al*., 2002). In addition, the yeast two-hybrid system revealed that pGBT9-*exe*D interacted with pGAD424- *exe*D, which suggests that ExeD

TABLE 3-2A. Protein-protein interactions in T2SS of *A. hydrophila* identified by yeast two-hybrid assay 2

Bait	Prey	Interaction
pGBT9-*exe*C	pGAD424-*exe*C	No
	pGAD424-*exe*D	No
	pGAD424-*exe*L	No
	pGAD424-*exe*M	No
	pGAD424-*exe*N	No
pGBT9-*exe*D	pGAD424-*exe*A	No
	pGAD424-*exe*B	**Yes**
	pGAD424-*exe*C	**Yes**
	pGAD424-*exe*D	**Yes**

TABLE 3-2B. The strength of protein-protein interactions in the T2SS of *A. hydrophila* identified by yeast two-hybrid assay 2

Bait	Prey	Inhibition by conc. of 3-AT
pGBT9-MUS81	pGAD424-MMS4	>1.2 mM
pGBT9-*exe*A	pGAD424-*exe*D	1.2 mM
pGBT9-*exe*D	pGAD424-*exe*B	1.2 mM
pGBT9-*exe*D	pGAD424-*exe*C	0.2 mM
pGBT9-*exe*D	pGAD424-*exe*D	1.2 mM

Gal4$_{BD}$ pGBT9	Gal4$_{AD}$ pGAD424
MUS81	MMS4
vector	vector
*exe*A	*exe*D
*exe*D	*exe*B
*exe*D	*exe*C
*exe*D	*exe*D
*exe*A	vector
vector	*exe*B
vector	*exe*C
vector	*exe*D

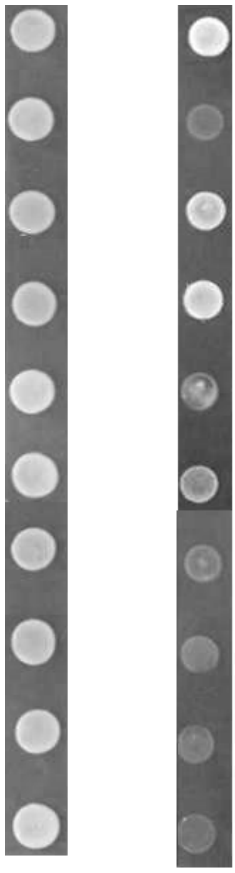

FIG. 3-1. ExeD-ExeA/B/C/D two-hybrid interactions. (A) I*n vivo* interactions of ExeD-ExeA/B/C/D and autoactivation determined by yeast two-hybrid assay. Yeast cells pJ69-4A transformed with Gal4$_{AD}$ and Gal4$_{BD}$ fusion constructs were used to test the interaction. Co-transformed plasmids were maintained in the cell by growth on media without Trp and Leu (shown on the left of the figure). Interactions of the hybrid proteins cause the expression of the *HIS3* reporter which allows growth on minimal medium lacking His since association of the Gal4 fusion proteins turns on the *GAL1* promoter which transcribes the *HIS3* reporter gene. Positive interactions are observed on media without His after 60 h incubation at 30 °C (shown on the right of the figure). The table on the left shows the bait and the prey plasmids used in the assay. The pair of pGBT9-MUS81 and pGAD424-MMS4 was used as the positive control, while the pair of the empty vectors pGBT9 and pGAD424 was used as the negative control.

$Gal4_{BD}$ pGBT9	$Gal4_{AD}$ pGAD424	$Gal4_{BD}$ pGBT9	$Gal4_{AD}$ pGAD424
MUS81	MMS4	MUS81	MMS4
vector	vector	vector	vector
*exe*A	*exe*D	*exeD*	*exeA*
*exe*B	*exe*D	*exe*D	*exe*B
*exe*C	*exeD*	*exe*D	*exe*C

Growth on SD media

–Trp -Leu **–Trp -Leu -His**

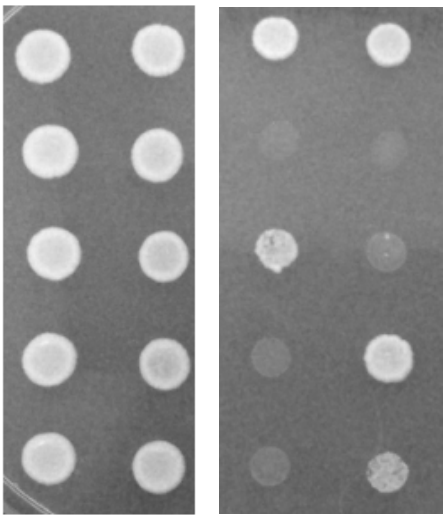

Fig. 3-1. ExeD-ExeA/B/C/D two-hybrid interactions. (B) ExeD-ExeA/B/C one-direction interactions determined by the yeast two-hybrid assay. Yeast cells pJ69-4A transformed with $Gal4_{AD}$ and $Gal4_{BD}$ fusion constructs were used to test the interaction. Co-transformed plasmids were maintained in the cell by growth on media without Trp and Leu (shown on the left of the figure). Physical interactions of the hybrid proteins cause the expression of the *HIS3* reporter which allows growth on minimal medium lacking His. Positive interactions are observed on media without His after 72 h incubation at 30 °C (shown on the right of the figure). The table on the left shows the bait and the prey plasmids used in the assay. The left part and the right part of the table show two directions of the assay, using the ExeD fragment as the prey and the bait respectively. The pair of pGBT9-MUS81 and pGAD424-MMS4 was used as the positive control, while the pair of the empty vectors pGBT9 and pGAD424 was used as the negative control.

can multimerize, corresponding to the previous studies showing that GspD is a dodecameric structure (Chami *et al*., 2005).

The strength of the interactions detected in the first two yeast two-hybrid assays were tested by replica plating colonies to SC-Trp-Leu-His containing 0.2-1.2 mM 3-AT (Table 3-2B, Fig. 3-1C). The strength of the interaction between ExeD and ExeC was the weakest among the four as it is inhibited by lower amounts (0.2 mM) of 3-AT. The strength of the other 3 interactions, including ExeA and ExeD, ExeD and ExeB, and ExeD multimerization are quite similar, and can be inhibited by 1.2 mM 3-AT. However, the interaction between ExeB and ExeD was slightly stronger than that of ExeA and ExeD, and the ExeAD interaction is stronger than ExeD mutimerization when the plates were examined after one day incubation (data not shown). Since the four interactions can be inhibited by 0.2 to 1.2 mM 3-AT, the results indicate that they are relatively weak compared with that of the positive control, pGBT9-MUS81 and pGAD424-MMS4.

3.3 Identification of the regions of ExeD involved in protein-protein interactions

To identify the region of the proteins responsible for the interaction between ExeD and ExeA, B, C and D, two-codon insertion mutagenesis (Howard *et al*., 2006) of the peri-ExeD was combined with the two-hybrid assay of ExeD interactions with ExeA, B, C and D. The two-codon ExeD mutant fusions were produced as described in 2.7.2, and the location of the mutations are shown in Fig. 3-2. The region of ExeD involved in the interaction between ExeD and ExeA, B, C, and ExeD multimerization were identified via yeast two-hybrid assays of the two-codon insertion mutants of ExeD and ExeA, B, C in the direction identified by the first yeast two-hybrid assay, whereas the region of ExeD responsible for ExeD multimerization was identified in both directions (Table 3-3). At the same time, the autoactivation tests were performed. The protocol was the same as that used in the second yeast two-hybrid assay described above.

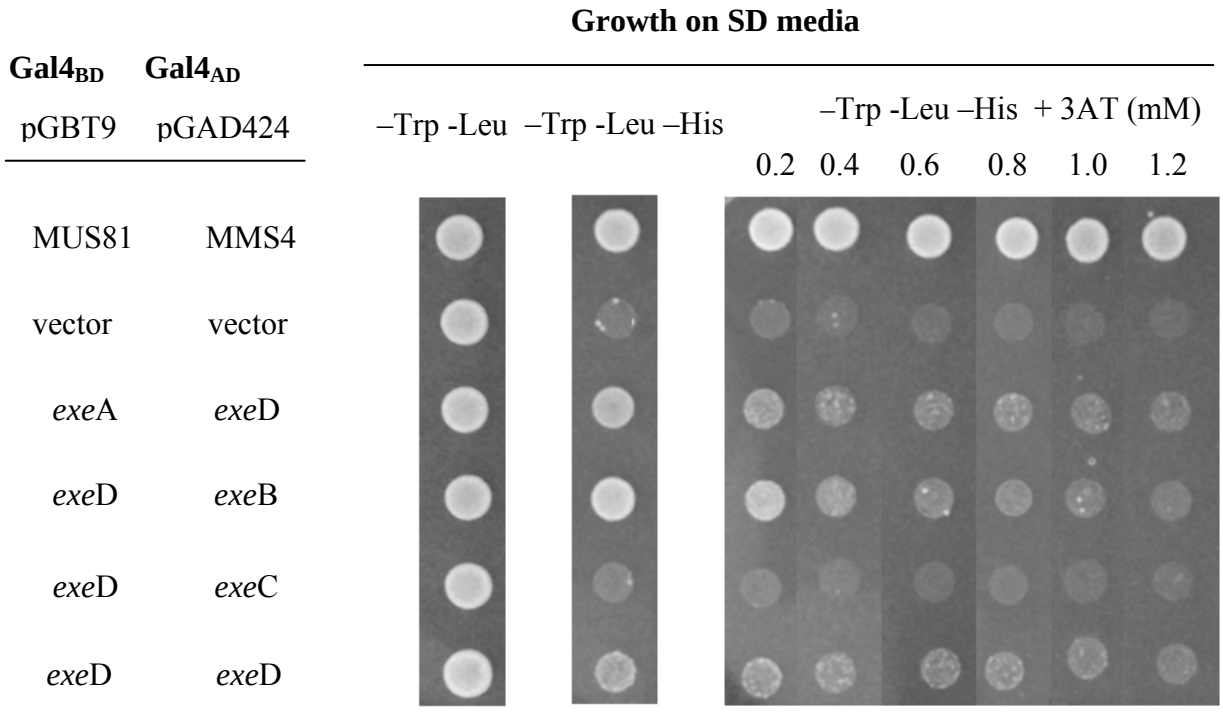

Fig. 3-1. ExeD-ExeA/B/C/D two-hybrid interactions. (C) The strength of the interactions determined by the yeast two-hybrid assay. Co-transformed plasmids were maintained in the cell by growth on media without Trp and Leu (shown on the left of the figure). Positive interactions are observed on media without His after 72 h incubation at 30 °C (shown in the middle of the figure). The strength of the interactions was determined with a gradient conc. of 3-AT added to the media without His (shown on the right of the figure). The table on the left shows the bait and the prey plasmids used in the assay, with the direction in which the positive interaction observed. The pair of pGBT9-MUS81 and pGAD424-MMS4 was used as the positive control, while the pair of the empty vectors pGBT9 and pGAD424 was used as the negative control.

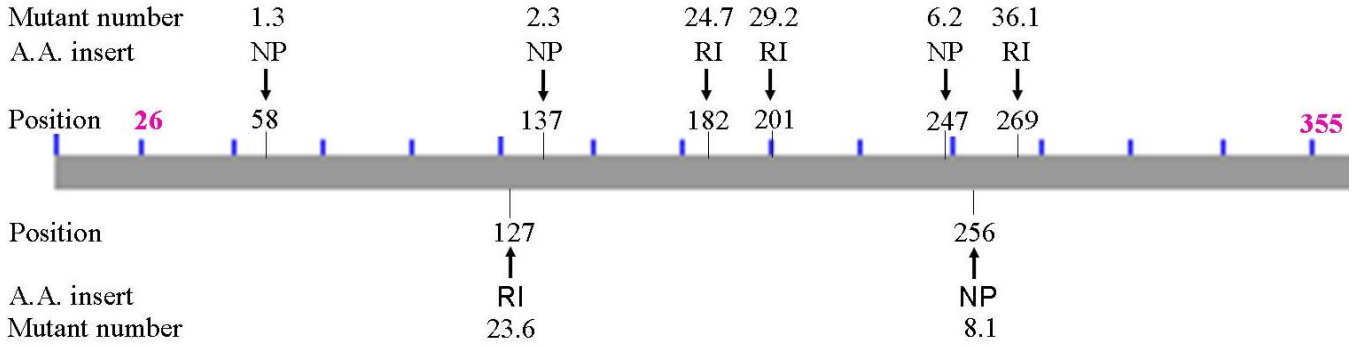

FIG. 3-2. Linker insertion mutagenesis of peri-*exe*D. The gray bar shows the periplasmic domain (residue 26-355) of the ExeD protein (residue 1-567). The mutant number is the name of the two-codon mutant constructed by Vivan Ast; A.A insert indicates the amino acids formed after two-codon (single stranded hexameric linkers CGGATC or GATCCG) insertion; the position shows the *Msp*I or *Hha*I restriction sites for insertion of the single stranded hexameric linkers CGGATC or GATCCG.

TABLE 3-3. Yeast two-hybrid assays of the interactions between *exe*D two-codon mutants and *exe*A, B, C and D

Bait	Prey
pGBT9-*exe*A	pGAD424-*exe*D (mutants)
pGBT9-*exe*D (mutants)	pGAD424-*exe*B
pGBT9-*exe*D (mutants)	pGAD424-*exe*C
pGBT9-*exe*D (mutants)	pGAD424-*exe*D
pGBT9-*exe*D	pGAD424-*exe*D (mutants)

3.3.1 Yeast two-hybrid assay of the interactions between pGBT9-*exe*A and pGAD424-*exe*D two-codon mutants

The first assay performed was between pGBT9-*exe*A (WT) and the pGAD424-*exe*D (two-codon mutants). The replica plate showed that there are interactions between pGBT9-*exe*A and all of the pGAD424-*exe*D mutants except for pGAD424-*exe*D (pVA1.3) (Table 3-4A, Fig. 3-3A). Among the interactions, pGBT9-*exe*A and pGAD424-*exe*D (pVA36.1) were the strongest, the second strongest interaction occurred between pGBT9-*exe*A and pGAD424-*exe*D (pVA23.6). The strength of these two interactions was stronger than that of WT, and was not completely inhibited by 1.2 mM 3-AT. The other interactions were inhibited by 0.4-0.8 mM 3-AT. The autoactivation test of the positive interactions is shown in Fig. 3-3B. Autoactivation was observed between pGBT9 and pGAD424-*exe*D (pVA23.6), and between pGBT9 and pGAD424-*exe*D (pVA8.1). However, compared with the interaction between pGBT9-*exe*A and pGAD424-*exe*D (pVA23.6), and pGBT9-*exe*A and pGAD424-*exe*D (pVA8.1), the autoactivations were much weaker (Table 3-4B, Fig. 3-3C). Therefore, there was still interaction between pGBT9-*exe*A and pGAD424-*exe*D (pVA23.6), and between pGBT9-*exe*A and pGAD424-*exe*D (pVA8.1). Since the interaction between pGBT9-*exe*A and pGAD424-*exe*D (pVA1.3) was completely inhibited, the results suggest that the region from amino acids residue 26 to 58 of peri-ExeD (26-355) is involved in the interaction between ExeA and ExeD (Fig. 3-4). In addition, the interaction between ExeA and other ExeD two-codon mutants in the fragment of periplasmic domain, ranging from amino acid residue 137 to 256, were partially inhibited, especially the interaction between pGBT9-*exe*A and pGAD424-*exe*D (pVA24.7.1) which is almost inhibited by 0.2 mM 3-AT. Therefore, the region around this mutation site may also be involved in the protein-protein interaction with ExeA according to these results.

3.3.2 Yeast two-hybrid assay of the interactions between pGBT9-*exe*D two-codon mutants and pGAD424-*exe*B

The region of ExeD involved in the interaction with ExeB was determined using the yeast two-hybrid assay between pGBT9-*exe*D (two-codon mutants) and pGAD424-*exe*B (WT). *In vivo* interactions of pGBT9-*exe*D (two-codon mutants)-pGAD424-*exe*B (WT) and the strength of

TABLE 3-4A. Interactions between pGBT9-*exe*A and pGAD424-*exe*D two-codon mutants

Bait	Prey	Inhibition by the conc. of 3-AT
pGBT9-*exe*A	pGAD424-*exe*D	>1.2 mM
pGBT9-*exe*A	pGAD424-*exe*D (pVA 1.3.1)	No interaction
pGBT9-*exe*A	*pGAD424-*exe*D (pVA 23.6.2)	>1.2 mM
pGBT9-*exe*A	pGAD424-*exe*D (pVA2.3.2)	0.6 mM
pGBT9-*exe*A	pGAD424-*exe*D (pVA24.7.1)	0.4 mM
pGBT9-*exe*A	pGAD424-*exe*D (pVA29.2.2)	0.8 mM
pGBT9-*exe*A	pGAD424-*exe*D (pVA6.2.1)	0.8 mM
pGBT9-*exe*A	* pGAD424-*exe*D (pVA8.1.1)	0.6 mM
pGBT9-*exe*A	pGAD424-*exe*D (pVA36.1.1)	>1.2 mM

* Autoactivation, the mutant interacts with the vector

TABLE 3-4B. Autoactivations of pGBT9 and pGAD424-*exe*D two-codon mutants

Bait	Prey	Inhibition by the conc. of 3-AT
pGBT9-*exe*A	pGAD424-*exe*D	>1.2 mM
pGBT9	pGAD424	No interaction
pGBT9	pGAD424-*exe*D (pVA 23.6.2)	0.4 mM
pGBT9-*exe*A	pGAD424-*exe*D (pVA 23.6.2)	>1.2 mM
pGBT9	pGAD424-*exe*D (pVA8.1.1)	0.2 mM
pGBT9-*exe*A	pGAD424-*exe*D (pVA8.1.1)	0.4 mM

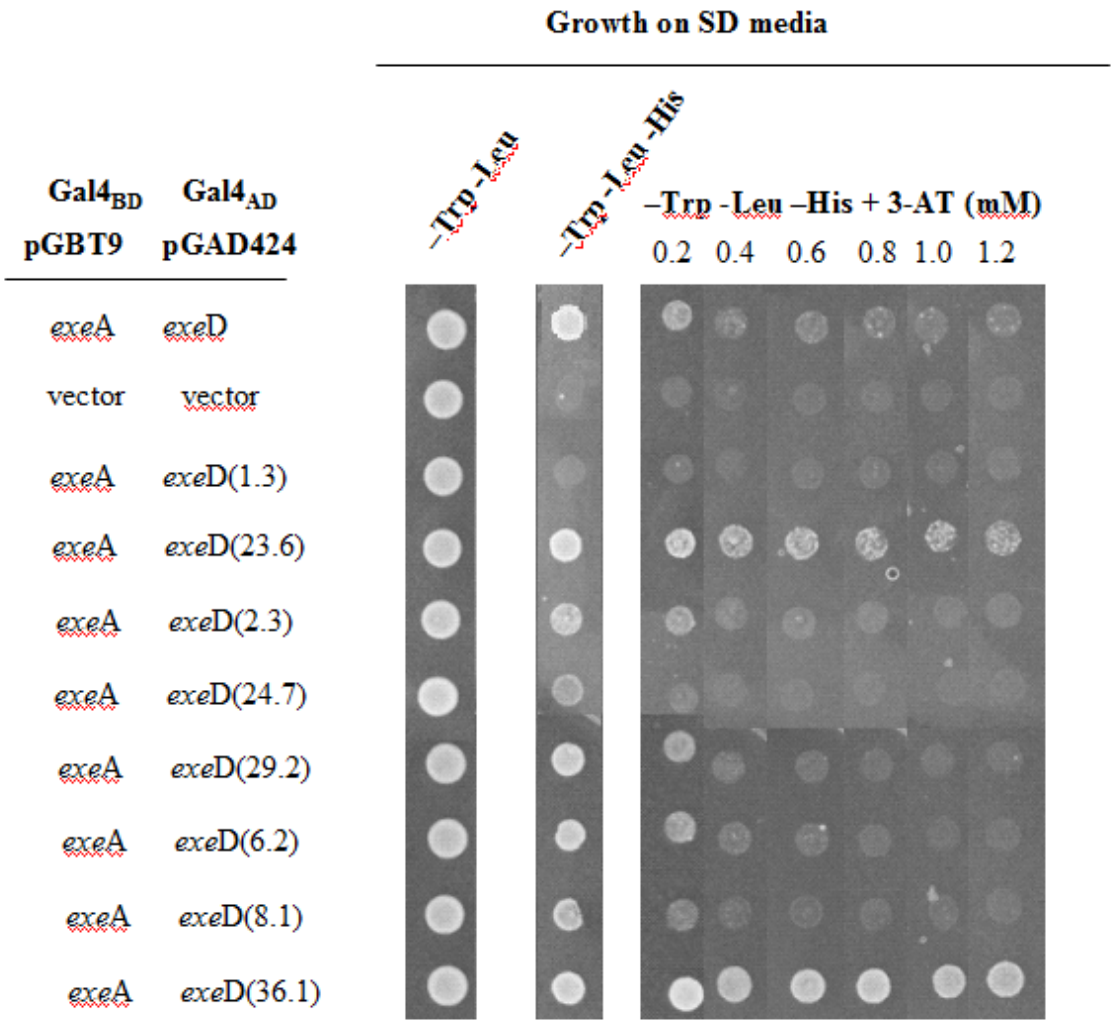

FIG. 3-3. *exe*A (WT)-*exe*D (two-codon mutants) two-hybrid interactions. (A) *In vivo* interactions of *exe*A (WT)-*exe*D (two-codon mutants) and the strength of the interactions determined by the yeast two-hybrid assay. Yeast cells pJ69-4A transformed with $Gal4_{AD}$ and $Gal4_{BD}$ fusion constructs were used to test the interaction. Co-transformed plasmids were maintained in the cell by growth on media without Trp and Leu (shown on the left of the figure). Positive interactions are observed on media without His after 72 h incubation at 30 °C (shown in the middle of the figure). The strength of the interactions was determined with a gradient conc. of 3-AT (0.2-1.2 mM) added to the media without His (shown on the right of the figure). The table on the left shows the pairs of pGBT9-*exe*A (WT) and pGAD424-*exe*D (two-codon mutants) used as the bait and the prey plasmid in the assay. The pair of *exe*A and *exe*D was used as the positive control, while the pair of the empty vectors pGBT9 and pGAD424 was used as the negative control.

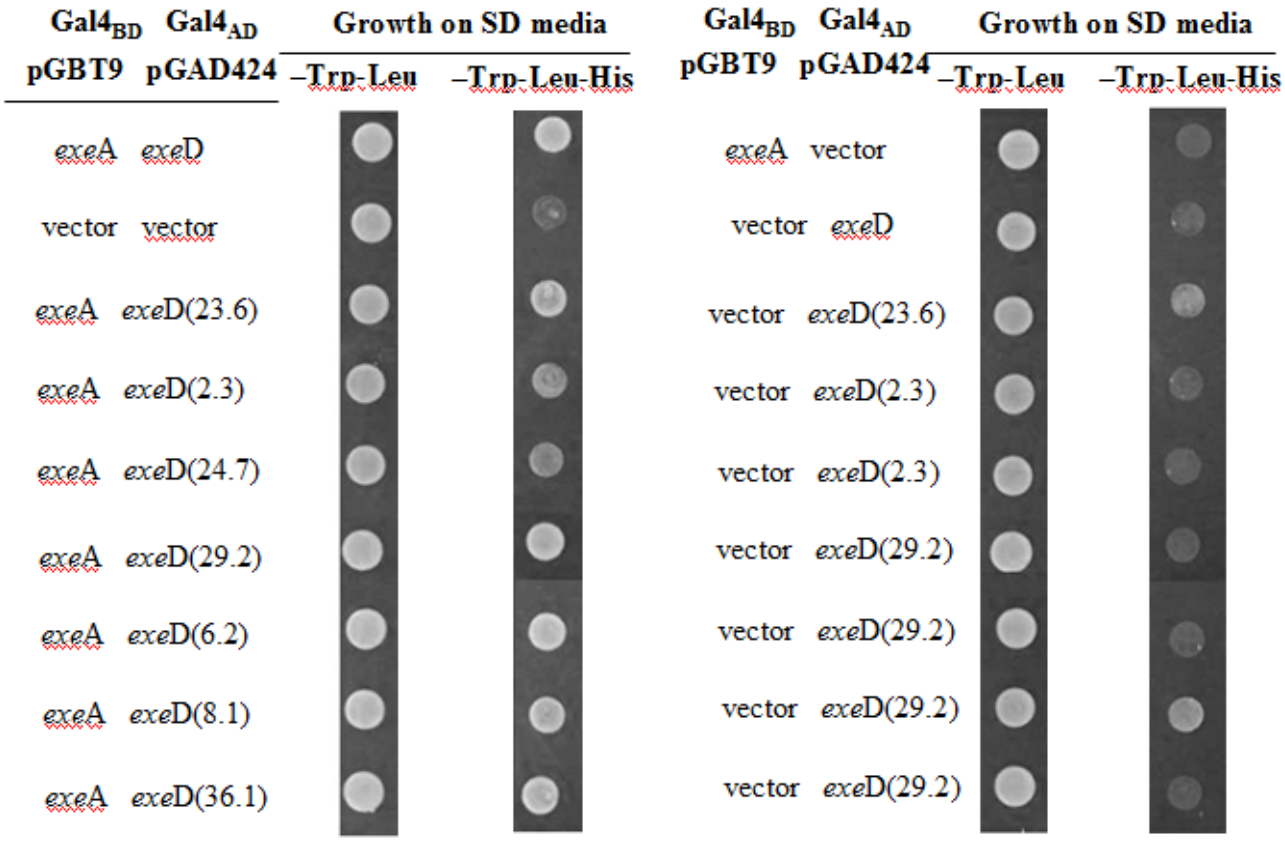

FIG. 3-3. *exe*A (WT)-*exe*D (two-codon mutants) two-hybrid interactions. (B) Autoactivations of the positive interactions determined by the yeast two-hybrid assay. The figure on the left shows the positive interactions between pGBT9-*exe*A (WT) and pGAD424-*exe*D (two-codon mutants), while the figure on the right shows the autoactivation test of these interactions. Co-transformed plasmids were maintained in the cell by growth on media without Trp and Leu (left columns of the figure). Positive interactions are observed on media without His after 60 h incubation at 30 °C (right columns of the figure). The tables on the left of each figure list the pairs of pGBT9-*exe*A (WT) and pGAD424-*exe*D (two-codon mutants) which shows physical interactions and the pairs of vector and WT of *exe*A/D as well as *exe*D mutants used for the autoactivation test. The pair of *exe*A and *exe*D was used as the positive control, while the pair of the empty vectors pGBT9 and pGAD424 was used as the negative control.

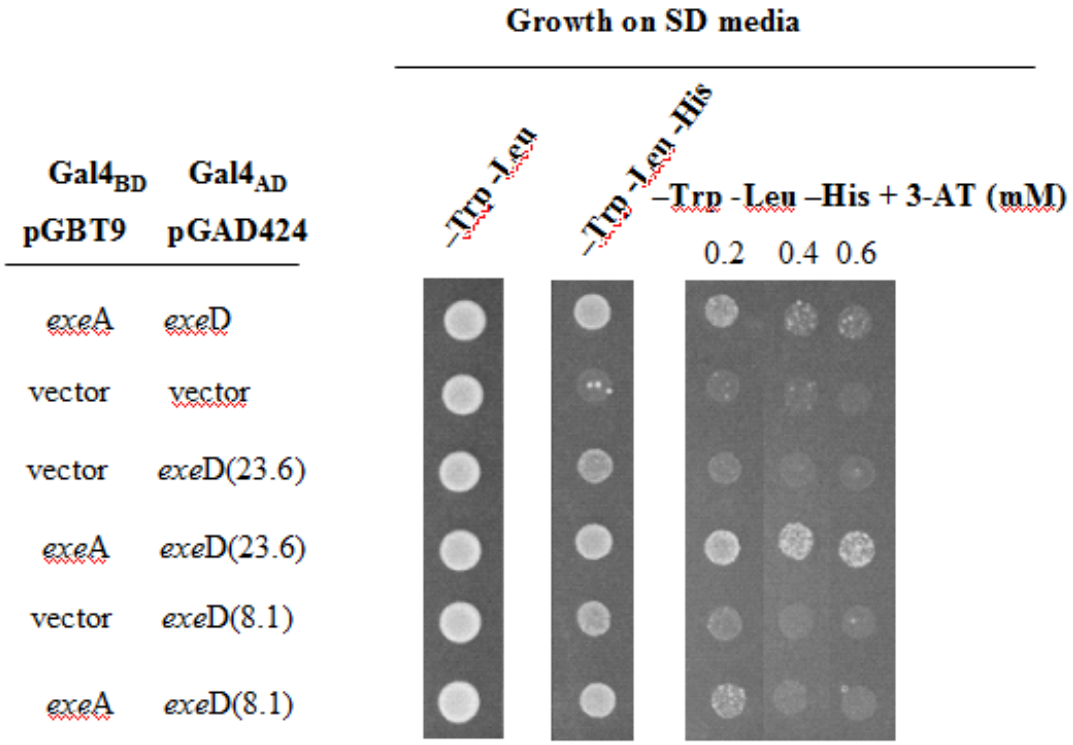

FIG. 3-3. *exe*A (WT)-*exe*D (two-codon mutants) two-hybrid interactions. (C) Comparison of the strength of interactions between positive interactions and autoactivations of *exe*A (WT)-*exe*D (two-codon mutants) by the yeast two-hybrid assay. Yeast cells pJ69-4A transformed with $Gal4_{AD}$ and $Gal4_{BD}$ fusion constructs were used to test the interaction. Co-transformed plasmids were maintained in the cell by growth on media without Trp and Leu (shown on the left of the figure). Positive interactions are observed on media without His after 72 h incubation at 30 °C (shown in the middle of the figure). The strength of the interactions was determined with a gradient conc. of 3-AT (0.2-0.6 mM) added to the media without His (shown on the right of the figure). The table on the left shows the pairs of *exe*A (WT)-*exe*D mutants used for determining the interaction and vector-*exe*D mutants used for the autoactivation test. The pair of *exe*A and *exe*D was used as the positive control, while the pair of the empty vectors pGBT9 and pGAD424 was used as the negative control.

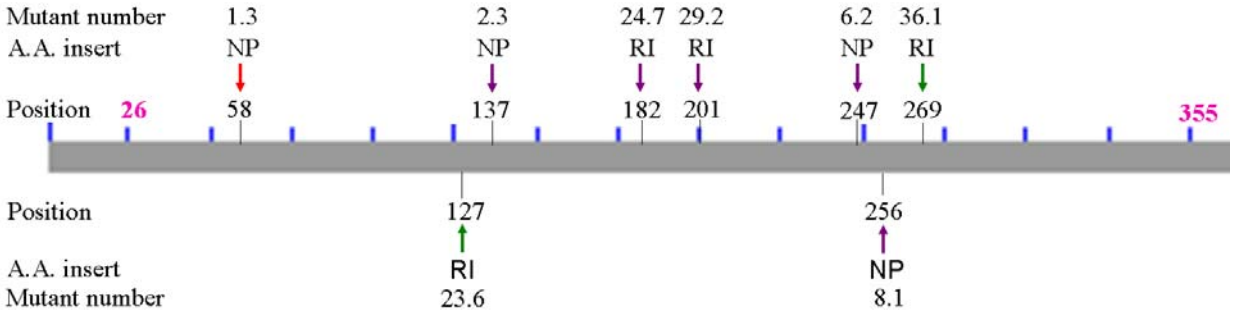

FIG. 3-4. Regions of ExeD involved in the interaction between ExeA and ExeD. The region of ExeD involved in the ExeA-ExeD interaction was determined by the yeast two-hybrid assay between ExeA (WT) and ExeD (two-codon mutants). The vertical arrows show the positions of the mutants. The red arrow stands for complete inhibition of the ExeA-ExeD interaction, the purple arrows stand for partial inhibition, and the green arrows stand for no inhibition of the interaction.

the interactions were shown in Table 3-5 and Fig. 3-5A. No interaction appeared between the first four pGBT9-*exe*D mutants and pGAD424-*exe*B, whereas the last four pGBT9-*exe*D mutants showed interaction with pGAD424-*exe*B. Among the interactions, the interaction between pGBT9-*exe*D (pVA29.2) and pGAD424-*exe*B was the strongest, and was only slightly inhibited by 1.2 mM 3-AT. The next strongest was the interaction between pGBT9-*exe*D (pVA36.1) and pGAD424-*exe*B, which was inhibited by 1.0 mM 3-AT. The interactions between ExeB and the other ExeD mutants were weak, and could be inhibited by 0.2-0.4 mM 3-AT. No autoactivation of the positive interactions was observed by the yeast two-hybrid assay as shown in Fig. 3-5B. The interactions between the first four pGBT9-*exe*D mutants and pGAD424-*exe*B were completely inhibited, suggesting that a region, from amino acid residue 26-182 of peri-ExeD was responsible for the interaction with ExeB (Fig. 3-6). However, the interaction between pGBT9-*exe*D (pVA6.2.1) and pGAD424-*exe*B, and between pGBT9-*exe*D (pVA8.1.1) and pGAD424-*exe*B are very week, so it can not be excluded that a region, from amino acid residue 247 to 256 of peri-ExeD is also involved in the ExeB-ExeD interaction.

3.3.3 Yeast two-hybrid assay of the interactions between pGBT9-*exe*D two-codon mutants and pGAD424-*exe*C

The yeast two-hybrid assay between pGBT9-*exe*D (two-codon mutants) and pGAD424-*exe*C (WT) was carried out although the interaction between pGBT9-*exe*D (WT) and pGAD424-*exe*C (WT) was very weak and sometimes hard to detect. *In vivo* interactions of pGBT9-*exe*D (two-codon mutants)-pGAD424-*exe*C (WT) and the strength of the interactions are shown in Table 3-6 and Fig. 3-7A. The interactions between seven of eight pGBT9-*exe*D mutants and pGAD424-*exe*C were hard to detect. Only pGBT9-*exe*D (36.1) and pGAD424-*exe*C showed a very weak interaction which was inhibited by 0.2 mM 3-AT. No autoactivation for this positive interaction was observed (Fig. 3-7B). Therefore, it can be concluded that the interactions between all the pGBT9-*exe*D mutants and pGAD424-*exe*C were completely inhibited except that between pGBT9-*exe*D (pVA36.1) and pGAD424-*exe*C, suggesting that the region from amino acid residue 26-256 of peri-ExeD is involved in the interaction with ExeC (Fig. 3-8).

TABLE 3-5. Interactions between pGBT9-*exe*D two-codon mutants and pGAD424-*exe*B

Bait	Prey	Inhibition by the conc. of 3-AT
pGBT9-*exe*D	pGAD424-*exe*B	>1.2 mM
pGBT9-*exe*D (pVA 1.3.1)	pGAD424-*exe*B	No interaction
pGBT9-*exe*D (pVA 23.6.2)	pGAD424-*exe*B	No interaction
pGBT9-*exe*D (pVA2.3.2)	pGAD424-*exe*B	No interaction
pGBT9-*exe*D (pVA24.7.1)	pGAD424-*exe*B	No interaction
pGBT9-*exe*D (pVA29.2.2)	pGAD424-*exe*B	>1.2 mM
pGBT9-*exe*D (pVA6.2.1)	pGAD424-*exe*B	0.4 mM
pGBT9-*exe*D (pVA8.1.1)	pGAD424-*exe*B	0.2 mM
pGBT9-*exe*D (pVA36.1.1)	pGAD424-*exe*B	1.0 mM

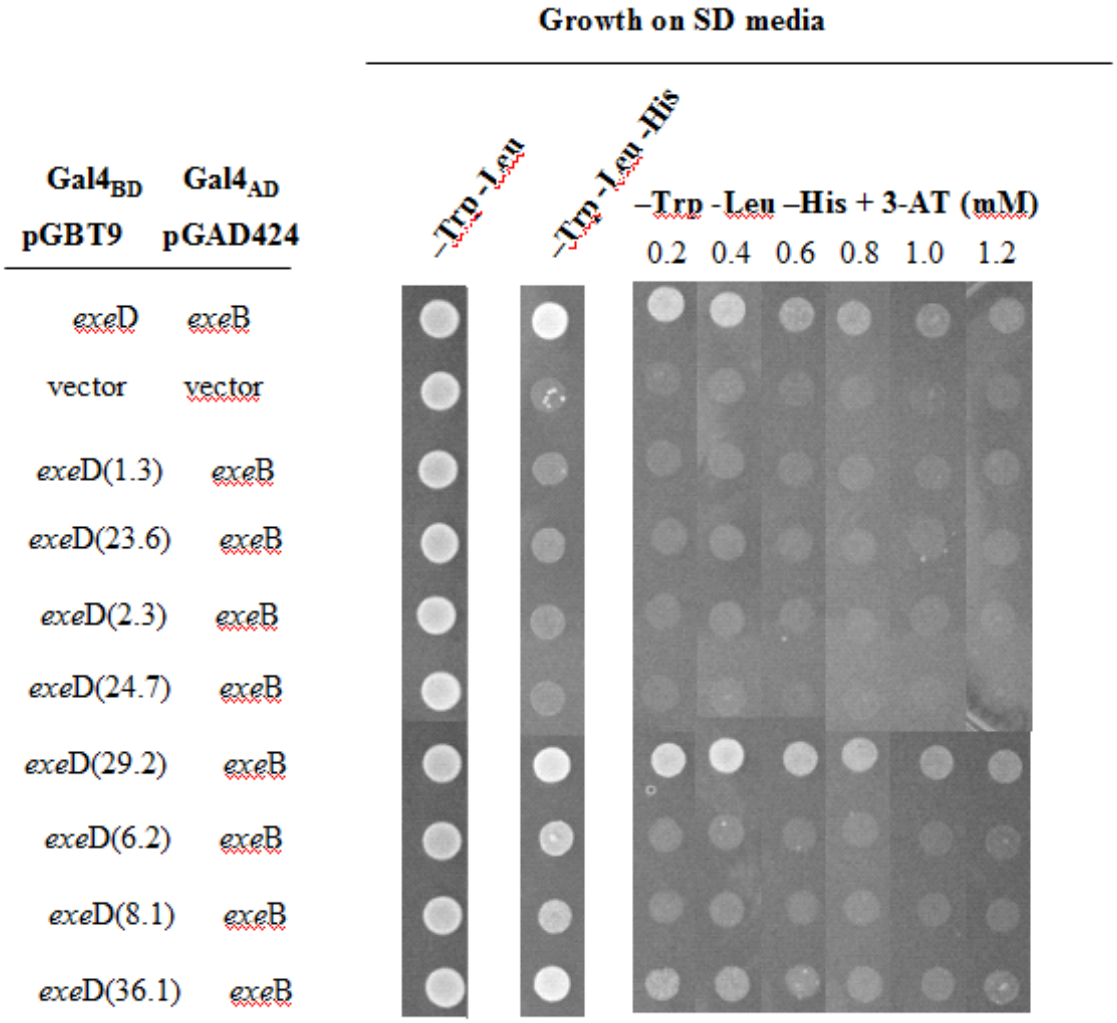

FIG. 3-5. *exe*D (two-codon mutants)-*exe*B (WT) two-hybrid interactions. (A) *In vivo* interactions of *exe*D (two-codon mutants-)-*exe*B (WT) and the strength of the interactions determined by the yeast two-hybrid assay. Yeast cells pJ69-4A transformed with fusion constructs were used to test the interaction. Co-transformed plasmids were maintained in the cell by growth on media without Trp and Leu (shown on the left of the figure). Positive interactions are observed on media without His after 72 h incubation at 30 °C (Showing in the middle of the figure). The strength of the interactions was determined with a gradient conc. of 3-AT (0.2-1.2 mM) added to the media without His (shown on the right of the figure). The table on the left shows the pairs of pGAD424-*exe*D (two-codon mutants) and pGAD424-*exe*B (WT) used as the bait and prey in the assay. The pair of *exe*D and *exe*B was used as the positive control, while the pair of the empty vector pGBT9 and pGAD424 was used as the negative control.

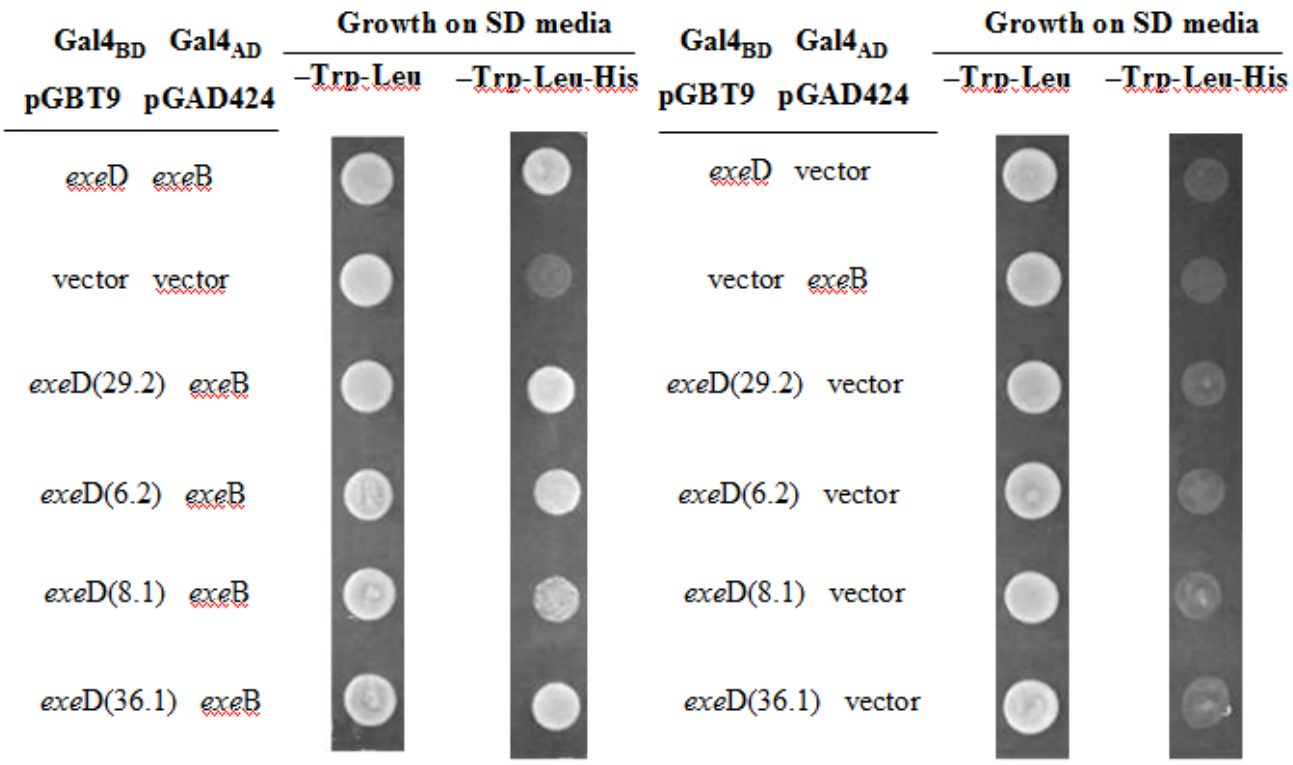

FIG. 3-5. *exe*D (two-codon mutants)-*exe*B (WT) two-hybrid interactions. (B) Autoactivation test of the positive interactions by the yeast two-hybrid assay. The panels on the left show the positive interactions between pGAD424-*exe*D (two-codon mutants) and pGAD424-*exe*B (WT), while the panels on the right show the autoactivation tests of these interactions. Co-transformed plasmids were maintained in the cell by growth on media without Trp and Leu (left columns of the figures). Positive interactions are observed on media without His after 60 h incubation at 30 °C (right columns of the figures). The tables on the left of each panel list the pairs of pGAD424-*exe*D (two-codon mutants) and pGAD424-*exe*B (WT) which shows interactions and the pairs of vector and *exe*B/D (WT) as well as *exe*D mutants used for the autoactivation test. The pair of *exe*D and *exe*B was used as the positive control, while the pair of the empty vectors pGBT9 and pGAD424 was used as the negative control.

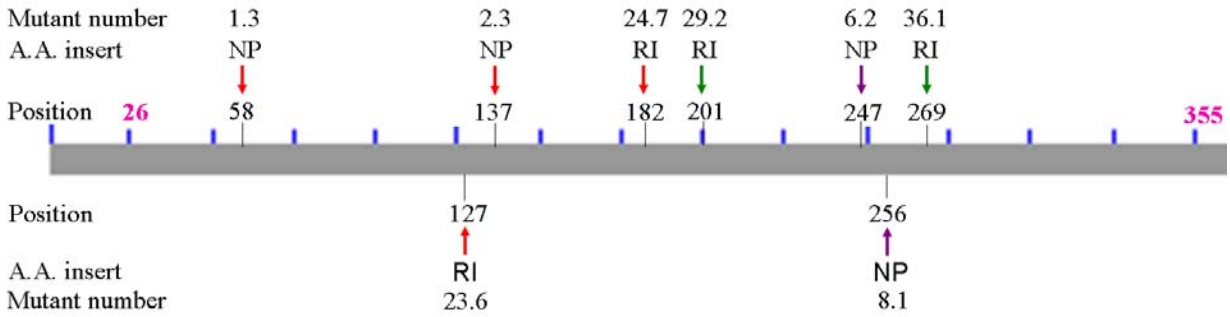

FIG. 3-6. Region of ExeD involved in the interaction between ExeD and ExeB. The region of ExeD involved in the ExeD-ExeB interaction was determined by the yeast two-hybrid assay between and ExeD (two-codon mutants) and ExeB (WT). The vertical arrows show the position of the mutants. The red arrow stands for complete inhibition of the ExeA-ExeD interaction, the purple arrows stand for partial inhibition, and the green arrows stand for no inhibition of the interaction.

TABLE 3-6. Interaction between pGBT9-*exe*D two-codon mutants and pGAD424-*exe*C

Bait	Prey	Inhibition by the conc. of 3-AT
pGBT9-*exe*D	pGAD424-*exe*C	0.2 mM
pGBT9-*exe*D (pVA 1.3.1)	pGAD424-*exe*C	No interaction
pGBT9-*exe*D (pVA 23.6.2)	pGAD424-*exe*C	No interaction
pGBT9-*exe*D (pVA2.3.2)	pGAD424-*exe*C	No interaction
pGBT9-*exe*D (pVA24.7.1)	pGAD424-*exe*C	No interaction
pGBT9-*exe*D (pVA29.2.2)	pGAD424-*exe*C	No interaction
pGBT9-*exe*D (pVA6.2.1)	pGAD424-*exe*C	No interaction
pGBT9-*exe*D (pVA8.1.1)	pGAD424-*exe*C	No interaction
pGBT9-*exe*D (pVA36.1.1)	pGAD424-*exe*C	0.2 mM

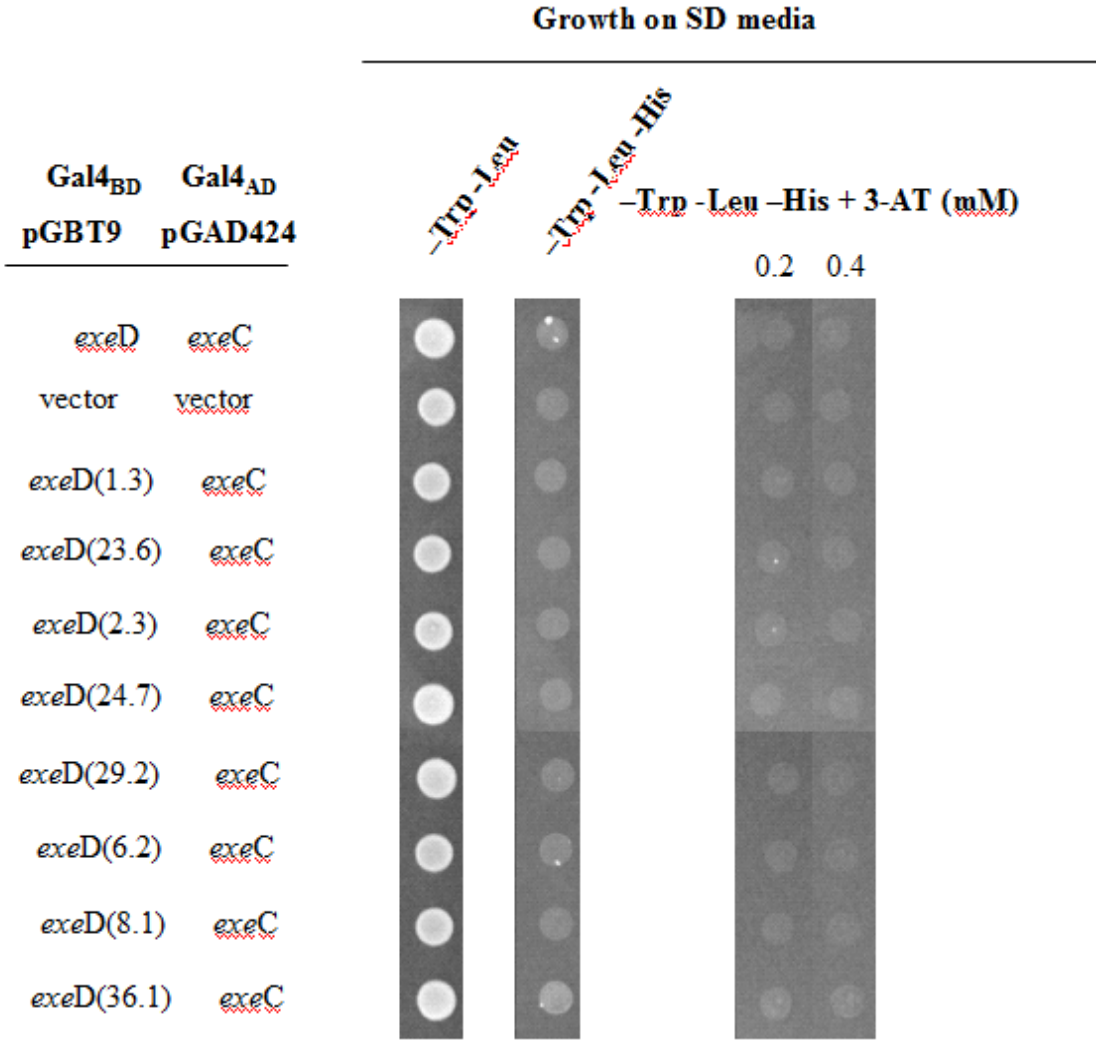

FIG. 3-7. *exe*D (two-codon mutants)-*exe*C (WT) two-hybrid interactions. (**A) *In vivo* interactions of *exe*D (two-codon mutants-)-*exe*C (WT) and the strength of the interactions determined by the yeast two-hybrid assay.** Yeast cells pJ69-4A transformed with $Gal4_{AD}$ and $Gal4_{BD}$ fusion constructs were used to test the interaction. Co-transformed plasmids were maintained in the cell by growth on media without Trp and Leu (shown on the left of the figure). Interactions of the hybrid proteins cause the expression of the *HIS3* reporter which allows growth on minimal medium lacking His. Positive interactions are observed on media without His after 72h incubation at 30 °C (shown in the middle of the figure). The strength of the interactions was determined with a gradient conc. of 3-AT (0.2-0.4 mM) added to the media without His (shown on the right of the figure). The table on the left shows the pairs of pGAD424-*exe*D (two-codon mutants) and pGAD424-*exe*C (WT) used as the bait and prey in the assay. The pair of *exe*D and *exe*C was used as the positive control, while the pair of the empty vectors pGBT9 and pGAD424 was used as the negative control.

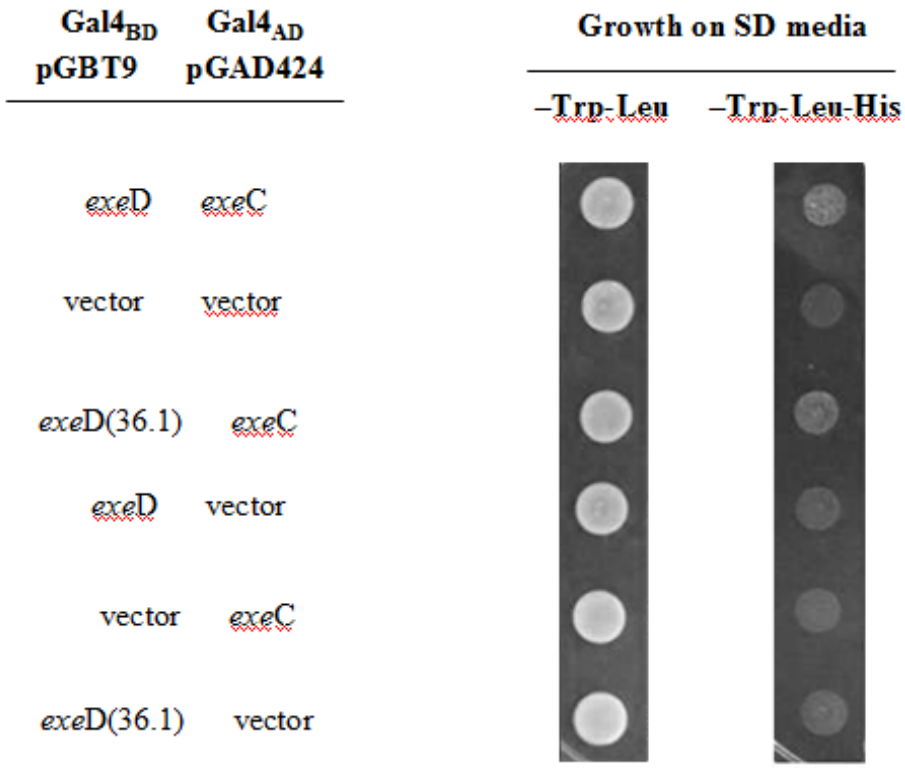

FIG. 3-7. *exe*D (two-codon mutants)-*exe*C (WT) two-hybrid interactions. (B) Autoactivation test of the positive interaction by the yeast two-hybrid assay. Yeast cells pJ69-4A transformed with $Gal4_{AD}$ and $Gal4_{BD}$ fusion constructs were used to test the interaction. Co-transformed plasmids were maintained in the cell by growth on media without Trp and Leu (left column of the figure). Positive interactions are observed on media without His after 60 h incubation at 30 °C (right column of the figure). The table on the left shows the pairs of fragments used in the test. The pair of vector/*exe*C and the pair of *exe*D (36.1)/vector are autoactivation tests of the pair of *exe*D (36.1)/*exe*C which shows positive interaction. The pair of vector/*exe*C and the pair of *exe*D/vector are autoactivation tests for the pair of *exe*D and *exe*C. The pair of *exe*D and *exe*C was used as the positive control, while the pair of the empty vectors pGBT9 and pGAD424 was used as the negative control.

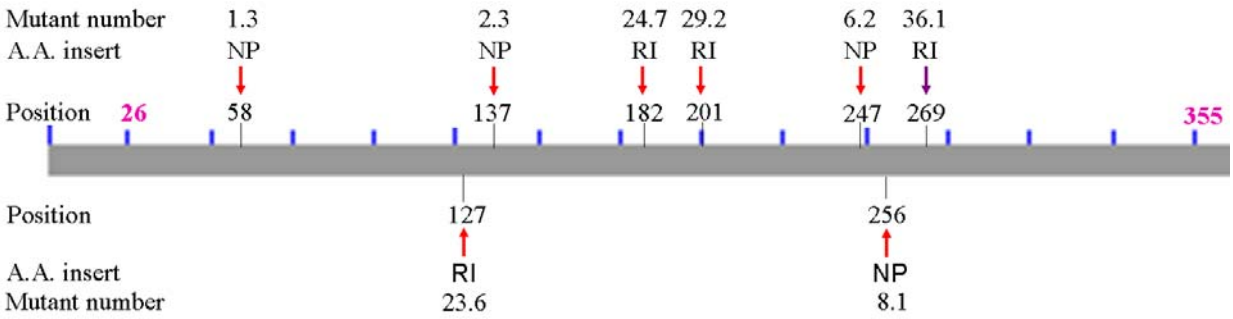

FIG. 3-8. Region of ExeD involved in the interaction between ExeD and ExeC. The region of ExeD involved in the ExeD-ExeC interaction was determined by the yeast two-hybrid assay between and ExeD (two-codon mutants) and ExeC (WT). The vertical arrows show the position of the mutants. The red arrow stands for complete inhibition of the ExeD-ExeC interaction, the purple arrows stand for partial inhibition.

3.3.4 Yeast two-hybrid assay of the interactions between pGBT9-*exe*D two-codon mutants and pGAD424-*exe*D, and between pGBT9-*exe*D and pGAD424-*exe*D two-codon mutants

The region involved in the ExeD dimerization was mapped in both directions by the yeast two-hybrid assay. *In vivo* interactions of pGBT9-*exe*D (two-codon mutants)-pGAD424-*exe*D (WT) and the strength of the interactions are shown in Table 3-7A and Fig. 3-9. An interaction between pGBT9-*exe*D (1.3) and pGAD424-*exe*D, and between pGBT9-*exe*D (36.1) and pGAD424-*exe*D were observed. These two interactions appeared stronger than that between the WT domains. The interaction was completely inhibited by all of the other mutations. In the other direction, two-hybrid assay of pGBT9-*exe*D (WT)-pGAD424-*exe*D (two-codon mutants) is shown in Table 3-7B and Fig. 3-10. The results indicated that there are three pairs of interactions, including pGBT9-*exe*D and pGAD424-*exe*D (1.3), pGBT9-*exe*D and pGAD424-*exe*D (23.6), and pGBT9-*exe*D and pGAD424-*exe*D (36.1), which were stronger than that of WT. In addition, there was a relatively weak interaction between pGBT9-*exe*D and pGAD424-*exe*D (2.3) which was inhibited by 0.6 mM 3-AT. In contrast, the interactions between pGBT9-*exe*D and the other pGAD424-*exe*D mutants were completely inhibited. The autoactivation test of the positive interactions in both directions is shown in Fig. 3-11. Autoactivation was only present between the bait vector pGBT9 and pGAD424-*exe*D (23.6). The strength of the interactions for the positive interaction and for the autoactivation of ExeD (WT) and the ExeD (23.6) mutant was determined and compared using 3-AT in the yeast two-hybrid assay (Table 3-7C, Fig. 3-12). Although there was autoactivation between pGBT9 and pGAD424-*exe*D (23.6), the interaction between pGBT9-*exe*D and pGAD424-*exe*D (pVA23.6) (inhibited by 1.2 mM 3-AT) was much stronger than the autoactivation (inhibited by 0.2 mM 3-AT), confirming the positive interaction between pGBT9-*exe*D and pGAD424-*exe*D (pVA23.6). In addition, the same test also found that there is a weak autoactivation between pGBT9 and pGAD424-*exe*D (pVA8.1) which can be inhibited by 0.2 mM 3-AT. However, neither direction of the yeast two-hybrid assay shows an interaction between ExeD (WT) and ExeD (8.1). Based on the two directions of the yeast two-hybrid assays, it can be concluded that from amino acid residue 182 to 256 of peri-ExeD is involved in the ExeD multimerization (Fig. 3-13).

TABLE 3-7A.Interactions between pGBT9-*exe*D two-codon mutants and pGAD424-*exe*D

Bait	Prey	Inhibition by the conc. of 3-AT
pGBT9-*exe*D	pGAD424-*exe*D	1.2 mM
pGBT9-*exe*D (pVA 1.3.1)	pGAD424-*exe*D	>1.2 mM
pGBT9-*exe*D (pVA 23.6.2)	pGAD424-*exe*D	No interaction
pGBT9-*exe*D (pVA2.3.2)	pGAD424-*exe*D	No interaction
pGBT9-*exe*D (pVA24.7.1)	pGAD424-*exe*D	No interaction
pGBT9-*exe*D (pVA29.2.2)	pGAD424-*exe*D	No interaction
pGBT9-*exe*D (pVA6.2.1)	pGAD424-*exe*D	No interaction
pGBT9-*exe*D (pVA8.1.1)	pGAD424-*exe*D	No interaction
pGBT9-*exe*D (pVA36.1.1)	pGAD424-*exe*D	>1.2mM

TABLE 3-7B. Interactions between pGBT9-*exe*D and pGAD424-*exe*D two-codon mutants

Bait	Prey	Inhibition by the conc. of 3-AT
pGBT9-*exe*D	pGAD424-*exe*D	1.2 mM
pGBT9-*exe*D	pGAD424-*exe*D (pVA 1.3.1)	>1.2 mM
pGBT9-*exe*D	* pGAD424-*exe*D (pVA 23.6.2)	>1.2 mM
pGBT9-*exe*D	pGAD424-*exe*D (pVA2.3.2)	0.6 mM
pGBT9-*exe*D	pGAD424-*exe*D (pVA24.7.1)	No interaction
pGBT9-*exe*D	pGAD424-*exe*D (pVA29.2.2)	No interaction
pGBT9-*exe*D	pGAD424-*exe*D (pVA6.2.1)	No interaction
pGBT9-*exe*D	* pGAD424-*exe*D (pVA8.1.1)	No interaction
pGBT9-*exe*D	pGAD424-*exe*D (pVA36.1.1)	>1.2 mM

*the mutants can autoactivate with the empty vector

TABLE 3-7C. Autoactivations of pGBT9-*exe*D and pGAD424-*exe*D two-codon mutants

Bait	Prey	Inhibition by the conc. of 3-AT
pGBT9-*exe*D	pGAD424-*exe*D	>1.2
pGBT9	pGAD424	No interaction
pGBT9	pGAD424-*exe*D (pVA 23.6.2)	0.2mM
pGBT9-*exe*D	pGAD424-*exe*D (pVA 23.6.2)	>1.2
pGBT9	pGAD424-*exe*D (pVA8.1.1)	0.2mM
pGBT9-*exe*D	pGAD424-*exe*D (pVA8.1.1)	No interaction

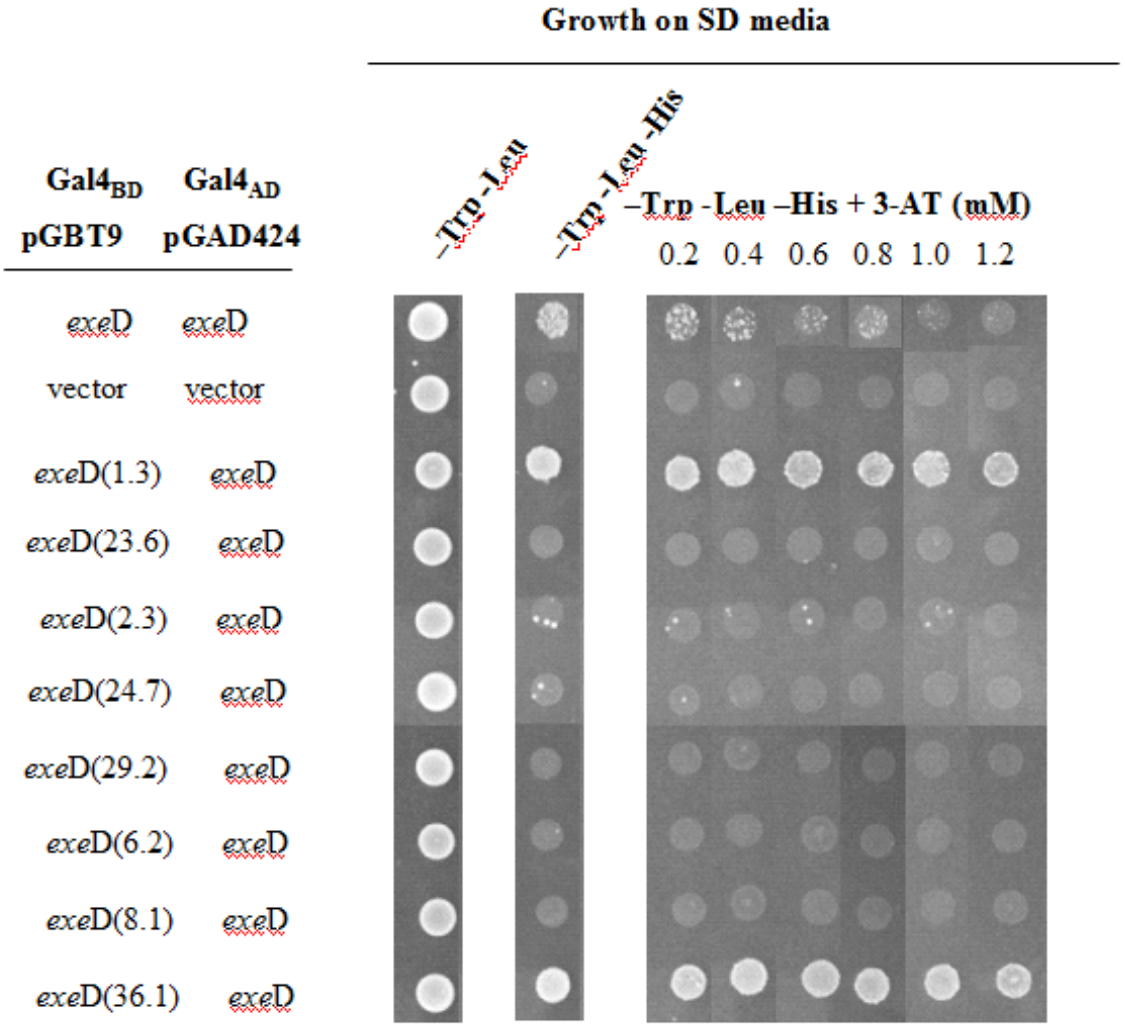

FIG. 3-9. *exe*D (two-codon mutants)-*exe*D (WT) two-hybrid interactions. *In vivo* interactions of *exe*D (two-codon mutants-)-*exe*D (WT) and the strength of the interactions were determined by the yeast two-hybrid assay. Yeast cells pJ69-4A transformed with $Gal4_{AD}$ and $Gal4_{BD}$ fusion constructs were used to test the interaction. Co-transformed plasmids were maintained in the cell by growth on media without Trp and Leu (shown on the left of the figure). Positive interactions are observed on media without His after 72 h incubation at 30 °C (shown in the middle of the figure). The strength of the interactions was determined with a gradient conc. of 3-AT (0.2-1.2 mM) added to the media without His (shown on the right of the figure). The table on the left shows the pairs of pGBT9-*exe*D (two-codon mutants) and pGAD424-*exe*D (WT) used as the bait and prey in the assay. The pair of *exe*D and *exe*D was used as the positive control, while the pair of the empty vectors pGBT9 and pGAD424 was used as the negative control.

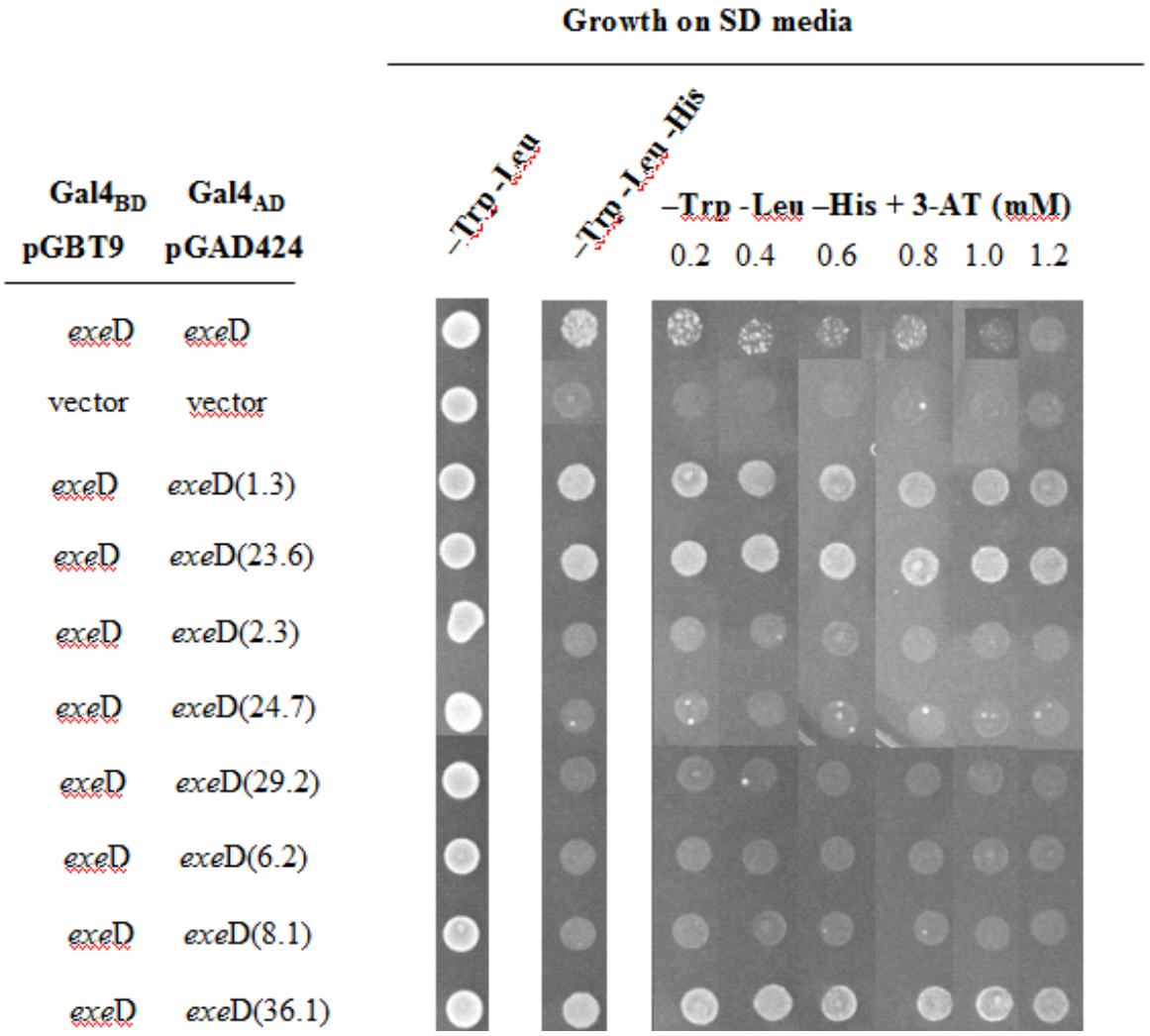

FIG. 3-10. *exe*D (WT)-*exe*D (two-codon mutants) two-hybrid interactions. *In vivo* interactions of *exe*D (WT)-*exe*D (two-codon mutants) and the strength of the interactions were determined by the yeast two-hybrid assay. Yeast cells pJ69-4A transformed with $Gal4_{AD}$ and $Gal4_{BD}$ fusion constructs were used to test the interaction. Co-transformed plasmids were maintained in the cell by growth on media without Trp and Leu (shown on the left of the figure). Positive interactions are observed on media without His after 72 h incubation at 30 °C (shown in the middle of the figure). The strength of the interactions was determined with a gradient conc. of 3-AT (0.2-1.2 mM) added to the media without His (shown on the right of the figure). The table on the left shows the pairs of pGBT9-*exe*D (WT) and pGAD424-*exe*D (two-codon mutants) used as the bait and prey in the assay. The pair of *exe*D and *exe*D was used as the positive control, while the pair of the empty vectors pGBT9 and pGAD424 was used as the negative control.

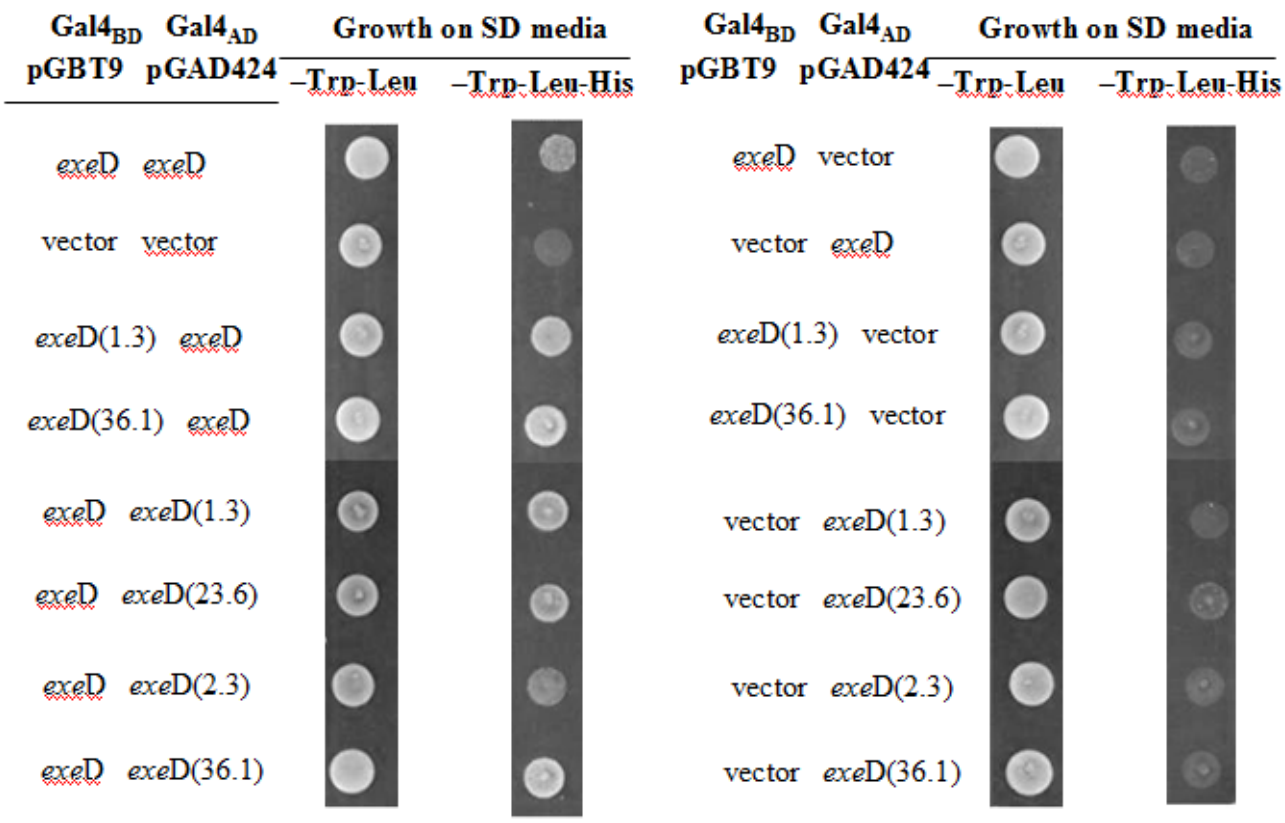

FIG. 3-11. Autoactivation test of *exe*D (two-codon mutants)-*exe*D (WT) and *exe*D (WT)-*exe*D (two-codon mutants). Autoactivation test of the positive interactions was determined by the yeast two-hybrid assay. The panels on the left show the positive interactions of pGBT9-*exe*D (two-codon mutants)-pGAD424-*exe*D (WT) and pGBT9-*exe*D (WT)-pGAD424-*exe*D (two-codon mutants), while the panels on the right show the autoactivation test of these interactions. Co-transformed plasmids were maintained in the cell by growth on media without Trp and Leu (left columns of the panels). Positive interactions are observed on media without His after 60 h incubation at 30 °C (right columns of the panels). The table on the left shows the pairs of pGBT9-*exe*D (two-codon mutants) and pGAD424-*exe*D (WT) as well as the pairs of pGBT9-*exe*D (WT)-pGAD424-*exe*D (two-codon mutants) used for determination of the positive interactions, while the table in the middle shows the pair of vector and WT of *exe*D as well as the *exe*D mutants used for the autoactivation test. The pair of *exe*D and *exe*D was used as the positive control, while the pair of the empty vectors pGBT9 and pGAD424 was used as the negative control.

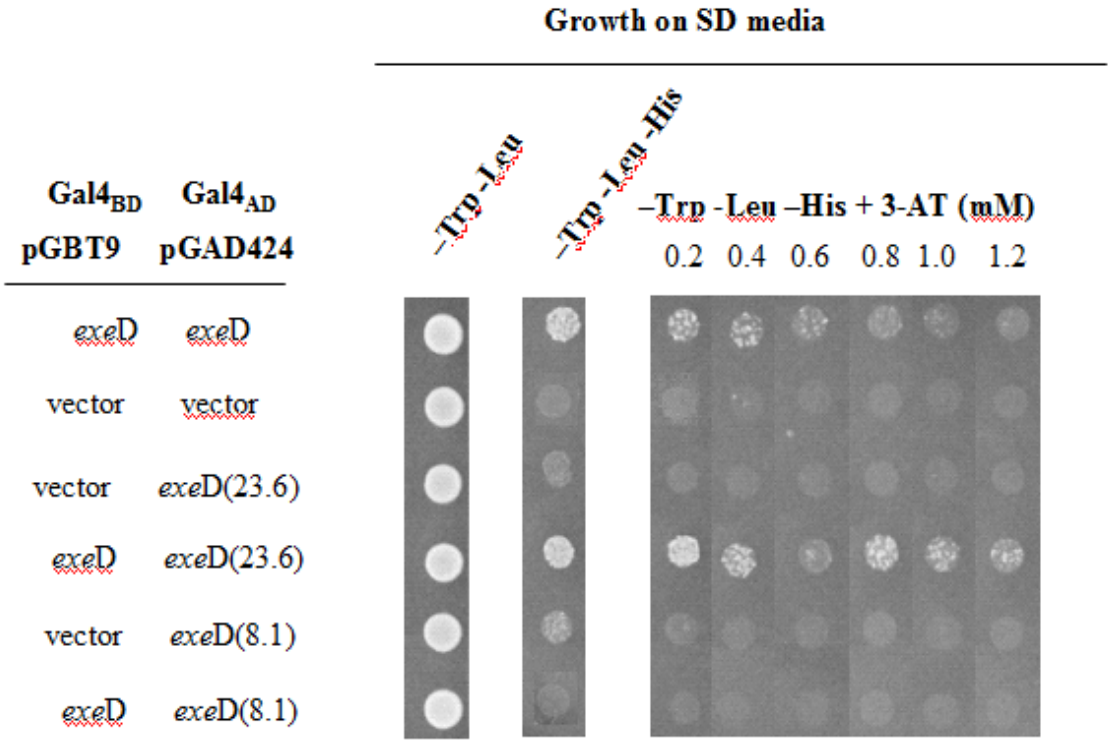

FIG. 3-12. Comparison of the strength of interactions between positive interaction and autoactivation of *exe*D (WT)-*exe*D (two-codon mutants) by the yeast two-hybrid assay. Yeast cells pJ69-4A transformed with $Gal4_{AD}$ and $Gal4_{BD}$ fusion constructs were used to test the interaction. Co-transformed plasmids were maintained in the cell by growth on media without Trp and Leu (shown on the left of the figure). Positive interactions are observed on media without His after 72 h incubation at 30 °C (shown in the middle of the figure). The strength of the interactions was determined with a gradient conc. of 3-AT (0.2-1.2 mM) added to the media without His (shown on the right of the figure). The table on the left shows the pairs of fragment used in the test. The pair of vector/*exe*D (23.6) and the pair of vector/*exe*D (8.1) show the autoactivation for the *exe*D-*exe*D (23.6) and *exe*D-*exe*D (8.1) interactions respectively. The pair of *exe*D and *exe*D was used as the positive control, while the pair of the empty vectors pGBT9 and pGAD424 was used as the negative control.

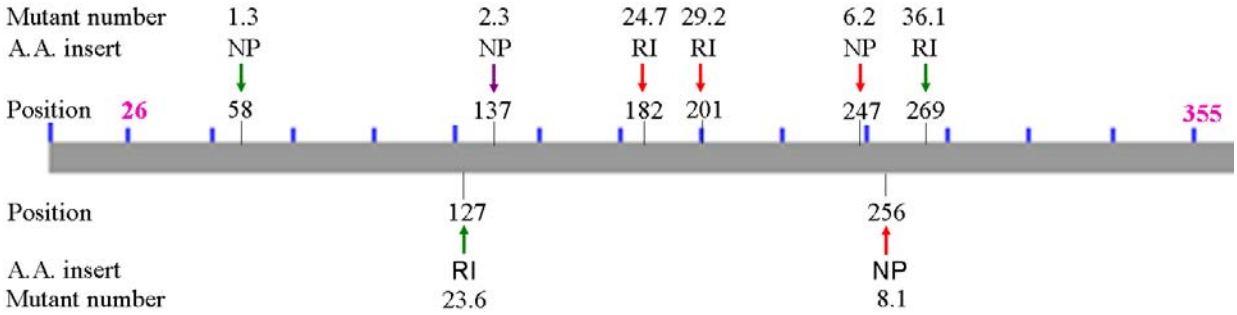

FIG. 3-13. Region of ExeD involved in ExeD multimerization. The region of ExeD involved in the ExeD-ExeD interaction was determined by the yeast two-hybrid assay between and ExeD (two-codon mutants) and ExeD (WT) in both directions. The vertical arrows show the position of the mutants. The red arrow stands for complete inhibition of the ExeA-ExeD interaction, the purple arrows stand for partial inhibition, and the green arrows stand for remaining of the interaction.

3.4 Yeast two-hybrid assay of *exe*D deletion mutants and *exe*A, B, C and D

The yeast two-hybrid assay of the ExeD two-codon mutants identified the regions of ExeD that were involved in the interactions; however, the mutations may alter the global structure of the proteins, meaning that a two-codon insertion mutation that interferes with the interaction may not correctly identify the region involved in that interaction. Therefore, based on the results of the two-hybrid assays, ExeD deletion mutants were constructed and the yeast two-hybrid assay was repeated. To construct the ExeD deletion mutants, the fragments which were suggested to be involved in the interactions as well as the regions which did not appear responsible for the interactions were cloned into pGBT9 and pGAD424 respectively, as described in 2.7.3. The ExeD deletion mutants used for the assay are shown in Fig. 3-14.

In vivo interactions between ExeA, B C and D (WT) and ExeD (deletion mutants) as well as autoactivation of all positive interactions were determined by the yeast two-hybrid assay (Table 3-8, Fig. 3-15, 3-16 and 3-17). The results showed that there were interactions between pGBT9-*exe*A and pGAD424-*exe*D:Δ201-355, between pGBT9-*exe*D:Δ201-355 and pGAD424-*exe*B, and between pGBT9-*exe*D:Δ201-355 and pGAD424-*exe*C which indicated that the ExeD fragment, from amino acid residue 26 to 200, is involved in the protein-protein interactions between secretin ExeD and each of the other components. No autoactivation of the positive interactions occurred in the assay. The interaction between pGBT9-*exe*D:Δ201-355 and pGAD424-*exe*C was not stable and sometimes could not be observed. The interaction could only be detected when cultures at an OD_{600} of 7-10 were used (Fig. 3-17). The interaction was even weaker than the GBT9-*exe*D (WT) and pGAD424-*exe*C (WT), which is the weakest among the interactions determined in this study. These results correspond to the yeast two-hybrid assay of the ExeD (two-codon mutants) and ExeA, B and C (WT), which showed protein-protein interactions between the respective proteins and ExeD with mutations in the first half of the fragment were completely inhibited while the last half showed weak or medium weak interactions. However, no interaction occurred between pGBT9-*exe*A and pGAD424-*exe*D:Δ121-355, perhaps because the structure of the protein fragment was not appropriate for the protein-protein interaction in yeast. Similarly, no interaction was found between the full length ExeD protein fragment and any of the ExeD deletion mutants as shown in Table 3-8.

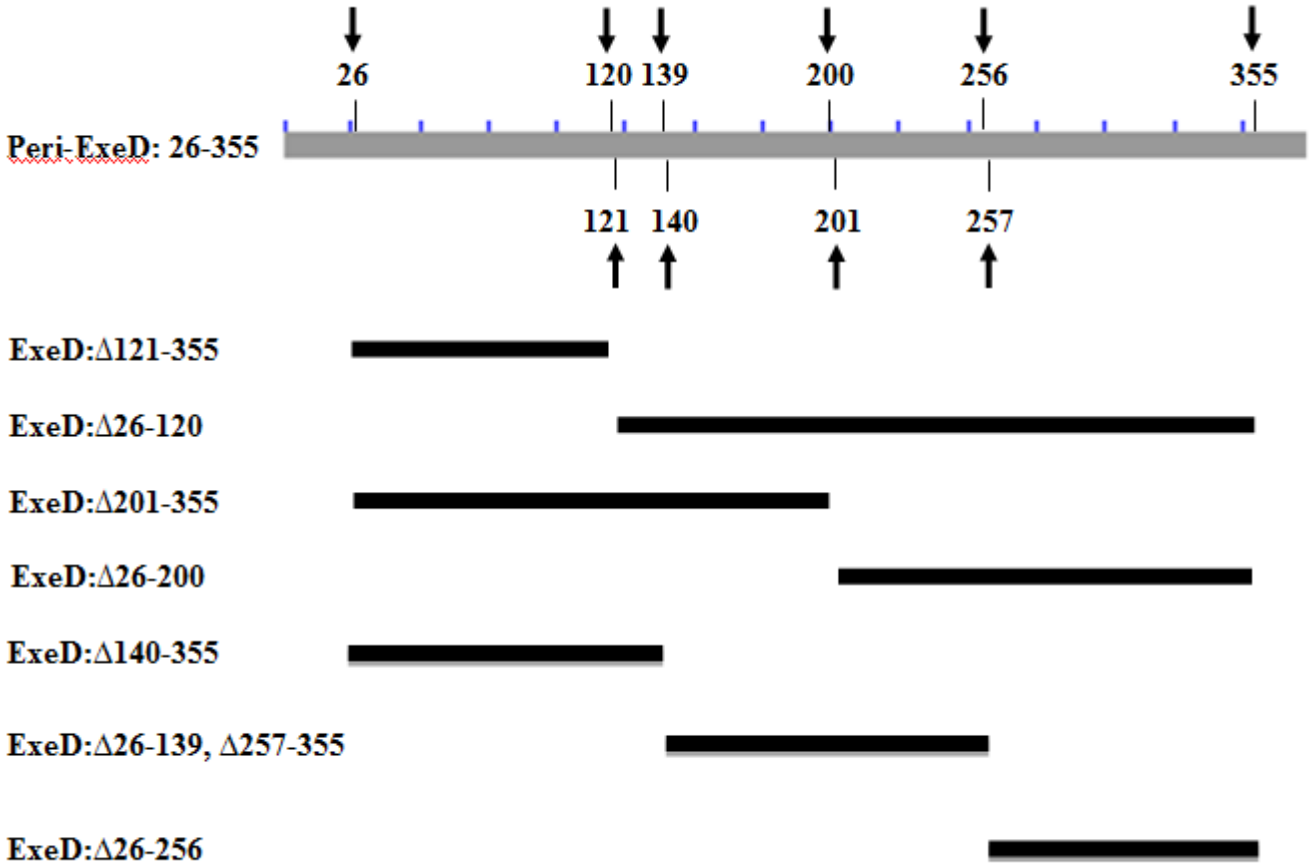

FIG. 3-14. Construction of the peri-*exe*D deletion mutants. The grey bar on the top shows the peri-*exe*D, the thinner black bars shows the fragments of *exe*D used in the assay. Fragments 26-120 and 121-355 were cloned into pGBT9 respectively and used as prey for yeast 2-hybrid assays of *exe*A and *exe*D interactions. Fragments 26-200 and 201-355 were cloned into both pGBT9 and pGAD424 and used as bait and prey for yeast 2-hybrid assays of *exe*D (deletion mutants) and *exe*A, B, C and D (WT). In addition, fragments 26-139, 140-256 and 257-355 were cloned into both pGBT9 and pGAD424 and used as bait and prey for yeast 2-hybrid assays of *exe*D (deletion mutants) and *exe*D (WT).

TABLE 3-8. Yeast two-hybrid assay between *exe*D deletion mutants and *exe*A, B, C, D

Bait	Prey	Interaction
pGBT9-*exe*A	pGAD424-*exe*D:Δ121-355	No
pGBT9-*exe*A	pGAD424-*exe*D:Δ26-120	No
pGBT9-*exe*A	pGAD424-*exe*D:Δ201-355	**Yes**
pGBT9-*exe*A	pGAD424-*exe*D:Δ26-200	No
pGBT9-*exe*D:Δ201-355	pGAD424-*exe*B	**Yes**
pGBT9-*exe*D:Δ26-200	pGAD424-*exe*B	No
pGBT9-*exe*D:Δ201-355	pGAD424-*exe*C	**Yes**
pGBT9-*exe*D:Δ26-200	pGAD424-*exe*C	No
pGBT9-*exe*D:Δ140-355	pGAD424-*exe*D	No
pGBT9-*exe*D:Δ26-139, Δ257-355	pGAD424-*exe*D	No
pGBT9-*exe*D:Δ26-256	pGAD424-*exe*D	No
pGBT9-*exe*D	pGAD424-*exe*D:Δ140-355	No
pGBT9-*exe*D	pGAD424-*exe*D:Δ26-139, Δ257-355	No
pGBT9-*exe*D	pGAD424-*exe*D:Δ26-256	No
pGBT9-*exe*D:Δ201-355	pGAD424-*exe*D	No
pGBT9-*exe*D:Δ26-200	pGAD424-*exe*D	No
pGBT9-*exe*D	pGAD424-*exe*D:Δ201-355	No
pGBT9-*exe*D	pGAD424-*exe*D:Δ26-200	No

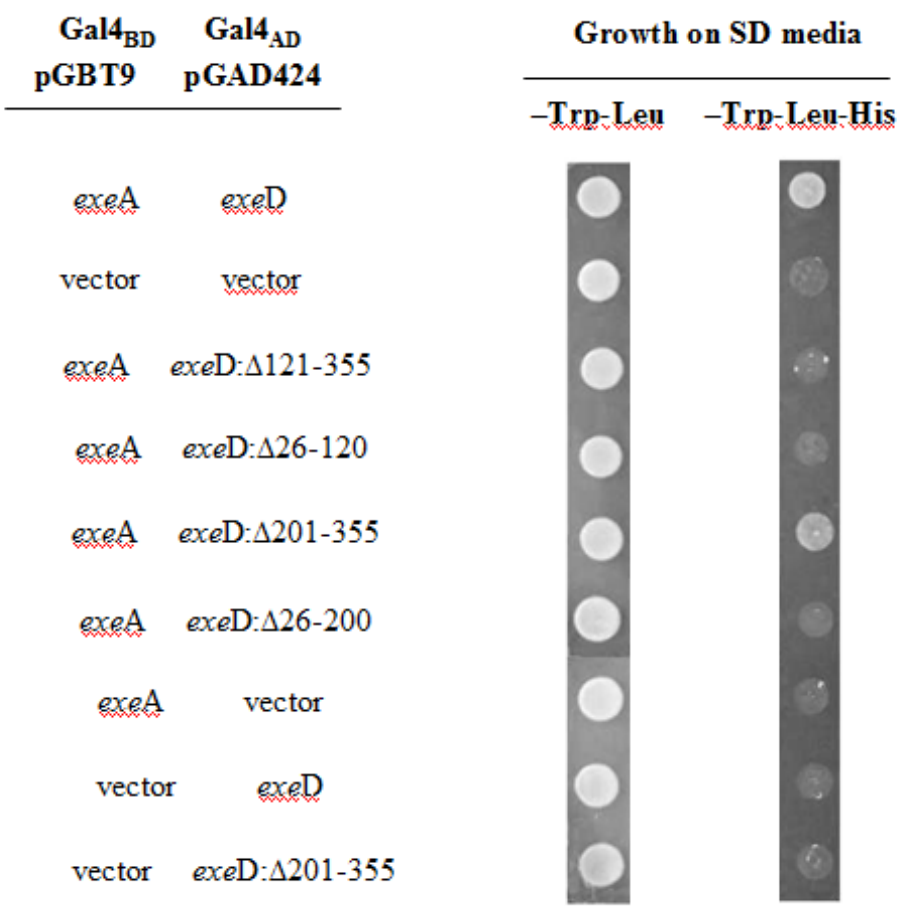

FIG. 3-15. *exe*A (WT)-*exe*D (deletion mutants) two-hybrid interaction. *In vivo* interactions between pGBT9-*exe*A (WT) and pGAD424-*exe*D (deletion mutants) as well as the autoactivation tests for the positive interaction were determined by the yeast two-hybrid assay. Co-transformed plasmids were maintained in the cell by growth on media without Trp and Leu (left column of the figure). Positive interactions are observed on media without His after 60 h incubation at 30 °C (right column of the figure). The table on the left shows the pairs of fragment used in the test. The pair of *exe*A/vector and the pair of vector/*exe*D:Δ201-355 are autoactivation tests of the pair of *exe*A/*exe*D:Δ201-355 which shows positive interaction. The pair of *exe*A/vector and the pair of vector/*exe*D are autoactivation tests of the pair of *exe*A/*exe*D which was used as the positive control, the pair of the empty vector pGBT9 and pGAD424 was used as the negative control.

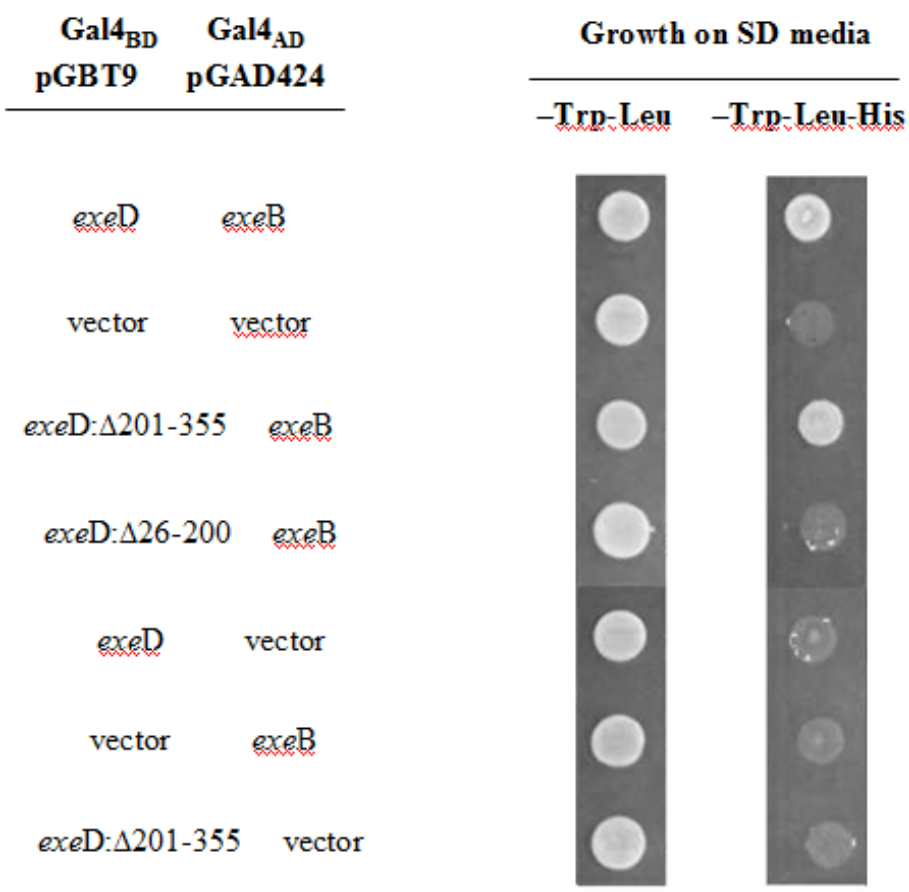

FIG. 3-16. *exe*D (deletion mutants)-*exe*B (WT) two-hybrid interaction. *In vivo* interactions between pGBT9-*exe*D (deletion mutants) and pGAD424-*exe*B (WT) as well as autoactivation test for the positive interaction were determined by the yeast two-hybrid assay. Co-transformed plasmids were maintained in the cell by growth on media without Trp and Leu (left column of the figure). Positive interactions are observed on media without His after 60 h incubation at 30 °C (right column of the figure). The table on the left shows the pairs of fragments used in the test. The pair of *exe*D:Δ201-355/vector and the pair of vector/*exe*B are autoactivation tests for the pair of *exe*D:Δ201-355/*exe*B which shows positive interaction. The pair of vector/*exe*B and the pair of *exe*D/vector are autoactivation tests for the pair of *exe*D/*exe*B which was used as the positive control, the pair of the empty vector pGBT9 and pGAD424 was used as the negative control.

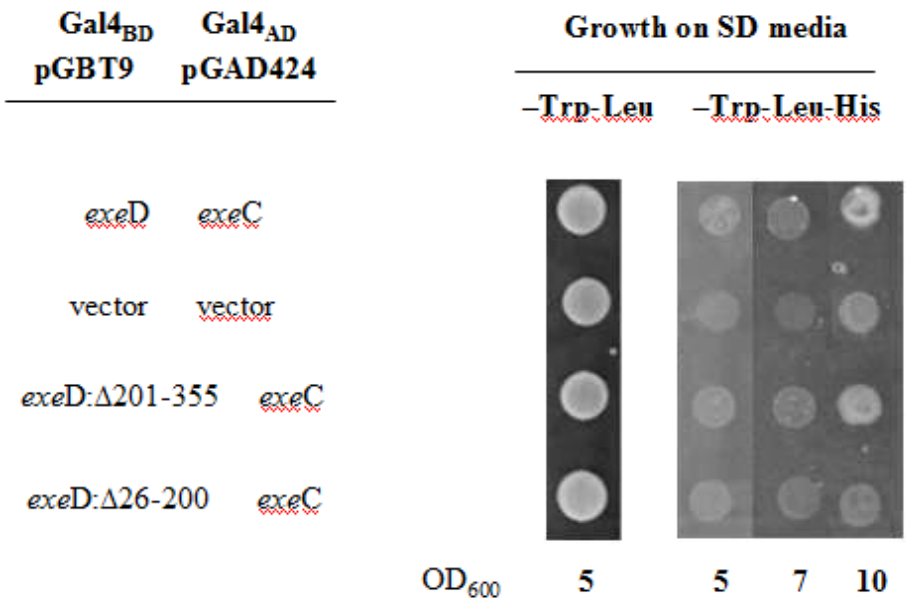

FIG. 3-17. *exe*D (deletion mutants)-*exe*C (WT) two-hybrid interaction. Co-transformed plasmids were maintained in the cell by growth on media without Trp and Leu (left column of the figure). Positive interactions are observed on media without His after 72 h incubation at 30 °C (right column of the figure). The table on the left shows the pairs of fragments used in the test. The pair of vector/*exe*C and the pair of *exe*D (36.1)/vector are autoactivation tests for the pair of *exe*D (36.1)/*exe*C which shows positive interaction. The pair of vector/*exe*C and the pair of *exe*D/vector are autoactivation test of the pair of *exe*D/*exe*C. The pair of *exe*D and *exe*C was used as the positive control, while the pair of the empty vectors pGBT9 and pGAD424 was used as the negative control.

3.5 Assay of the interactions between ExeD and ExeA, B, C and D via co-purification

3.5.1 Induction of the constructed bait and prey plasmids

In order to further confirm the interactions between the Exe proteins (WT) identified in the yeast two-hybrid assays, co-purification tests were performed. In this experiment, the bait plasmids, N-terminal His tag pET30-*exe*A and *exe*B, and N-terminal His tag pET47-*exe*C and *exe*D, as well as the prey plasmids, pCDFDuet-*exe*A, B, C and D were constructed as described in 2.7.4. Expression of the constructed His tag and S tag Exe proteins were examined as described in 2.7.5. SDS-PAGE showed that all the proteins express well except that pCDFDuet-*exe*C could not be induced (Table 3-9, Fig. 3-18A). However, the induction of pCDFDuet-*exe*C could be detected by immunoblot (Fig. 3-18B) which indicated that the clone was correct but did not express well. Therefore, pCDFDuet-*exe*C could not be used for the co-purification test.

3.5.2 Co-purification of pET30-*exe*A and pCDFDuet-*exe*D

In order to confirm the positive interactions between ExeD and ExeA, B, C and D identified by the yeast two-hybrid assay, the pET30 and pET47b His-tag fused protein and pCDFDuet unfused proteins were constructed as described in 2.7.4, and co-purification was assayed in both directions using metal-chelate affinity chromatography as described in 2.9. The samples were analysed by SDS-PAGE and immunoblot as described in 2.10. For pET30-*exe*A and pCDFDuet-*exe*D, samples comprised of the cell lysate of pET30-*exe*A (bait), pCDFDuet-*exe*D (prey), and a mixture of pET30-*exe*A and pCDFDuet-*exe*D lysates were applied to a Ni-NTA column individually. The sample was then washed with the binding buffer and eluted with binding buffer containing 10-500 mM imidazole (Fig. 3-19A). Fractions A1 to B6 contain the flow through of the mixture which contains material not bound to the column (not shown). A peak appears in the elution gradient from fraction C6 to C11 which contains the His-ExeA. This peak was also observed in the chart of pET30-*exe*A alone (data not shown). Similarly, Fig. 3-19B shows the chromatograph for the bait pCDFDuet-*exe*D. In this case, a very small peak eluted during the elution gradient.

TABLE 3-9. Expression of the Exe proteins

Lane	Sample	MW (kDa)	Expression
1-3	pCDFDuet-*exe*B	20.7	Yes
4-6	pET30-*exe*B	19.0	Yes
7-9	pET47-*exe*C	27.3	Yes
10-12	pCDFDuet-*exe*C	28.7	No
13-15	pCDFDuet-*exe*A	30.7	Yes
16-18	pET30-*exe*A	30.0	Yes
19-21	pCDFDuet-*exe*D	38.2	Yes
22-24	pET47-*exe*D	36.8	Yes

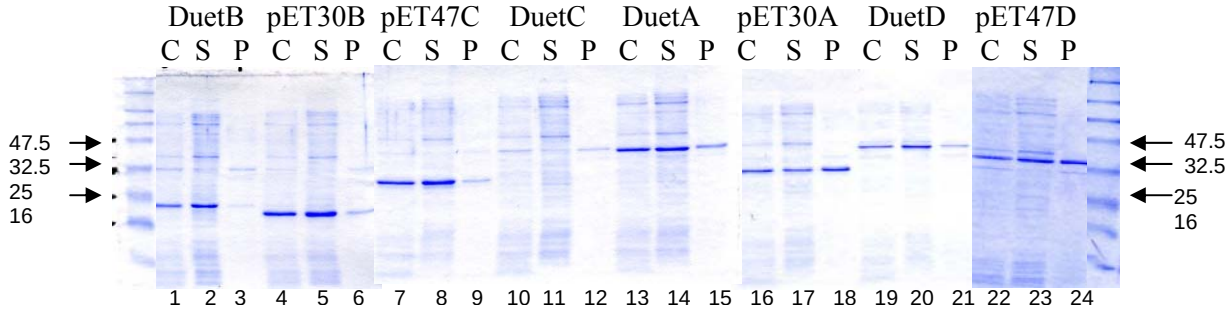

FIG. 3-18A. Determination of Exe protein induction by SDS-PAGE. The His-tag (pET30, pET47) and S-tag (pCDFDuet) Exe plasmids were electroporated to BL21 and induced with 1 mM IPTG for 3 h as described in 2.7.4. Culture, supernatant (soluble cytoplasmic fraction) and pellet (inclusion bodies) of each protein were examined. Cultures were harvested after 3-h induction; supernatants and pellets were collected via centrifugation at 31, 000 × g for 20 min or 19, 8000 × g for 20 min after French pressure cell lysis at 1, 000 p.s.i. Pellets were resuspended in 10 ml NTA buffer A. Samples were mixed with 2 × sample buffer and heated at 95 ºC for 3 min. 5µl of each sample was loaded on a 12% SDS-PAGE gel. C: culture, S: supernatant, P: pellet.

FIG. 3-18B. Determination of pCDFDuet-*exe*C induction by immunoblot. The sample used for the blot was the same as the SDS-PAGE of Fig. 3-18A. The ExeC expression was determined by Anti-ExeC immunoblot. The film was developed for 5 s. C: culture, S: supernatant, P: pellet.

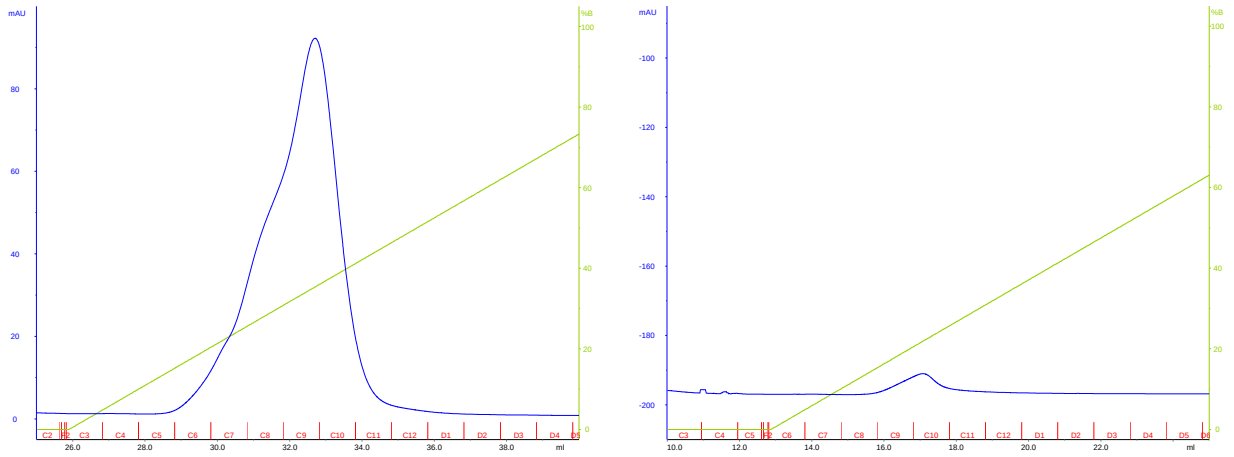

A **B**

FIG. 3-19. A. Co-purification of pET30-*exe*A and pCDFDuet-*exe*D via FPLC. BL21 cells containing pET30-*exe*A and pCDFDuet-*exe*D were induced and extracted as described in 2.9. The cell lysates of pET30-*exe*A and pCDFDuet-*exe*D were mixed and incubated at 4 °C for 5 h. After equilibration of the Ni-NTA agarose column, the mixture was then applied to the column which was washed with binding buffer and then eluted with a gradient of binding buffer containing 10-500 mM imidazole. **B. Determination of the binding of pCDFDuet-*exe*D to Ni-NTA column.** BL21 cells containing pCDFDuet-*exe*D were induced and extracted as described in 2.9. The cell lysate was applied to the Ni-NTA agarose column, which was washed with binding buffer and then eluted with a gradient of binding buffer containing 10-500 mM imidazole.

SDS-PAGE gels were run on the various column fractions, and the gels stained with coomassie blue or used to prepare an anti-ExeD immunoblot. As shown in Fig. 3-20, the His-ExeA fragment of 30 kDa appears in fractions C7 to C11 in the elution of the pET30-*exe*A and pCDFDuet-*exe*D mixture, with the peak occurring in fraction 9. This indicates that pET30-*exe*A bound to the column properly as the bait. There is also a prominent ExeD fragment of 38.2 kDa, in both the pET30-*exe*A + pCDFDuet-*exe*D extracts and the flow through fractions, indicating that it did not bind to the column as expected. To determine if small amounts of the ExeD fragment had bound to ExeA in the pET30-*exe*A + pCDFDuet-*exe*D extracts, an immunoblot using anti-ExeD antibody was performed on the peak His-ExeA fractions from the pET30-*exe*A + pCDFDuet-*exe*D extract fractionation and on the corresponding fractions from the pCDFDuet-*exe*D extract fractionation. As shown in Fig. 3-21, the 38.2 kDa ExeD fragment is observed in the His-ExeA elution fragments, but not in the corresponding fractions when the pCDFDuet-*exe*D extract alone was fractionated on the column. Therefore, it can be concluded that there is an *in vitro* interaction between ExeA and ExeD, confirming the yeast two-hybrid assay results.

Because the level of apparent ExeD binding was very low, a second co-purification test of pET30-*exe*A and pCDFDuet-*exe*D was performed with increased amounts of cell lysate. This time 100 ml cultures were grown and the pellet was re-suspended in 5 ml binding buffer. 1 ml of the cell lysates or mixed lysates was loaded to the Ni-NTA column. The chromatographs are shown as Fig. 3-22A, B, C. The SDS-PAGE gels again showed that the 30 kDa His-ExeA eluting in the imidazole gradient (Fig. 3-23). In this case however even on the coomassie blue stained gel, a band that appeared to be 38.2 kDa ExeD fragment could be observed in the His-ExeA peak fractions from the pET30-*exe*A + pCDFDuet-*exe*D extracts fractionation. This fragment was also detected in the anti-ExeD immunoblot of the pET30-*exe*A + pCDFDuet-*exe*D extracts imidazole gradient elution fractions, but only very faintly in the corresponding elution fractions from the column to which only the pCDFDuet-*exe*D extract had been applied (Fig. 3-24A). However, the immunoblot revealed a strongly reacting band of 27 kDa and also a band of 47 kDa in the pET30-*exe*A + pCDFDuet-*exe*D extracts elution fractions. A further anti-ExeD immunoblot on the various extracts showed that the fragment of 27 kDa was neither a fragment of ExeD nor a fragment of ExeA because it occurred in the extracts of both pET30-*exe*A and pCDFDuet-*exe*D (Fig. 3-24B). It co-binds with ExeA but not ExeD because it did

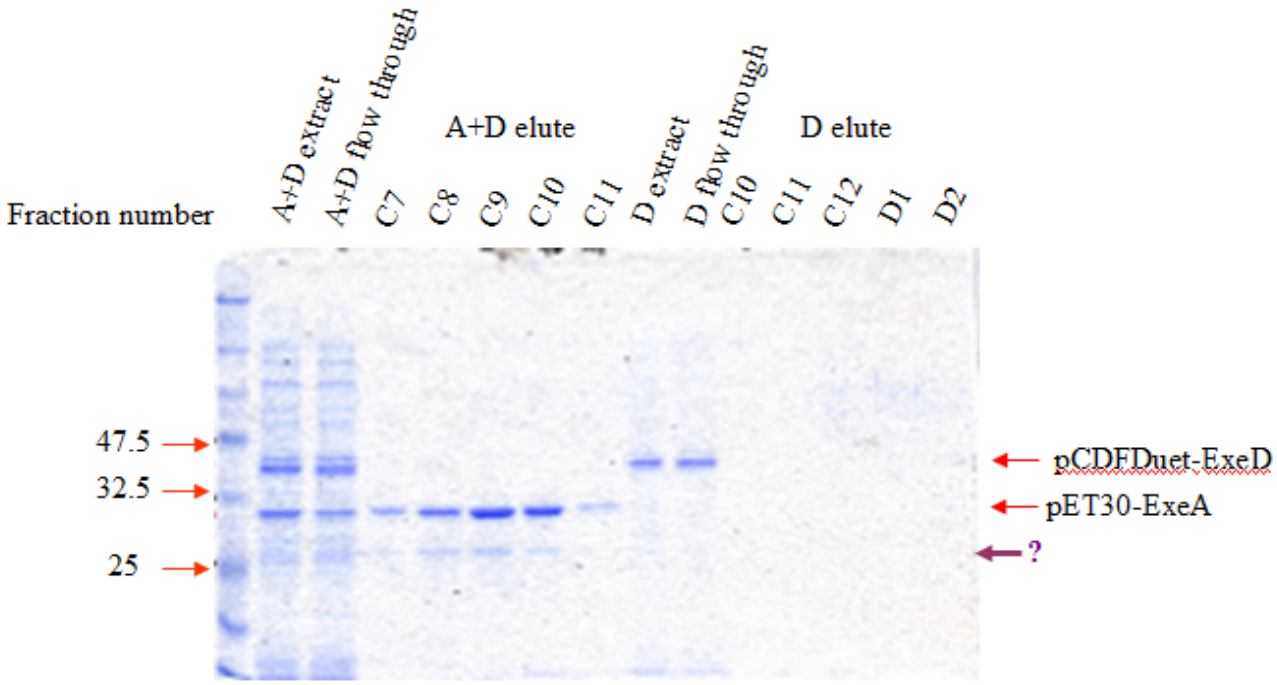

FIG. 3-20. SDS-PAGE of pET30-*exe*A + pCDFDuet-*exe*D elution and pCDFDuet-*exe*D elution. 10% SDS-PAGE showing the co-purification of the peri-ExeD expressed from pCDFDuet-*exe*D (38.2 kDa) with the His-tagged **peri-ExeA** expressed from pET30-*exe*A (30 kDa). The extract and flow through of pET30-*exe*A + pCDFDuet-*exe*D, and the imidazole gradient elution fractions following the application of a mixture of cell extracts from cells containing pET30-*exe*A + pCDFDuet-*exe*D are shown on the left, while the extract and flow through of pCDFDuet-*exe*D, the elution fractions of an extract from cells containing only pCDFDuet-*exe*D are shown on the right.

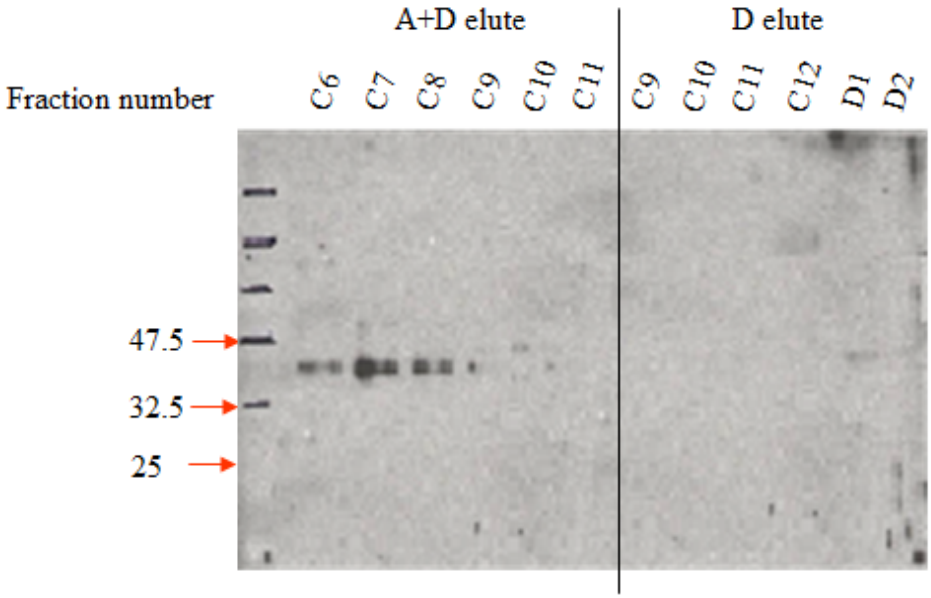

FIG. 3-21. Immunoblot of pET30-*exe*A + pCDFDuet-*exe*D elution and pCDFDuet-*exe*D elution. Anti-ExeD immunoblot showing the co-purification of the peri-ExeD expressed from pCDFDuet-*exe*D (38.2 kDa) with the His-tagged **peri-ExeA** expressed from pET30-*exe*A (30 kDa). The imidazole gradient elution fractions following the application of a mixture of cell extracts from cells containing pET30-*exe*A and pCDFDuet-*exe*D are shown on the left, while the elution fractions of an extract from cells containing only pCDFDuet-*exe*D are shown on the right. Anti-ExeD antiserum was used at a dilution of 1:50, 000, and the film was developed for 3 min.

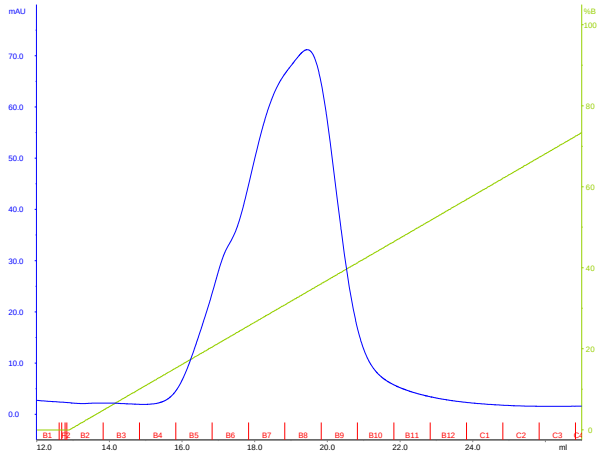

FIG. 3-22A. Co-purification of pET30-*exe*A and pCDFDuet-*exe*D via FPLC. BL21 cells containing pET30-*exe*A and pCDFDuet-*exe*D were induced and extracted as described in 2.9. The cell lysates of pET30-*exe*A and pCDFDuet-*exe*D were mixed and incubated at 4° C for 4 h. After equilibration of the Ni-NTA agarose column, the mixture was applied to the column which was washed with binding buffer and then eluted with a gradient of binding buffer containing 10-500 mM imidazole.

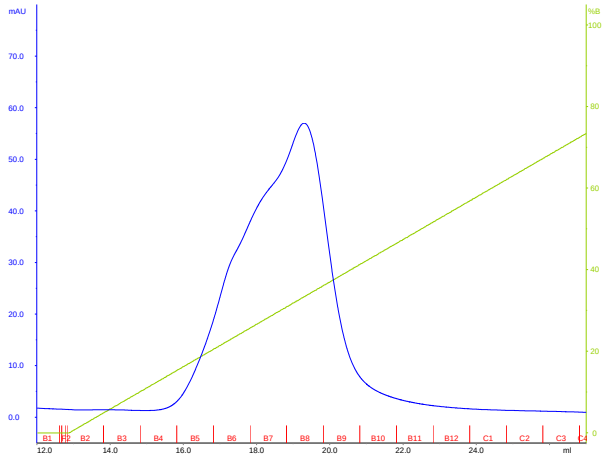

B. Determination of the binding of pET30-*exe*A to Ni-NTA column. BL21 cells containing pET30-*exe*A were induced and extracted as described in 2.9. After equilibration of the Ni-NTA agarose column, the cell lysate of pET30-*exe*A was applied to the column which was washed with binding buffer and then eluted with a gradient of binding buffer containing 10-500 mM imidazole.

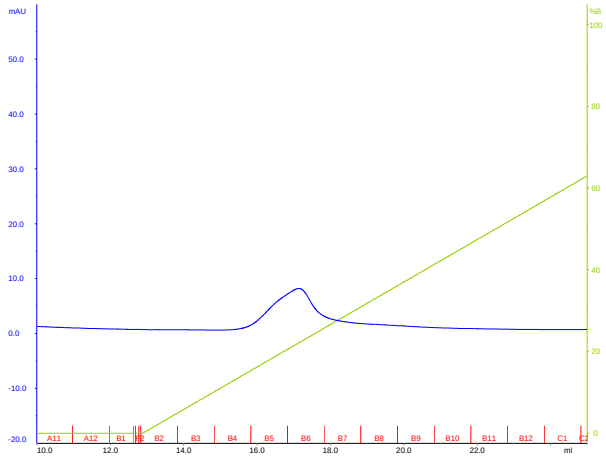

C. Determination of the binding of pCDFDuet-*exe*D to Ni-NTA column. BL21 cells containing pCDFDuet-*exe*D were induced and extracted as described in 2.9. After equilibration of the Ni-NTA agarose column, the cell lysate of pCDFDuet-*exe*D was applied to the column which was washed with binding buffer and then eluted with a gradient of binding buffer containing 10-500 mM imidazole.

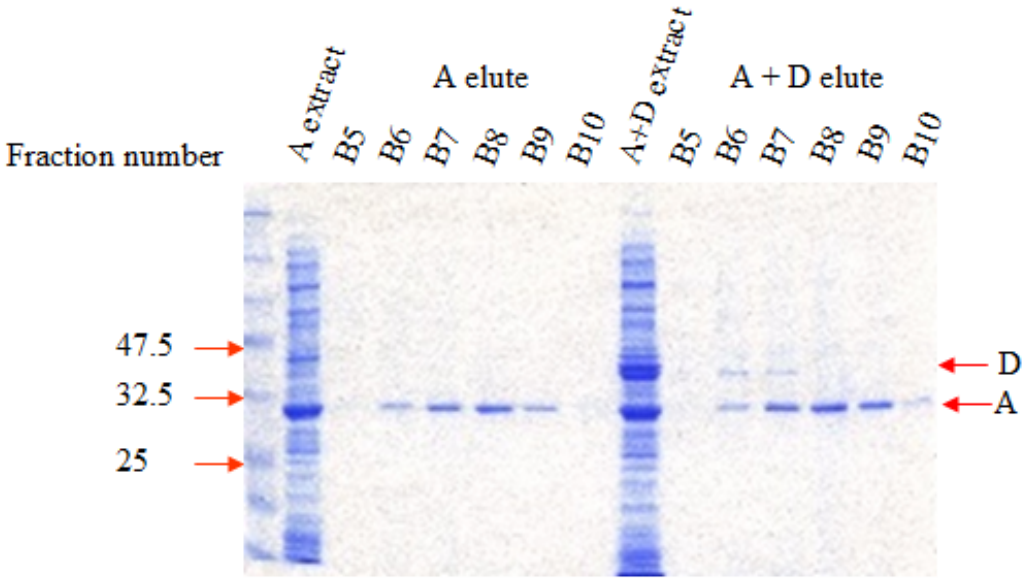

FIG. 3-23. SDS-PAGE of pET30-*exe*A elution and pET30-*exe*A + pCDFDuet-*exe*D elution. 10% SDS-PAGE showing the co-purification of the peri-ExeD expressed from pCDFDuet-*exe*D (38.2 kDa) with the His-tagged **peri-ExeA** expressed from pET30-*exe*A (30 kDa). The pET30-*exe*A extract and imidazole gradient elution fractions following the application of the cell extract from cells containing pET30-*exe*A are shown on the left, while the pET30-*exe*A + pCDFDuet-*exe*D extract and the elution fractions of an extract from cells containing pET30-*exe*A + pCDFDuet-*exe*D are shown on the right.

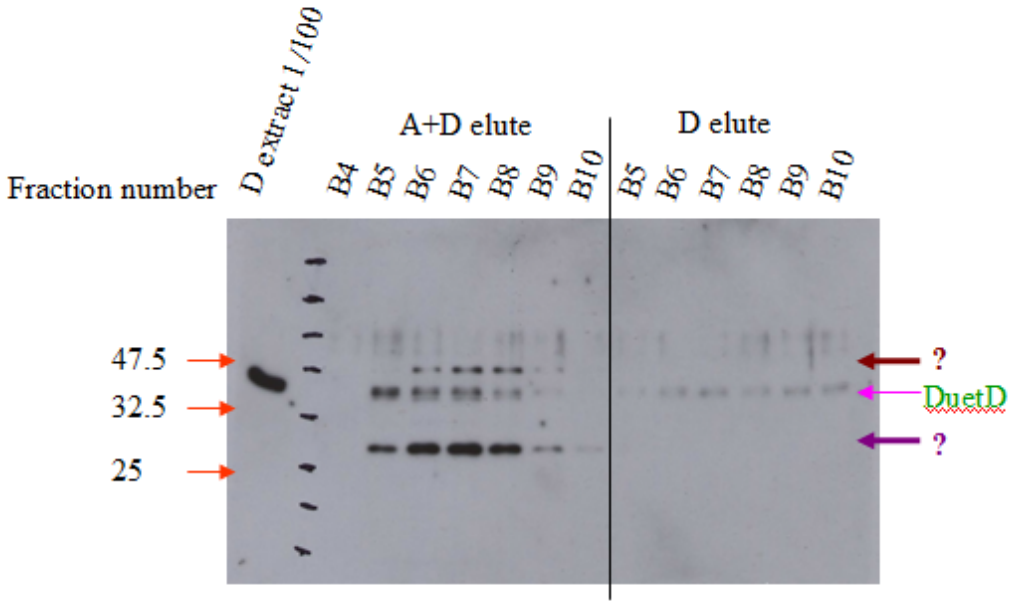

FIG. 3-24A. Immunoblot of pET30-*exe*A + pCDFDuet-*exe*D elution and pCDFDuet-*exe*D elution. Anti-ExeD immunoblot showing the co-purification of the peri-ExeD expressed from pCDFDuet-*exe*D (38.2 kDa) with the His-tagged peri-ExeA expressed from pET30-*exe*A (30 kDa). The pCDFDuet-*exe*D extract (1:100 dilution) and the imidazole gradient elution fractions following the application of a mixture of cell extracts from cells containing pET30-*exe*A and pCDFDuet-*exe*D are shown on the left, while the elution fractions of an extract from cells containing only pCDFDuet-*exe*D are shown on the right. Anti-ExeD antiserum was used at a dilution of 1:50, 000, and the film was developed for 3 min.

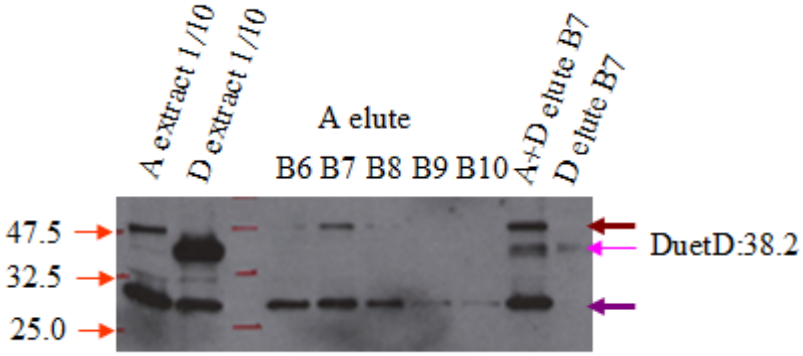

FIG. 3-24B. Immunoblot of 26 kDa and 47 kDa fragment. The pET30-*exe*A extract (1:10 dilution), pCDFDuet-*exe*D extract (1:10 dilution), fraction B6 to B10 of the pET30-*exe*A lysate elution; fraction B7 of the pET30-*exe*A + pCDFDuet-*exe*D elution and fraction B7 of pCDFDuet-*exe*D elution are shown. Anti-ExeD antiserum was used at a dilution of 1:20, 000, and the film was developed for 1 min.

not occur in pCDFDuet-*exe*D elution fractions (Fig. 3-24A). In addition, the fragment of 47 kDa could not be a fragment of ExeD because it occurred in pET30-*exe*A extract only (Fig. 3-24B). Evidently these proteins co-purify with His-ExeA and also can react with the anti-ExeD antiserum. In addition to these two experiments, other co-purification tests were also performed, including examining the interaction between the bait pET30-*exe*A and the prey pCDFDuet-*exe*A, pCDFDuet-*exe*B, pCDFDuet-*exe*C, and the bait pET47-*exe*D and the prey pCDFDuet-*exe*A. No other protein-protein interactions could be detected using this method.

4. DISCUSSION

4.1 The C-terminal periplasmic domains of ExeA and ExeB interact with a region of the periplasmic domain of ExeD

As described in the introduction, the T2SS of *A. hydrophila* is composed of two operons, *exe*AB and *exe*C-N (Howard *et al*., 1993; Jahagirdar and Howard, 1994). Although ExeA and ExeB homologues in T2SS have been found in many bacterial species, their presence is not universal (Jahagirdar and Howard, 1994; Condemine and Shevchik, 2000). Recent studies have shown that ExeA and ExeB are two ancillary factors of ExeD in the T2SS of *A. hydrophila*, with ExeA forming a complex with ExeB which is required for the assembly and/or multimerization of the ExeD secretin in the OM (Ast *et al*., 2002; Howard, *et al*., 2006). However, the exact functions of ExeA and ExeB are not clear. Although ExeB has been proposed to interact directly with ExeD in a TonB-like fashion to open the secretin channel (Howard *et al*., 1996; Ast *et al*., 2002), no ExeA-ExeD or ExeB-ExeD interactions have been observed in our lab. In *Erwinia*, OutB was found to stabilize OutD when they were co-expressed in *E. coli* and these two proteins could be cross-linked using formaldehyde (Condemine and Shevchik, 2000), while no protein-protein interaction has been found between GspA and any part of the secreton in other species.

In this study, yeast two-hybrid assays were used to demonstrate for the first time that both ExeA and ExeB interact directly with ExeD. Specifically, the first group of the yeast two-hybrid assays was accomplished between the periplasmic domains of ExeA/ExeB (bait) and those of Exe A, B, C, D, L, M and N (prey). The results showed that there was an interaction between pGBT9-*exe*A and pGAD424-*exe*D, no other interactions were observed. The negative result for the ExeB and ExeD interaction is contradictory to previous studies which have suggested that the C-terminal domain including the peri-OutB interacts with OutD (Condemine and Shevchik, 2000). In addition, the ExeAB complex has been demonstrated to play either a direct or indirect role in the transport of ExeD into the OM (Ast *et al*., 2002). To further confirm the results, the yeast two-hybrid assays between ExeD and ExeA/ExeB in the opposite direction were performed, and the results showed that there was interaction between pGBT9-*exe*D (bait) and pGAD424-*exe*B (prey) while no protein-protein interaction occurred between pGBT9-*exe*D and pGAD424-*exe*A. Therefore, it can be concluded that there are protein-protein

interactions between ExeA and ExeD, and between ExeB and ExeD, both of which only occurred in one direction in the Gal4 yeast two-hybrid system. This phenomenon might be caused by the obstruction of normal structure formation in the Gal4 yeast two-hybrid system. Another explanation for the phenomenon could be that oligomerization of the proteins required for interactions could not be formed in some of the fusion pairs. Electron microscopy analysis of negatively stained PulD-PulS complexes showed that PulD forms a ring-like structure (Nouwen *et al*., 1999). The side views of electron microscopy suggested that the protease-resistant C-terminal domain was composed of two stacked rings and there was protein structure in the center of the ring (Nouwen *et al*., 2000). A recent study further revealed that the C-domain contributed to the outer chamber, the central disc and the plug, while the N-terminal domain of PulD fold back into the large cavity of the channel formed by the C-terminal domain (Chami *et al*., 2005). As the result, the full-length GspD in an oligomeric ring-like structure may be required for the interaction with other components including GspA, GspB and GspC. However, such an assembly is unlikely to form in the Gal4 yeast two-hybrid systems but could be present during biochemical approaches such as pulldown experiments or co-expression and co-purification (Korotkov *et al*., 2006).

The yeast two-hybrid assay showed that the co-transformants of pGBT9-*exe*A and pGAD424-*exe*D could not grow on SC-Trp-Leu-Ade, and that the interaction between pGBT9-*exe*A and pGAD424-*exe*D could not be detected by the liquid β-galactosidase assay (data not shown), indicating that the interaction between the ExeA and ExeD fragments are weak. The strength analysis of the interaction between ExeA and ExeD, and between ExeB and ExeD also suggested that both interactions were weak. To determine the strength of the ExeA-ExeD interaction and ExeB-ExeD interaction, the yeast two-hybrid assays were carried out by replica plating colonies to SC-Trp-Leu-His containing 0.2-1.2 mM 3-AT. The results showed that both interactions were inhibited by 1.2 mM 3-AT, which is much weaker than the positive control.

To map the region of ExeD involved in these interactions with ExeA and ExeB, eight two-codon mutants distributed in the peri-ExeD were constructed and the yeast two-hybrid assay were performed between the ExeD (two-codon mutants) and ExeA/ExeB (WT). The results showed that the fragment, from amino acid residue 26 to 58 of ExeD contribute to the interaction with ExeA, and that the segment of ExeD, from amino acid residue 26 to182 is

involved in the ExeB-ExeD interaction. This is because the mutations in these two fragments completely inhibit the interactions. In addition, the interaction between ExeA (WT) and the ExeD (two-codon mutants) in the fragment from amino acid residue 137 to 256, was partially inhibited, especially the interaction between ExeA and the ExeD mutant at residue 182, was very weakly inhibited compared with the other strongly inhibited mutant interactions. Therefore, it can not be excluded that the region around residue 182 of ExeD may also be involved in the interaction with ExeA. Similarly, a region, from amino acid 247 to 256 of ExeD may also be involved in the ExeB-ExeD interaction since the yeast two-hybrid assay showed partial inhibition of the interaction between ExeB and mutants in the region of ExeD.

Although the regions of ExeD that were involved in the interactions with ExeA and ExeB were revealed by the yeast two-hybrid assays between the ExeD (two-codon mutants) and ExeA/ExeB (WT), a two-codon insertion mutation that interferes with the interaction may not correctly identify the region involved in that interaction because the ExeD mutations may alter the global structure of the proteins. Therefore to confirm these results, ExeD deletion mutants were constructed and the yeast two-hybrid assay was repeated. Based on the results of the two-hybrid assay between ExeD two-codon mutants and ExeA, the region, from residue 26 to 58 of ExeD, is involved in the interaction with ExeA, and the region around residue 182 may also be important for the interaction, indicating that the fragment, form residue 26 to 120 of ExeD, and/or the fragment, from residue 26 to 200 of ExeD, may be important for the ExeA-ExeD interaction. Therefore, four ExeD deletion mutants were constructed, including pGAD424-*exe*D:Δ121-355, pGAD424-*exe*D:Δ26-120, pGAD424-*exe*D:Δ201-355 and pGAD424-*exe*D:Δ26-200. Similarly, the two-hybrid assay between ExeD (two-codon mutants) and ExeB (WT) showed that the region from residue 26 to 182 of ExeD, is involved in the interaction with ExeB, indicating that the fragment, form residue 26 to 200 of ExeD, may be required for the ExeB-ExeD interaction. Thus two ExeD deletion mutants including pGBT9-*exe*D:Δ201-355 and pGBT9-*exe*D:Δ26-200 were constructed for the yeast two-hybrid assay. Although a region, from amino acid residue 247 to 256 of ExeD may also be involved in the ExeB-ExeD interaction, this fragment is very short and the mutants near this region still showed relatively strong interaction with ExeB, therefore this fragment was not used for the ExeD deletion analysis. The yeast two-hybrid assays between the ExeD deletion mutants and ExeA/ExeB (WT) showed that there were interactions between pGBT9-*exe*A and pGAD424-*exe*D:Δ201-

355, and between pGBT9-*exe*D:Δ201-355 and pGAD424-*exe*B, indicating that the same ExeD fragment (amino acid residue 26–200), is involved in the protein-protein interactions with both ExeA and ExeB. This result is consistent with the yeast two-hybrid assays between the ExeD two-codon mutants and ExeA/ExeB (WT), which showed protein-protein interactions between ExeA/ExeB and ExeD with mutations in the first half of the fragment were completely inhibited while the mutations in the last half of the fragments showed weak or medium weak interactions (Fig. 4-1A and B). Therefore, it can be hypothesized that the region from amino acid residue 26 to 200 of the peri-ExeD is involved in the interaction with ExeA and ExeB. This corresponds to previous studies showing that the periplasmic N-terminal domain of GspD facilitates interactions with other components of the secretion apparatus (Bitter *et al*., 1998, Brok *et al*., 1999; Nouwen *et al*., 2000).

Earlier studies showed that ExeA forms a stable complex with ExeB in the IM (Howard *et al*., 1996; Schoenhofen *et al*., 1998). Schoenhofen *et al*. (1998, 2005) also suggested that both ExeA and ExeB might be homodimers since ExeA could be cross-linked as a 120 kDa homodimer and thus the functional ExeAB complex could be a heterotetramer. These results were confirmed by gel filtration analysis of the ExeAB complex indicating that ExeAB was a large oligomer possibly consisting of three dimers of each protein (Schoenhofen *et al*., 2005). However, neither self-interaction of ExeA/ExeB nor ExeA-ExeB interaction could be detected by the yeast two-hybrid assay. Similar to the one-direction interaction between ExeA and ExeD, and between ExeB and ExeD, the negative results for ExeA-ExeA, ExeB-ExeB and ExeA-ExeB interactions could be caused by incorrect folding of the ExeA and ExeB fusion protein used in the assay. Another possible explanation for the negative results might be that the protein-protein interaction occurs in a different region of the proteins. Since ExeA and ExeB are cytoplasmic membrane proteins, the protein interactions may occur at the TM domain. In addition, the formation of the ExeAB complex may require dimerization of ExeA and ExeB. However, the conformation of ExeA and ExeB required for self-interactions may not have formed in the Gal4 yeast two-hybrid system, thus further resulting in the failure of interaction between ExeA and ExeB.

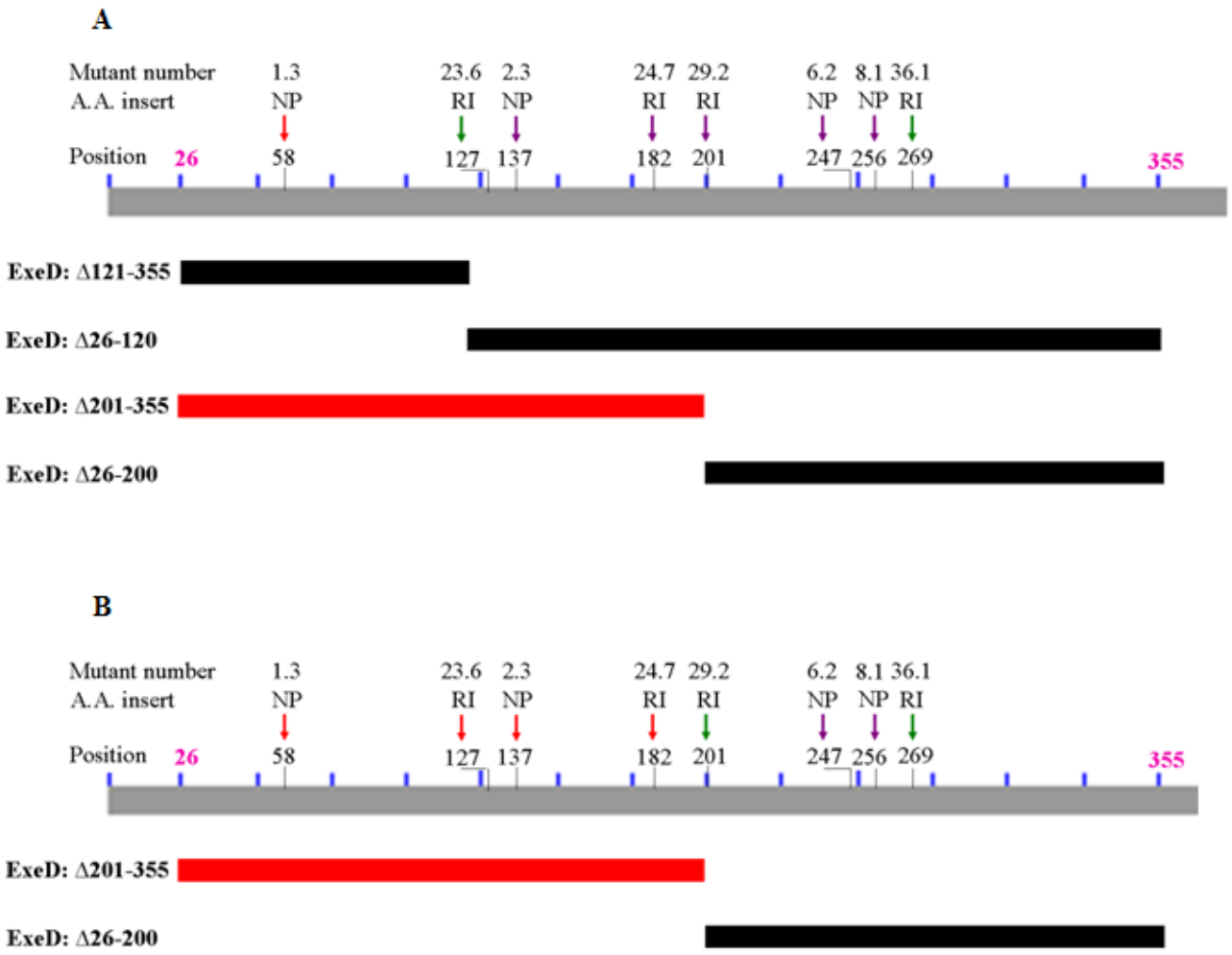

FIG. 4-1. Summary of results indentifying the ExeD region involved in the interaction between (A) ExeA and ExeD and between (B) ExeB and ExeD The region of ExeD involved in the ExeA-ExeD and ExeB-ExeD interactions were determined by the yeast two hybrid assays between ExeA/ExeB (WT) and ExeD (two-codon mutants) and between ExeA/ExeB (WT) and ExeD (deletion mutants) . The vertical arrows show the position of the mutants. The red arrows indicate complete inhibition of the ExeA-ExeD or ExeB-ExeD interaction, the purple arrows indicate partial inhibition, and the green arrows indicate no inhibition of the interaction. The black and red bars show the ExeD deletion mutants used in the tests. The red bar stands for the region of ExeD involved in the interactions with ExeA and ExeB.

In order to confirm the positive interactions identified by the yeast two-hybrid assay, co-purification assays of ExeD with ExeA/ExeB in both directions were carried out. When His-tagged ExeA was used as the bait, the chromatograph and the SDS-PAGE gels showed that the His-tagged ExeA bound to the column properly, and immunoblot using anti-ExeD antibody showed that the ExeD fragment (pCDFDuet-*exe*D) bound to the His-ExeA since the ExeD fragment was observed in the elution fraction when pET30-*exe*A + pCDFDuet-*exe*D extracts were incubated together before application to the column. Thus the results indicated that there is an *in vitro* interaction between ExeA and ExeD, confirming the results of the yeast two-hybrid assay. Unfortunately, the ExeA-ExeD interaction in the other direction (pET47-*exe*D and pCDFDuet-*exe*A) and the ExeD-ExeB interactions could not be confirmed via co-purification due to background binding. This phenomenon often occurs when the interactions are weak, as was indicated by the yeast two-hybrid assay in this study.

An earlier study in our lab has proved that ExeAB complex is required for the localization and assembly of the ExeD secretion port multimer in the OM (Ast *et al*., 2002). This is based on a series of experiments showing that the ExeD secretin was not able to multimerize and remained in the IM as a monomer in the absence of ExeAB, however, expression of ExeAB from a plasmid in an *exe*AB mutant strain resulted in an increased amount of ExeD multimer corresponding to the restored aerolysin secretion. Moreover, induction of ExeAB complexes could promote the assembly of previously synthesized ExeD monomer into the multimer. The same study also found that overproduced ExeD in C5.84 cells, an *exe*A::Tn5-751 mutant, would result in ExeD multimerization in the IM without the presence of ExeAB, and the amount fractionated with the OM of the overproducing cells was similar to that in WT. This result further suggests that the ExeAB complex plays either a direct or indirect role in the transport of ExeD into the OM, probably via interacting directly with ExeD. The function of the ExeAB complex in secretin assembly was further examined by Howard *et al*. (2006) and the result showed that mutations in a putative PG binding motif in the peri-ExeA lost the ability to assemble the ExeD secretin or secrete aerolysin, while retaining the ability to form a complex with ExeB, suggesting that the PG binding motif of ExeA was required for ExeD secretin assembly while not involved in ExeAB complex formation. The study also revealed that ExeA (WT) could be cross-linked to PG, whereas three substitution mutants in the putative PG

binding motif of ExeA could not, indicating that there was an interaction between ExeA and PG. Therefore, it can be concluded that PG binding to ExeA is required for the function of the ExeAB complex in ExeD secretin assembly. In addition, the *in vivo* cross-linking analysis also showed that ExeB and ExeC interact with PG in the presence of ExeA. This result leads to a hypothesis that ExeA, B, C, D and PG may form a complex during assembly of the ExeD secretin. Therefore, the ExeABCD-PG complex is probably involved in localization and assembly of the ExeD secretion port multimer in the OM. However, no interaction was identified between ExeA and ExeC and between ExeB and ExeC in the yeast two-hybrid assays described here. This could be because the regions and structures of ExeA, B and C involved in such interactions were not present in these assays. The C-terminal periplasmic domain of ExeA, ExeB and ExeC would be presumed to be involved in the interactions as a previous study suggested that both PDZ domain of PulC and coiled coil structure of GspC in the periplasm were involved in the protein-protein interactions (Bleves *et al.*, 1999; Bouley *et al*., 2001; Gérard-Vincent, *et al*., 2002; van Ham and Hendriks, 2003). In contrast, other studies showed that both the coiled coil structure and the PDZ domain of GspC could be involved in the formation of homo-multimeric complexes (DaeGérard-Vincent *et al*., 2002) or contribute to the recognition of secreted proteins and confer secretion specificity to a subgroup of secreted proteins (Bouley *et al*., 2001), indicating that the C-terminal coiled coil structure and the PDZ domain of GspC might not be required for interaction with other proteins of T2SS. Moreover, other studies suggested that the TMS and/or N-terminal cytoplasmic domain of GspC formed a complex with GspL and GspM (DaeGérard-Vincent *et al*. 2002; Lee *et al*. 2004), and it could be that these two domains of ExeC may be responsible for interactions with ExeA and ExeB. In the study of Howard *et al*. (2006), full length ExeA, ExeB and ExeC (WT) were used and the interactions of ExeA/PG, ExeB/PG and ExeC/PG were detected by *in vivo* cross-linking and immunoblot with anti-ExeA, anti-ExeB and anti-ExeC individually. In this study, only the C-terminal periplasmic domains of the three proteins were cloned into the yeast vector for the two-hybrid assay. Therefore, possible interactions between ExeA and ExeC and between ExeB and ExeC might not have been detected due to the deletion of TMS and cytoplasmic domain of the proteins. In addition, GspC has also been shown to form a homo-trimer or homo-multimer in the IM via the C-terminal coiled coil/PDZ domain or TMS (Possot *et al*., 1999, DaeGérard-Vincent *et al*., 2002, Login and Shevchik, 2006). Therefore it is also possible that the

mutimerization of ExeC is required for any interaction with ExeA and ExeB, and this mutimerization might not have occurred in the yeast two-hybrid system.

4.2 The C-terminal periplasmic domain of ExeC interacts with the N-terminal periplasmic domain of ExeD

In addition to ExeA and ExeB, ExeC and secretin ExeD also form important protein-protein interactions in the T2SS according to previous work. It has been suggested that GspC and GspD are essential for toxin secretion in T2SS as they confer specificity for substrate recognition and/or secreton assembly (Gerard-Vincent *et al*., 2002), and evidence for GspC and GspD interactions has been reported (Shevchik *et al*., 1997; Possot *et al*., 1999; Lee *et al*., 2000; Johnson *et al*., 2006). In this study, the yeast two-hybrid assay showed that there was a very weak interaction between ExeC and ExeD which could be inhibited by 0.2 mM 3-AT, confirming the ExeC-D interaction in *A. hydrophila*. However, previous results have shown discrepancies concerning the region of GspC involved in the interaction with GspD. Most studies suggest that C-terminal peri-GspC is involved in the interaction with GspD (Bleves *et al*., 1999**;** Gerard-Vincent *et al*., 2002; Robert *et al*., 2005a; Korotkov *et al*., 2006). In this study, the peri-ExeC, from amino acid residue 47 to 290, was used for the yeast two-hybrid assay and the positive result corresponds to previous studies mentioned above. Based on the studies described in the introduction, it can be hypothesized that the high homology region in the peri-ExeC is important for the interaction with ExeD. In addition, the region of ExeD involved in the interaction with ExeC was also examined by the yeast two-hybrid assay between ExeD (two-codon mutants) and ExeC (WT) and between ExeD (deletion mutants) and ExeC (WT). The yeast two-hybrid assay between the ExeD two-codon mutants and ExeC suggested that the fragment containing amino acid residue 26-256 of peri-ExeD is involved in the interaction with ExeC. Similarly, the yeast two-hybrid assay between the ExeD deletion mutants and ExeC also showed that a region in peri-ExeD, from amino acid residue 26 to 200, is probably responsible for the interaction with ExeC. However, since the interaction between the ExeD mutants and ExeC is very weak and not stable, the exact region of ExeD that contributes to the ExeC-ExeD interaction could not be determined in this study. Although the exact region of ExeD involved was not mapped, the positive result of the ExeC-D interaction is

consistent with most studies suggesting that the N-terminal peri-GspD is involved in protein-protein interactions with ExeC (Bitter *et al*., 1998, Brok *et al*., 1999; Nouwen *et al*., 2000).

Previous studies suggested that the C-terminal coiled coil/PDZ domain of GspC could be involved in the formation of homo-multimeric complexes (DaeGérard-Vincent *et al*., 2002). However, in this study, self-interaction of ExeC was not observed in the yeast two-hybrid assay, which corresponds to recent studies indicating that the TM domain drives the self-association of GspC whereas the periplasmic region is dispensable for homodimerization (Robert *et al*. 2005a; Korotkov *et al.* 2006; Login and Shevchik 2006).

Interactions between ExeC and ExeL/ExeM were also not observed using the yeast two-hybrid assay in this study. The negative result is contradictory to previous studies showing that GspC could associate with the IM proteins GspL and GspM and stabilize the GspLM subcomplex (Possot *et al*., 1999, 2000; Gérard-Vincent *et al*., 2002; Robert *et al*., 2002, 2005b; Lee *et al*., 2004). This discrepancy might be caused by the region of ExeC used in the assay. Many studies have suggested that the N-terminal TM domain and/or TM/HR domain of GspC interacts with the components of the IM complex (Bleves *et al*., 1999; Bouley *et al*., 2001; Lee *et al*., 2001; Gerard-Vincent *et al*., 2002), while other studies suggested that the N-terminal cytoplasmic domain of GspC is required for the interaction with GspLM and stabilization of the IM complex. In this study, however, only the peri-ExeC was used for the yeast two-hybrid assay.

4.3 Residue 182 to 256 of the periplasmic domain of ExeD contributes to the multimerization of ExeD.

In this study, the N-terminal periplasmic domain, from amino acid residue 26 to 355 of ExeD was found to be able to dimerize in the Gal4 yeast system. Compared with the positive control, the interaction is very weak and can be inhibited by 1.2 mM 3AT. This result corresponds to previous studies showing that the secretin GspD forms a highly stable large oligomeric ring in the OM which consists of approximately 12-14 monomers (Bitter *et al*., 1998; Nouwen *et al*., 1999, 2000; Chami *et al*., 2005). However, most studies have suggested that the C-terminal domain of GspD is responsible for OM insertion and multimerization (Chen *et al*., 1996;

Shevchik *et al.*, 1997; Bitter *et al*., 1998, Brok *et al*., 1999; Nouwen *et al*., 2000; Bouley *et al*., 2001). Chen *et al*. (1996) for example revealed that two fragments, from residue 429 to 544 and from residue 544 to 759 in the C-terminal domain of XpsD were required for OM insertion and multimerization. However, Guilvout *et al*. (1999) suggested that both the N-terminal and C-terminal region of PulD were required for multimerization. The study found that the C-terminal domain is responsible for multimer stability while the N domain contributes to multimer formation. Moreover, Chami *et al*. (2005) also suggested that only a small part of C-terminal domain of PulD was embedded within the OM, suggesting that the N-terminal domain of PulD might also be involved in homo-multimerization. Therefore, it can be hypothesized that the periplasmic N-terminal domain of GspD is also involved in the mutimerization in addition to interacting with other components of the T2SS. In addition, the exact region of the ExeD involved in the ExeD dimerization was further mapped using the yeast two-hybrid assay between ExeD (two-codon mutants) and ExeD (WT), and the result showed that the region from amino acid residue 182 to 256 of peri-ExeD is involved in the ExeD multimerization. This result, together with the results concerning the interactions between ExeD and ExeA and B lead to the hypothesis that the region from amino acid residue 26 to 200 of peri-ExeD is involved in the interaction with other components of the secretion apparatus and exoproteins in the periplasm while the region from amino acid residue 182 to 256 of peri-ExeD contributes to the multimerization of ExeD in addition to the C-terminal domain of ExeD. The region of ExeD involved in the dimerization of ExeD could not be examined by the yeast two-hybrid assay between ExeD (deletion mutants) and ExeD (WT), this is probably because the self-interaction requires full length or a longer sequence of ExeD to form the dimer in the yeast, the lack of these sequences resulting in the structure needed for the interaction not being formed in the yeast.

4.4 A hypothetical model for the type II secretion apparatus of *A. hydrophila*

Base on the previous results and the findings in this study, a model of the T2SS of *A. hydrophila* is described as follows. The T2SS is part of the GSP which includes 2 steps, passage across the inner and outer membranes (Fig. 1-1). In the first step, exoproteins to be secreted such as aerolysin are synthesized as precursors containing N-terminal cleavable signal peptides that target them to the Sec machinery in the IM. Following secretion into the

periplasm, signal peptides are removed by the activity of leader peptidase, and the mature exoproteins are released into the periplasmic space, where they fold. In the second step, the fully folded exoproteins in the periplasm are recognized and translocated across the OM by components of the T2SS. This process is accomplished by the coordination of the ExeEFLM complex, ExeABCD-PG complex and the pseudopilus structure composed of ExeG-K. First, the IM proteins ExeL and ExeM assemble into homomultimers and protect each other from proteolytic degradation via direct interaction. At the same time, the cytoplasmic protein ExeE arranges itself into a hexameric ring which leads to its association with the N-terminal cytoplasmic domain of ExeL. ExeE oligomerization might be triggered by ATP binding, and ATPase activity might require a properly formed conformation of EpsE resulting from association of ExeE and ExeL. The IM protein ExeF also joins the complex via interacting with the ExeE hexameric ring and ExeL homomultimer and is stabilized by these two proteins. ExeC strengthens the association between ExeL and ExeM via forming a reversible ternary complex with these two proteins. The resulting IM complex formed of ExeE, ExeF, ExeL and ExeM via a reversible association is thus used as a platform for assembling the pseudopilus composed of ExeG to ExeK. During the formation of the ExeE, F, L and M complex, ExeA, another ATPase in addition to ExeE in the T2SS of *A. hydrophila*, triggers the formation of a large and stable complex composed of three ExeA dimmers and three ExeB dimers in the IM via ATP-binding to its consensus ATP-binding site . At the same time, ExeA and ExeB bind to PG. During this process, ExeAB interact directly with the amino-terminal domain of ExeD, leading to the assembly and multimerization of the secretin into the PG and OM. These activities may be triggered or regulated using energy derived from ATP hydrolysis. In addition, ExeC and ExeN connect the IM complex ExeEFLM and the OM by interacting with ExeLM of the IM complex and the OM protein ExeD. ExeB, ExeC and ExeN may control the opening of the ExeD secretin channel directly or via interacting with ExeD in a TonB-like fashion to open the secretin channel, leading to efficient secretion. The pseudopilins composed of ExeG to ExeK extend from the ExeEFLM complex and form a pilus structure spanning the cell envelope to the ExeD pore of the OM. During the secretion process, ExeG is assembled in the pseudopilus and interacts directly with the secretin ExeD, a process dependent on ExeN via ExeG-ExeN interaction. ExeC may also play a direct role during pseudopilus assembly or activity by regulating the ExeG-ExeD contact. The pseudopilus assembly and elongation

process is controlled by ExeK via interactions with ExeG. ExeK forms a ternary complex with ExeI and ExeJ and the complex might locate at the tip of the pseudopilus. Once the T2SS is assembled, the exoproteins in the periplasm are recognized by ExeD, and ExeK-ExeI-ExeJ tip probably interacts transiently with the secretin ExeD, thus acting as a piston to translocate exoproteins out of the cell through the OM secretin pore.

5. FUTURE WORK

In this study, four pairs of protein-protein interactions including ExeA-ExeD, ExeD-ExeB, ExeD-ExeC and ExeD-ExeD, were identified by the Gal4 yeast two hybrid system. However, some interactions which were expected were not obtained, for example between ExeA and ExeB. As previously discussed this may be because either the regions of the proteins used for the tests were not involved in the interaction or the conformation of the proteins required for interactions could not be formed in some of the fusion pairs in the yeast two-hybrid system. In addition, some of the interactions observed were not stable and the system was not sensitive enough for some of the weak interactions between Exe proteins. For these reasons, a bacterial two-hybrid system is suggested as an alternative for future study. The BacterioMatch II two-hybrid system has been proved to be an efficient method for detecting protein-protein interactions *in vivo* (Wu *et al*., 2003). Protein-protein interaction is examined via transcriptional activation of *his*3, the first reporter gene, which allows growth in the absence of histidine. Positives are verified by the secondary reporter *aad*A gene, which confers Sm resistance. Compared with the yeast two-hybrid system, the bacterial two-hybrid system has the following advantages: First, it may take less time due to the much faster growth of bacteria compared to yeast; second, higher efficiency of transformation can result in larger numbers of interactions being screened more rapidly and easily, and third, easier isolation of plasmid DNA from *E. coli* than from yeast.

In this study, both pull-down (data not shown) and co-purification were performed to verify the yeast two-hybrid result. Certain protein structures or assembly required for the protein-protein interaction might be unable to form in the two-hybrid studies but could be present during biochemical approaches such as pull-down experiments or co-expression and co-purification (Korotkov *et al*., 2006). For example, the full-length GspD forms an oligomeric ring-like

structure. However, there was always background binding in both methods. Therefore, another method is necessary for confirming the protein-protein interactions between Exe proteins. *In vivo* cross-linking with bifunctional cross-linking reagents between the full length Exe proteins would be one way to confirm the interactions observed in this study. One problem however is that the full length ExeD is a highly stable large oligomer, which may be diffcult to identify the ExeA-ExeD interaction on the SDS-PAGE gel and immunoblot since the large protein complex of ExeA + ExeD multimer would be at the very top of the gel. Therefore, trichloroacetic acid (TCA) or phenol could be used to break the ExeD oligomer into monomers for the analysis. To identify the protein-protein interaction between ExeA or ExeB and ExeD, *A. hydrophila* containing full length ExeD (WT) and ExeA (WT) would be grown and cross-linking reagent would be added. After phenol or TCA extraction, ExeA and ExeD would be immunoprecipitated by anti-ExeA and anti-ExeD antibody irrespectively. If there is protein-protein interaction, in addition to the presence of full length ExeA and monomer ExeD in the precipitates, complexes reacting with both antiserum would be observed. This would also involve full length Exe proteins compared to the fragments used in this study.

In this study, the interacting region of the N terminal domain of ExeD has been mapped via the yeast two-hybrid assay between the ExeD (two-codon mutants) and ExeA, B, C and D (WT), and between the ExeD (deletion mutants) and ExeA, B, C and D (WT). Based on these results, the ExeD fragment, from amino acid residue 26 to 200, is proposed to be involved in the protein-protein interaction with ExeA, B and C, which may contribute to ExeD assembly and to function of the T2SS. To confirm the importance of these interactions to T2SS function, a complementation test of the ExeD (two-codon mutants) used in this study could be performed and the effect on ExeD assembly determined. To do so, the ExeD two-codon mutants could be cloned to pVACD-P, a plasmid containing ExeD in pMMB207 constructed by Vivan Ast (Ast *et al*., 2002). The plasmids would be conjugated into AhD14, a Δ*exe*D *A. hydrophila* strain and the complementation test would be performed to assess the effect of the two-codon insertion mutants on secretion assembly.

6. Concluding Remarks

The most striking result obtained in this study is the evidence for interactions between ExeA/B and ExeD. Previous studies have revealed that the ExeAB complex is required for the assembly and/or multimerization of the ExeD secretin in the OM, possibly using energy derived from ATP hydrolysis. In this study, the yeast two-hybrid assay was used to demonstrate interactions of ExeA/D and ExeB/D, suggesting that the ExeAB complex plays a direct role in the transport of ExeD into the OM. However, it is not clear if the association of the ExeAB complex and ExeD homododecamer occurs during or after transport/assembly. Furthermore, it has been suggested that the pilotin GspS, a component of the OM complex, is required to protect secretins from proteolysis and to direct its insertion to the OM (Hardie *et al*, 1996a, b; Daefler and Russel, 1998; Shevchik and Condemine, 1998; Guilvout *et al*., 2006), suggesting that ExeA and ExeB are analogs of GspS which play a similar role in *A. hydrophila*. However, the Out system of *E. chrysanthemi* contains OutB and OutS while no GspA homologue has been found, and both OutS and OutB are apparently involved in the stability and OM localization of OutD. It is not clear whether they perform overlapping, the same or separate functions. Another general OM insertion factor Omp85 (YaeT) in *N. meningitides* has also been proposed to be involved in secretin assembly (Voulhoux *et al*, 2003; Bayan *et al*, 2006). However, Collin *t al*. (2007) suggested that multimerization and OM association of PulD was YaeT-independent. It is possible that the GspA, GspB, GspS and Omp85 (YaeT) carry out similar or overlapping functions in the localization and assembly of GspD, with various combinations of these factors acting in different systems for the successful assembly of the secretin. In addition to the interaction between ExeA/ExeB and ExeD, the interaction between ExeC and ExeD in the periplasm was confirmed by the yeast two-hybrid assay of this study, corresponding to the previous results showing that the C-terminal peri-GspC is involved in an interaction with GspD (Robert *et al*., 2005a; Korotkov *et al*., 2006).

References

Abendroth, J., Bagdasarian, M., Sandkvist M. and Hol Wim G. J. 2004a. The structure of the cytoplasmic domain of EpsL, an inner membrane component of the type II secretion system of *Vibrio cholerae*: An unusual member of the actin-like ATPase superfamily. J. Mol. Biol. **344:**619-633.

Abendroth, J., P. Murphy, M. Sandkvist, M. Bagdasarian, and W. G. J. Hol. 2005. The X-ray structure of the type II secretion system complex formed by the N-terminal domain of EpsE and the cytoplasmic domain of EpsL of *Vibrio cholerae*. J. Mol. Biol. **348:**845-855.

Abendroth, J; Rice, A. E.; McLuskey, K.; Bagdasarian, M. and Hol, W. G. J. 2004b. The crystal structure of the periplasmic domain of the type II secretion system protein EpsM from *Vibrio cholerae*: The simplest version of the ferredoxin fold. J. Mol. Biol. **338:**585-596.

Altwegg, M. and Gless, H.K. 1989. *Aeromonas* as a human pathogen. Crit. Rev. Microbiol. **16:**253-286.

Arts, J.; Groot, A.; Ball, G.; Durand, E.; Khattabi, M. E.; Filloux, A.; Tommassen, J. and Koster, M. 2007. Interaction domains in the *Pseudomonas aeruginosa* type II secretory apparatus component XcpS (GspF). Microbiology **153**:1582-1592.

Ast, V. M., Schoenhofen, I.C., Langen, G.R., Stratilo, C.M., Chamberlain, D. and Howard, S.P. 2002. Expression of the ExeAB complex of *Aeromonas hydrophila* is required for the localization and assembly of the ExeD secretion port multimer. Mol. Microbiol. **44:** 217-231.

Ball, G., Chapon-Herve, V., Bleves, S., Michel, G. and Bally, M. 1999. Assembly of XcpR in the cytoplasmic membrane is required for extracellular protein secretion in Pseudomonas aeruginosa. J. Bacteriol. **181:**382-388.

Barany, F. 1985. Two-Codon Insertion Mutagenesis of Plasmid Genes by Using Single-Stranded Hexameric Oligonucleotides. Proc. Natl. Acad. Sci. **82:** 4202-4206.

Bartei, P. L., Chien, C.T., Sternglanz, R., and Fields, S. 1993a. Using the two-hybrid system to detect protein-protein interactions. Cellular Interactions in Development: A Practical Approach. 153-179.

Bartei, P. L., Chien, C.T., Sternglanz, R., and Fields, S. 1993b. Elimination of false positives that arise in using the two-hybrid system. Biotechniques. **14:**920-924.

Bayan, N., Guilvout, I. and Pugsley, A.P. 2006. Secretins take shape. Mol. Microbiol. **60:**1–4.

Bitter, B., Ria van Boxtel, Mathijs Groeneweg, Patricia Sa´nchez Carballo, Ulrich Za¨hringer, Jan Tommassen and Margot Koster. 2007. Species-Specific Functioning of the

Pseudomonas XcpQ Secretin: Role for the C-Terminal Homology Domain and Lipopolysaccharide. J. Bacteriol. **189:**2967–2975.

BitterW, Koster M, Latijnhouwers M, de Cock H and Tommassen J. 1998. Formation of oligomeric rings by XcpQ and PilQ, which are involved in protein transport across the outer membrane of Pseudomonas aeruginosa. Mol. Microbiol. **27:**209–219.

Bleves, S., Gérard-Vincent, M., Lazdunski, A. and Filloux, A. 1999. Structure-function analysis of XcpP, a component involved in general secretory pathway-dependent protein secretion in *Pseudomonas aeruginosa*. J. Bacteriol. **181:**4012–4019.

Bleves, S., A Lazdunski, and A Filloux. 1996. Membrane topology of three Xcp proteins involved in exoprotein transport by Pseudomonas aeruginosa. J. Bacteriol. **178:**4297-4300.

Bouley, J., Condemine, G., and Shevchik, V.E. 2001. The PDZ domain of OutC and the N-terminal region of OutD determine the secretion specificity of the type II out pathway of *Erwinia chrysanthemi.* J. Mol. Biol. **308:**205-219.

Bram, R. J., Lue, N.F., and Kornberg, R.D. 1986. A GAL family of upstream activating sequences in yeast: roles in both induction and repression of transcription. EMBO J. **5:**603-608.

Brok, R., Gelder, P.V., Winterhalter, M., Ziese, U., Koster, A.G., Cock, H.de., Koster, M., Tommassen, J. and Bitter, W. 1999. The C-terminal domain of the Pseudomonas secretin XcpO forms the oligomeric rings with pore activity. J. Mol. Biol. **294:** 1169-1179.

Camberg, J.L., Sandkvist, M. 2005. Molecular analysis of the *Vibrio cholerae* type II secretion ATPase EpsE. J. Bacteriol. **187**: 249–256.

Chami, M., Guilvout, I., Gregorini, M., Remigy, H.W., Muller, S.A., Valerio, M., Engel, A., Pugsley, A.P. and Bayan, N. 2005. Structural insights into the secretin PulD and its trypsin resistant core. J. Biol. Chem. **280:**37732–37741.

Camberg, J. L., Tanya L Johnson, Marcella Patrick, Jan Abendroth, Wim G J Hol and Maria Sandkvist. 2007. Synergistic stimulation of EpsE ATP hydrolysis by EpsL and acidic phospholipids. EMBO J. **26:**19–27.

Chen LY, Chen DY, Miaw J and Hu NT. 1996. XpsD, an outer membrane protein required for protein secretion by Xanthomonas campestris pv. campestris, forms a multimer. J. Biol. Chem. **271:**2703–2708.

Collin, Séverine; Guilvout, Ingrid; Chami, Mohamed; Pugsley, Anthony P. 2007. YaeT-independent multimerization and outer membrane association of secretin PulD. Mol. Microbio. **64:**1350-1357.

Condemine, G. and Shevchik, V. E. 2000. Overproduction of the secretin OutD suppresses the secretion defect of an *Erwinia chrysanthemi out*B mutant. Microbiology. **146:**639–647.

Crowther, L.J., Anantha, R.P. and Donnenberg, M.S. 2004. The inner membrane subassembly of the enteropathogenic Escherichia coli bundle-forming pilus machine. Mol. Microbiol. **52:**67–79.

Crowther, L.J., Yamagata, A., Craig, L., Tainer, J.A. and Donnenberg, M.S. 2005. The ATPase activity of BfpD is greatly enhanced by zinc and allosteric interactions with other Bfp proteins. J. Biol. Chem. **280:**24839–24848.

Daefler, S., Guilvout, I., Hardie, K.R., Pugsley, A.P. and Russel, M. 1997. The C-terminal domain of the secretin PulD contains the binding site for its cognate chaperone, PulS, and confers PulS dependence on pIVf1 function. Mol. Microbiol. **24:**465–475.

Daefler, S. and Russel, M. 1998. The Salmonella typhimurium InvH protein is an outer membrane lipoprotein required for the proper localization of InvG. Mol Microbiol. **28:**1367-1380.

de Groot, A., M. Koster, M. Gérard-Vincent, G. Gerritse, A. Lazdunski, J. Tommassen, and A. Filloux. 2001. Exchange of Xcp (Gsp) secretion machineries between *Pseudomonas aeruginosa* and *Pseudomonas alcaligenes*: species specificity unrelated to substrate recognition. J. Bacteriol. **183:**959-967.

de Keyzer J, van der Does C. and Driessen AJM 2003. The bacterial translocase: a dynamic protein channel complex. Cellular and Molecular life Sciences. **60:**2034-2052.

Desvaux M, Parham NJ, Scott-Tucker A and Henderson IR 2004. The general secretory pathway: a general misnomer? Trends Microbiol. **12:**306–309.

Douet, V., Loiseau, L., Barras, F. and Py, B. 2004. Systematic analysis, by the yeast two-hybrid, of protein interaction between components of the type II secretory machinery of *Erwinia chrysanthemi*. Res. Microbiol. **155:**71–75.

Durand, E. *et al.* 2005. XcpX controls biogenesis of the Pseudomonas aeruginosa XcpT-containing pseudopilus. J. Biol. Chem. **280:**31378–31389.

Fields, S. and Song, O. 1989. A novel genetic system to detect protein-protein interactions. Nature. **340:**245-246.

Fields, S. 1993. The two-hybrid system to detect protein-protein interactions. Methods: A Companion to Meth. Enzymol. **5:**116-124.

Filloux, A. 2004. The underlying mechanisms of type II protein secretion. Biochimica et Biophysica Acta **1694:**163-179.

Filloux, A., Michel, G. and Bally, M. 1998. GSP-dependent protein secretion in Gram-negative bacteria: the Xcp system of Pseudomonas aeruginosa. FEMS Microbiol. Rev. **22:**177–198.

Fivaz,M. L., Abrami, Y., Tsitrin and F. G. Van Der Goot. 2001. Aerolysin from *Aeromonas hydrophila* and related Toxins. Pore-Forming Toxins.

Forest, K.T. 2008. The type II secretion arrowhead: the structure of GspIÂ–GspJÂ–GspK. Nature Structural & Molecular Biology **15:**428-430.

Forest, K.T., Satyshur KA, Worzalla GA, Hansen JK & Herdendorf TJ. 2004. The pilus-retraction protein PilT: ultrastructure of the biological assembly. Acta Crystallogr D Biol Crystallogr. **60:**978–982.

Francetic, O., D. Belin, C. Badaut, and A. P. Pugsley. 2000. Expression of the endogenous type II secretion pathway in *Escherichia coli* leads to chitinase secretion. EMBO J. **19:**6697–6703.

Francetic, O., and A. P. Pugsley. 1996. The cryptic general secretory pathway (*gsp*) operon of *Escherichia coli* K-12 encodes functional proteins. J. Bacteriol. **178:**3544–3549.

Genin, S., and Boucher, C.A. 1994. A superfamily of proteins involved in different secretion pathways in gram-negative bacteria: modular structure and specificity of the N-terminal domain. Mol. Gen. Genet. **243:**112-118.

Gérard-Vincent, M., Robert, V., Ball, G., Bleves, S., Michel, G. P. F., Lazdunski, A., and Filloux, A. 2002 Identification of XcpP domains that confer functionality and specificity to the Pseudomonas aeruginosa type II secretion apparatus. Mol. Microbiol. **44:**1651-1665.

Guilvout I; Chami M; Engel A; Pugsley AP and Bayan N. 2006. Bacterial outer membrane secretin PulD assembles and inserts into the inner membrane in the absence of its pilotin. EMBO. J. **25:**5241-9.

Guilvout, I, Hardie, K. R., Sauvonnet, N. and Anthony P. Pugsley. 1999. Genetic Dissection of the Outer Membrane Secretin PulD: Are There Distinct Domains for Multimerization and Secretion Specificity? J. Bacteriol. **181:**7212-7220.

van Ham, M. and Hendriks, W. 2003. PDZ domains glue and guide. Mol. Biol. **30:**69–82.

Hardie KR, Lory S and Pugsley AP. 1996a. Insertion of an outer membrane protein in Escherichia coli requires a chaperone-like protein. **EMBO. J.** 15:978–988.

Hardie KR, Seydel A, Guilvout I and Pugsley AP. 1996b. The secretinspecific, chaperone-like protein of the general secretory pathway: separation of proteolytic protection and piloting functions. Mol. Microbiol. **22:**967–976.

Heidelberg, J.F., Eisen, J.A., Nelson, W.C., Clayton, R.A., Gwinn, M.L. and Dodson, R.J., *et al*. 2000. DNA sequence of both chromosomes of the cholera pathogen *Vibrio cholerae*. Nature. **406:**477–483.

Hill, J., K A Donald, D E Griffiths, and G Donald. 1991. DMSO-enhanced whole cell yeast transformation. Nucleic Acids Res. **19:**5791.

Hobbs, M. & Mattick, J.S. 1993. Common components in the assembly of type 4 fimbriae, DNA transfer systems, filamentous phage and protein-secretion apparatus: a general system for the formation of surface-associated protein complexes. Mol. Microbiol. **10:**233–243.

Howard, S. P., Critch, J. and Bedi, A. 1993. Isolation and analysis of eight exe genes and their involvement in extracellular protein secretion and outer mebrane assembly in *Aeromonas hydrophila*. J. Bacteriol. **175:**6695-6703.

Howard, S. P., Gebhart, C., Langen, G. R., Gang, L. and Timothy, S.G. 2006. Interactions between peptidoglycan and the ExeAB complex during assembly of the type II secretin of *Aeromonas hydrophila.* Mol. Microbiol. **59:**1062-1072.

Howard, S. P., Meiklejohn, H. G., Shivak, D. and Jahagirdar, R. 1996. A TonB-like protein and a novel membrane protein containing an ATP-binding cassette function together in exotoxin secretion. Mol. Microbiol. **22:**595-604.

Jahagirdar, R. and Howard., S. P. 1994. Isolation and characterization of a second *exe* operon required for extacellar protein secetion in *Aeromonas hydrophila*. J. Bacteriol. **176:** 6819-6826.

James, P., Halladay, J. and Craig, E. A. 1996. Genomic libraries and a host strain designed for highly efficient two- hybrid selection in yeast. Genetics **144:**1425-1436.

Jiang, N. B. and S P Howard. 1991. Mutagenesis and isolation of Aeromonas hydrophila genes which are required for extracellular secretion. **J. Bacteriol.** 173:1241-1249.

Jiang, B., and Howard, S.P. 1992. The *Aeromonas hydrophila exeE* gene, required both for protein secretion and normal outer membrane biogenesis, is a member of a general secretion pathway. Mol. Microbiol. **6:**1351–1361.

Johnson, T., L., Maria E. Scott, and Maria Sandkvist. 2007. Mapping Critical Interactive Sites within the Periplasmic Domain of the *Vibrio cholerae* Type II Secretion Protein EpsM J. Bacteriol. **89:**9082-9089.

Johnson, T. L., Abendroth, J., Hol, W.G.J., and Sandkvist, M. 2006. Type II secretion: from structure to function. FEMS Microbiol. Letters. **255**:175–186.

de Keyzer J, van der Does C and Driessen AJ. 2003. The bacterial translocase: a dynamic protein channel complex. Cell Mol. Life Sci. **60:**2034–2052.

Korotkov, K. V., Krumm, B., Bagdasarian, M., and Hol, W. G.J. 2006. Structural and Functional Studies of EpsC, a Crucial Component of the Type 2 secretion system from *Vibrio cholerae.* J. Mol. Bio**. 363:**311-321.

K¨ohler R, Schafer K, Muller S, Vignon G, Diederichs K, Philippsen A, Ringler P, Pugsley AP, Engel A and Welte, W. 2004. Structure and assembly of the pseudopilin PulG. Mol. Microbiol. 54:647–664.

Korotkov, K. V. and Wim G J Hol. 2008. Structure of the GspK–GspI–GspJ complex from the enterotoxigenic *Escherichia coli* type 2 secretion system. Nature Structural and Molecular Biology **15:**462-468.

Lee, MS, Chen, LY, Leu, WM, Rong-Jen Shiau, and Nien-Tai Hu. 2005. Associations of the Major Pseudopilin XpsG with XpsN (GspC) and Secretin XpsD of *Xanthomonas campestris* pv. campestris Type II Secretion Apparatus Revealed by Cross-linking Analysis. J. Biol. Chem. **280:**4585-4591.

Lee, H.M., Ruey Chen, J.R., Lee, H.L., Leu, W.M., Chen, L.Y., and Hu, N.T. 2004. Functional Dissection of the XpsN (GspC) Protein of the *Xanthomonas campestris* pv. campestris Type II Secretion Machinery. J. Bacteriol. **186:**2946-2955.

Lee, Hsien-Ming.;Tyan, Shiaw-Wei.;Leu, Wei-Ming.;Chen, Ling-Yun.;Chen, David Chanhen. And Hu, Nien-Tai. 2001. Involvement of the XpsN Protein in Formation of the XpsL-XpsM Complex in Xanthomonas campestris pv. campestris Type II Secretion Apparatus. J. Bacteriol. **183:**528–535.

Lee, H.M., Wang, K.C., Liu, Y.L. Yew, H.Y., Chen, L.Y., Leu, W.M., Chen, D.C., and Hu, N.T. 2000. Association of the Cytoplasmic Membrane Protein XpsN with the Outer Membrane Protein XpsD in the Type II Protein Secretion Apparatus of *Xanthomonas campestris* pv. Campestris. J. Bacteriol. **182:**1549-1557.

Letellier, L., Howard, S.P., and Buckley, J.T. 1997. Studies on the energetics of proaerolysin secretion across the outer membrane of *Aeromonas* species. Evidence for a requirement for both the protonmotive force and ATP. J. Biol. Chem. **272:**11109–11113.

Lindeberg, M., G.P. Salmond and A. Collmer. 1996. Complementation of deletion mutations in a cloned functional cluster of *Erwinia chrysanthemi out* genes with *Erwinia carotovora out* homologues reveals OutC and OutD as candidate gatekeepers of species-specific secretion of proteins via the type II pathway. Mol. Microbiol. **20:**175–190.

Login F. H., and Shevchik V. E. 2006. The single transmembrane segment drives self-assembly of OutC and the formation of a functional type II secretion system in Erwinia chrysanthemi. J. Biol. Chem. **281:**33152-33162.

Luban, J., and Goff, S.P. 1995. The yeast two-hybrid system for studying protein-protein interactions. Analytical biotechnology. **6:**59-64.

Mattick, J.S. and Alm, R.A. 1995. Response from Mattick and Alm: common architecture of type 4 fimbriae and complexes involved in macromolecular traffic. Trends Microbiol. **3:** 411-413.

McAlister-Henn, L., Gibson, N., and Panisko, E. 1999. Applications of the yeast two-hybrid system. Methods. **19:**330-337.

Michel, G., S. Bleves, G. Ball, A. Lazdunski, and A. Filloux. 1998. Mutual stabilization of the XcpZ and XcpY components of the secretory apparatus in *Pseudomonas aeruginosa*. Microbiology. **144:**3379-3386.

Nunn, D. 1999. Bacterial type II protein export and pilus biogenesis: more than just homologies? Trends Cell Biol. **9:**402–408.

Nunn, D.N. and Lory, S. 1993. Cleavage, methylation, and localization of the Pseudomonas aeruginosa export proteins XcpT, -U, -V, and -W. J. Bacteriol. **175:**4375–4382.

Nouwen N., Ranson N., Saibil H., Wolpensinger, B., Engel, A., Ghazi, A. and Pugsley, A. P. 1999. Secretin PulD: Association with pilot PulS, structure, and ion-conducting channel formation. Proc. Natl. Acad. Sci. **96:**8173-8177.

Nouwen, N., Stahlberg, H., Pugsley, A.P. and Engel, A. 2000. Domain structure of secretin PulD revealed by limited proteolysis and electron microscopy EMBO J. **19:**2229-2236.

Palmer T, Sargent F and Berks BC. 2005. Export of complex cofactor-containing proteins by the bacterial Tat pathway. Trends Microbiol. **13:**175–180.

Pallen, M. J. and Ponting, C. P. 1997. PDZ domains in bacterial proteins. Mol. Microbiol. **26:**411–415.

Peabody CR, Chung YJ, Yen MR, Vidal-Ingigliardi D, Pugsley AP & Saier MH Jr. 2003. Type II protein secretion and its relationship to bacterial type IV pili and archaeal flagella. Microbiology. **149:**3051–3072.

Phizicky, E. M. and Fields, S. 1995. Protein-protein interactions: methods for detection and analysis. Microbiological Reviews. **59:**94-123.

Planet PJ, Kachlany SC, DeSalle R and Figurski DH. 2001. Phylogeny of genes for secretion NTPases: Identification of the widespread tadA subfamily and development of a diagnostic key for gene classification. Proc. Natl. Acad. Sci. **98:**2503-2508.

Possot O. M., Gerard-Vincent, M. and Pugsley A.P. 1999. Membrane association and multimerization of secreton component PulC. J. Bacteriol. **181:**4004-4011.

Possot, O. M., Vignon, G., Bomchil, N., Ebel, F. and Anthony P. Pugsley 2000. Multiple Interactions between Pullulanase Secreton Components Involved in Stabilization and cytoplasmic Membrane Association of PulE. J. Bacteriol. **182:**2142-2152.

Py B, Loiseau L, Barras F 1999. Assembly of the type II secretion machinery of *Erwinia chrysanthemi*: Direct interaction and associated conformational change between OutE, the putative ATPbinding component and the membrane protein OutL. J. Mol. Biol. **289:**659–670.

Py, B., Loiseau, L. and Barras, F. 2001. An inner membrane platform in the type II secretion machinery of Gram-negative bacteria. EMBO reports. **2:**244–248.

Robert V, Filloux A & Michel GP. 2005a. Role of XcpP in the functionality of the *Pseudomonas aeruginosa* secreton. Res. Microbiol. **156:**880–886.

Robert, V; Filloux, A. and Gérard. P.F. M. 2005b. Subcomplexes from the Xcp secretion system of *Pseudomonas aeruginosa*. FEMS Microbiology Letters **252:**43–50.

Robert, V., F. Hayes, A. Lazdunski, and G. P. Michel. 2002. Identification of XcpZ domains required for assembly of the secreton of *Pseudomonas aeruginosa*. J. Bacteriol. **184:**1779-1782.

Robien, M.A., Krumm, B.E., Sandkvist, M., Hol, W.G. 2003. Crystal structure of the extracellular protein secretion NTPase EpsE of *Vibrio cholerae*. J. Mol. Biol. **333:**657–674.

Sandkvist, M. 2001a. MicroReview: Biology of type II secretion. Mol. Microbiol. **40:**271-283.

Sandkvist, M. 2001b. Type II secretion and pathogenesis. Infect. Immun. **69:**3523–3535.

Sandkvist M, Bagdasarian M, Howard SP. 2000. Characterization of the multimeric Eps complex required for cholera toxin secretion. International Journal of Medical Microbiology. **290:**345-350.

Sandkvist M, Bagdasarian M, Howard SP, DiRita VJ. 1995. Interaction between the autokinase EpsE and EpsL in the cytoplasmic membrane is required for extracellular secretion in Vibrio cholerae. EMBO J. **14:**1664–1673.

Sandkvist, M., L. P. Hough, M. M. Bagdasarian, and M. Bagdasarian. 1999. Direct interaction of the EpsL and EpsM proteins of the general secretion apparatus in *Vibrio cholerae*. J. Bacteriol. **181:**3129-3135.

Sandkvist, M., J. M. Keith, M. Bagdasarian, and S. P. Howard. 2000. Two regions of EpsL involved in species-specific protein-protein interactions with EpsE and EpsM of the general secretion pathway in *Vibrio cholerae*. J. Bacteriol. **182:**742-748.

Sauvonnet, N., Vignon, G., Pugsley, A.P. and Gounon, P. 2000. Pilus formation and protein secretion by the same machinery in Escherichia coli. EMBO J. **19:**2221–2228.

Savvides SN, Yeo HJ, Beck MR, Blaesing F, Lurz R, Lanka E, Buhrdorf R, Fischer W, Haas R, Waksman G. 2003. VirB11 ATPases are dynamic hexameric assemblies: new insights into bacterial type IV secretion. EMBO J. **22:**1969–1980.

Schoenhofen, I. C., Gang, L., Strozen, T. G., and Howard, S. P. 2005. Purification and Characterization of the N-terminal Domain of ExeA: a Novel ATPase Involved in the Type II Secretion Pathway of *Aeromonas hydrophila*. J. Bacteriol. **187:** 6370-6378.

Schoenhofen, I. C., Stratilo, C. and Howard, S.P. 1998. An ExeAB complex in the type II secretion pathway of *Aeromonas hydrophila*: effect of ATP-binding cassette mutations on complex formation and function. Mol. Microbiol. **29:**1237-1247.

Shevchik, V.E. and Condemine, G. 1998. Functional characterization of the Erwinia chrysanthemi OutS protein, an element of a type II secretion system. Microbiology. **144:**3219-3228.

Shevchik VE, Robert-Baudouy J and Condemine G. 1997. Specific interaction between OutD, an Erwinia chrysanthemi outer membrane protein of the general secretory pathway, and secreted proteins. EMBO. J. **16:**3007–3016.

Shiue, Sheng-Jie; Chien, I-Ling; Chan, Nei-Li; Leu, Wei-Ming; Hu, Nien-Tai. 2007. Mutation of a key residue in the type II secretion system ATPase uncouples ATP hydrolysis from protein translocation. Mol. Microbiol. **65:**401-412.

Shiue SJ; Kao KM; Leu WM; Chen LY; Chan NL and Hu NT. 2006. XpsE oligomerization triggered by ATP binding, not hydrolysis, leads to its association with XpsL. EMBO J. **25:**1426–1435.

Tsai, R. T., Wei-Ming Leu, Ling-Yun Chen, and Nien-Tai Hu. 2002. A reversibly dissociable ternary complex formed by XpsL, XpsM and XpsN of the Xanthomonas campestris pv. campestris type II secretion apparatus. Biochem J. **367:**865–871.

Thomas, J. D., Reeves, P. J., and Salmond, G. P. C. 1997. The general secretion pathway of *Erwinia carotovora* subsp. *carotovora*: analysis of the membrane topology of OutC and OutF. Microbiology. **143:**713–720.

Traut, T. W. 1994. The functions and consensus motifs of nine types of peptide segments that form different types of nucleotide-binding sites. Eur.J. Biochem. **222:**9–19.

Voulhoux R, Ball G, Ize B, Vasil ML, Lazdunski A, Wu LF and Filloux A. 2001. Involvement of the twin-arginine translocation system in protein secretion via the type II pathway. EMBO J. **20:**6735–6741.

Voulhoux R, Bos MP, Geurtsen J, Mols M. and Tommassen J. 2003. Role of a highly conserved bacterial protein in outer membrane protein assembly. Science. **299:**262-265.

Walker, J. E., M. Saraste, M. J. Runswick, and N. J. Gay. 1982. Distantly related sequences in the alpha- and beta-subunits of ATP synthase, myosin, kinases and other ATP-requiring enzymes and a common nucleotide binding fold. EMBO J. **1:**945–951.

Wong, K. R., and Buckley, J. T. 1989. Proton motive force involved in protein transport across the outer membrane of *Aeromonas salmonicida.* Science. **246:**654–656.

Wu, Bonnie; Rebecca L. Mullinax, and Joseph A. Sorge. 2003. Identifying Interacting Proteins in an *Escherichia coli*-Based Two-Hybrid System. Humana Press. **221:**295-309.

Yang, M., Wu, Z., and Fields, S. 1995. Protein-peptide interactions analyzed with the yeast two-hybrid system. Nucleic Acids Research **23:**1152-1156.

Yeo HJ, Savvides SN, Herr AB, Lanka E and Waksman G. 2000. Crystal structure of the hexameric traffic ATPase of the Helicobacter pylori type IV secretion system. Mol. Cell. **6:** 1461–1472.

Yu, H. B., Kaur, R., Lim, S, Wang, X. H. and Leun, K. Y. 2007. Characterization of extracellular proteins produced by *Aeromonas hydrophila* AH-1. Proteomics **7:**436–449.